ON THE STABILITY AND PROPAGATION OF BAROTROPIC MODONS IN SLOWLY VARYING MEDIA

by

GORDON EDWIN SWATERS

B.Math.(Honours), University Of Waterloo, 1980
M.Sc., University Of British Columbia, 1983

A THESIS SUBMITTED IN PARTIAL FULFILMENT OF

THE REQUIREMENTS FOR THE DEGREE OF

DOCTOR OF PHILOSOPHY

in

THE FACULTY OF GRADUATE STUDIES

Department Of Mathematics
Institute Of Applied Mathematics
Department Of Oceanography

We accept this thesis as conforming

to the required standard

THE UNIVERSITY OF BRITISH COLUMBIA

July 1985

In presenting this thesis in partial fulfilment of the requirements for an advanced degree at the University of British Columbia, I agree that the Library shall make it freely available for reference and study. I further agree that permission for extensive copying of this thesis for scholarly purposes may be granted by the Head of my Department or by his or her representatives. It is understood that copying or publication of this thesis for financial gain shall not be allowed without my written permission.

Department of Mathematics

The University of British Columbia
2075 Wesbrook Place
Vancouver, Canada
V6T 1W5

Date: July 1, 1985

Abstract

Two aspects of the theory of barotropic modons are examined in this thesis. First, sufficient neutral stability conditions are derived in the form of an integral constraint for westward and eastward-travelling modons. It is shown that eastward-travelling and westward-travelling modons are neutrally stable to perturbations in which the energy is contained mainly in spectral components with wavenumber magnitudes ($|\eta|$) satisfying $|\eta|<\kappa$ and $|\eta|>\kappa$, respectively, where κ is the modon wavenumber. These results imply that when $\kappa/|\eta|>1$ the slope of the neutral stability curve proposed by McWilliams et al.(1981) for eastward-travelling modons must begin to increase as $\kappa/|\eta|$ increases. The neutral stability condition is computed with mesoscale wavenumber eddy energy spectra representative of the atmosphere and ocean. Eastward-travelling atmospheric modons are neutrally stable to the observed seasonally- and annually-averaged atmospheric eddies. The neutral stability of westward-travelling atmospheric modons and oceanic modons cannot be inferred on the basis of the observed wavenumber eddy energy spectra for the atmosphere and ocean.

Second, a leading order perturbation theory is developed to describe the propagation of barotropic modons in a slowly varying medium. Two problems are posed and solved. A perturbation solution is obtained describing the propagation of an eastward-travelling modon modulated by a weak bottom Ekman boundary layer. The results predict that the modon radius and translation speed decay exponentially and that the modon

wavenumber increases exponentially, resulting in an exponential amplitude decay in the streamfunction and vorticity. These results agree with the numerical solution of McWilliams et al.(1981). A leading order perturbation theory is also developed describing modon propagation over slowly varying topography. Nonlinear hyperbolic equations are derived to describe the evolution of the slowly varying modon radius, translation speed and wavenumber for arbitrary finite-amplitude topography. To leading order, the modon is unaffected by meridional gradients in topography. Analytical perturbation solutions for the modon radius, translation speed and wavenumber are obtained for small-amplitude topography. The perturbations take the form of westward and eastward-travelling transients and a stationary component proportional to the topography. The general solution is applied to ridge-like and escarpment-like topographic configurations.

Table of Contents

List of Figures

Acknowledgement

It is a pleasure to thank Dr. Lawrence A. Mysak for many discussions on applied mathematics and physical oceanography, and for his enthusiastic encouragement of and interest in this research. The author also thanks Dr. Paul LeBlond, Dr. Kevin Hamilton, Dr. Uri Ascher and Dr. Brian Seymour for many helpful discussions pertaining to his research. This research was supported by Natural Sciences and Engineering Research Council of Canada and U.S. Office of Naval Research grants awarded to Dr. Lawrence A. Mysak, and by a U.B.C. Department of Mathematics Teaching Assistantship. Of special note I wish the oceanography beer garden regulars and in particular Don Dunbar, Karen Perry, Keith Thomson and Tom Kessler long life and prosperity. If it was not for you people the whole thing would not nearly have been as much fun.

I have resolved to quit only abstract geometry, that is to say, the consideration of questions that serve only to exercise the mind, and this, in order to study another kind of geometry, which has for its object the explanation of the phenomena of nature.

Rene Descartes

I. INTRODUCTION

Rings and eddies play an important role in the overall dynamics of the ocean. Flierl(1977) has argued, for example, that in the northwestern Atlantic Ocean the observed distribution of fluctuation kinetic energy and a theoretical estimate of this distribution based on quasigeostrophic dynamics (QGD) of eddies and their dispersive wave field are comparable. Lai and Richardson(1977) estimate from historical data that the lifespan of a Gulf Stream eddy is typically between 2 to 3 years, the average translation speeds are on the order of 5 km day^{-1}, the radii are about 100 km and the vertical extent is up to one kilometer. The number of rings and eddies observed at any given time was approximately 15 with maximum counts about twice this value. These observations suggest that eddy and ring dynamics must be important for thermal, vorticity and nutrient mixing in the ocean on mesoscales (i.e., length scales on the order of 100 km).

Eddies and rings can be generated from a variety of flow-geometry configurations. Observations of eddies have been theoretically described by coastal current instability (Ikeda et al., 1984), topographic-mean flow interactions (Swaters and Mysak, 1985), planetary wave reflection off coastal geometry (Willmott and Mysak, 1980) and the meandering of western boundary currents (Lai and Richardson, 1977 and Csanady, 1979). In addition to the above mechanisms, planetary eddies can also be obtained when the effects of phase dispersion

balance amplitude dispersion in planetary waves (Clarke, 1971) to produce the solitary planetary waves.

Malanotte-Rizzoli(1982) classified models of atmospheric and oceanic solitary planetary waves into one of two categories according to the nonlinearity of the potential vorticity equation (PVE). Steadily translating solutions of the PVE reduce to describing the potential vorticity as a function (P) of the pathlines. Rossby solitons and solitary waves are described by assuming P to be analytic. Examples of this approach include the Maxworthy and Redekopp(1976) derivation of Korteweg-De Vries (KdV) and modified-KdV equations from QGD in zonal channel models with a sheared zonal flow. Similar derivations by Malanotte-Rizzoli and Hendershott(1980) and Malanotte-Rizzoli(1984) with cross-channel topographic variation also resulted in a KdV equation and hence a solitary wave solution. Also, Flierl(1979) has obtained radially symmetric quasigeostrophic solitary wave solutions on an infinite β-plane assuming P to be analytic.

The second category is to specify P as a nonanalytic function. The solutions that this procedure yields, hereafter called modons, have the property that the streamfunction is only differentiable to some finite order (usually two). Stern(1975) obtained the prototype modon solution (and named them as such) by assuming P to be a linear function in a bounded circular domain on the β-plane with the streamfunction vanishing identically outside this region. These solutions were continuous but not differentiable at the boundary and had a

dipole vortex structure.

Larichev and Reznik(1976) obtained what is now called the barotropic modon by determining a form for P in the exterior region when the streamfunction vanishes at infinity (see Figure 1 for a three-dimensional plot of a modon). These solutions have smooth vorticity everywhere except at the boundary where the vorticity has a finite step discontinuity in its radial derivative. These solutions have been subsequently generalized to two-layer fluids (Flierl et al., 1980) and spherical geometry (Tribbia, 1984 and Verkley, 1984). Kloeden(1985a,1985b) claims to have established a theorem that states that the modon is the unique localized separable solitary wave solution of the PVE assuming that P is piecewise linear.

Studies of modon dynamics have primarily focussed on numerical integrations of the PVE. For example, McWilliams et al.(1981) numerically calculated the effect of Ekman dissipation on modon propagation and concluded that the decay was approximately exponential and shape preserving. The details of the decay in the amplitude and translation speed could not be explicitly determined except that they appeared to occur on the modon "dispersion curve". Other numerical experiments with random vorticity perturbations indicated that the onset of instability was determined by the length scale of the perturbations.

McWilliams and Zabusky(1982) numerically simulated collisions between barotropic modons. Depending on the parameter values, a wide range of interaction possibilities were

observed, from soliton-like, fusion-like and fission-like interactions to the complete annihilation of the vortices. The multitude of interaction possibilities resulted in some debate as to whether or not the modon is in fact a two-dimensional soliton (Flierl et al., 1980 and McWilliams, 1980). No theoretical framework has yet been developed from which to understand these interactions.

Mied and Lindemann(1982) and McWilliams(1983) have considered the problem of modon genesis. It had been suggested (Flierl, 1976) that a pure baroclinic eddy would naturally tend to develop into a barotropic modon. Mied and Lindemann(1982) subsequently numerically calculated the evolution of a baroclinic eddy with a tilted vertical axis and counter-rotating upper and lower layers. Their results indicated that when the vertical axis lies in the north-south plane modon genesis ensues unless the horizontal separation between the centers of the vortices is too large. If the vertical axis lay in other directions the two vortices tended to separate with no coupling taking place. McWilliams(1983) was also able to create modon-like dipoles by the collision of two quasigeostrophic vortices.

Laboratory studies of modon genesis (Flierl et al., 1983) indicated that dipole vortex formation likely evolves from very general initial conditions. This conclusion was formulated as a theorem (Flierl et al., 1983) which states that any slowly varying isolated disturbance on a β-plane must have zero net angular momentum. The modon is one of the simplest nontrivial flow configurations with this property.

In summary, previous research on modon dynamics has indicated the following results. Modon stability is dependent on the structure of the perturbation field. Modon genesis is conjectured to evolve from rather general initial conditions and is one of the simplest realizations of isolated steadily translating fluid motions on a β-plane. Modons in a dissipative environment appear to preserve their shape, at least initially. Modon-modon interactions appear to have many possibilities, some of which are soliton-like others not.

However, several questions in modon dynamics remain to be answered before we can understand the role of modons to atmospheric and oceanic dynamics. No theoretical or analytical framework has yet been developed which can be used to describe the above numerical results. Such a framework would seem to be required if modon dynamics is to be understood in terms of known geophysical fluid dynamic mechanisms. In particular, nothing is known about basic problems such as how modons might interact with their environment. For example, the interaction of modons with currents and Rossby waves have yet to be studied. In addition, questions relating to the stability of modons are unanswered. For example, the specification of stability conditions and the solution of the linearized stability problem are unknown.

This thesis examines two aspects of barotropic modon dynamics. The first aspect is examined in Chapter II, in which sufficient neutral stability conditions are derived for normal-mode small-amplitude perturbations of westward and eastward-

travelling modons in the form of an integral constraint. These conditions are derived from the spatially-integrated perturbation energy and enstrophy equations (Charney and Flierl(1981) and Malanotte-Rizzoli(1982)) for steadily translating quasigeostrophic fluid motions. It is shown that eastward-travelling modons are neutrally stable to normal-mode perturbations that are solely composed of spectral components with wavelength magnitudes larger than $2\pi/\kappa$ where κ is the modon wavenumber (see Chapter 2). Westward-travelling modons are neutrally stable to normal-mode perturbations solely composed of spectral components with wavelengths smaller than $2\pi/\kappa$.

These results imply that when $\kappa/|\eta|>1$, where $|\eta|$ is the magnitude of the perturbation wavenumber vector $\eta=(\eta_1,\eta_2)$, the slope of the neutral stability curve proposed by McWilliams et al.(1981) should begin to increase as $|\eta|$ decreases. A similar trend in the neutral stability curve has been numerically determined for topographically-forced planetary solitary waves (Malanotte-Rizzoli, 1982).

The neutral stability integral is tested using observed eddy energy spectra for the atmosphere and ocean. For the atmospheric calculation, seasonally- and annually-averaged mid-latitude 300, 500 and 700 mb two-dimensional wavenumber eddy energy spectra were inferred from Tomatsu(1979), Saltzman and Fleisher(1962) and Eliasen and Machenhauer(1965). It is argued on the basis of the calculations contained in this thesis that eastward-travelling atmospheric modons are neutrally stable to the observed seasonally- and annually-averaged fluctuations in

the atmosphere. Westward-travelling atmospheric modons may not satisfy the neutral stability condition and thus their stability or instability cannot be inferred.

The only published barotropic wavenumber eddy energy spectrum available for the oceans is contained in Fu(1983). Simple scaling arguments are presented to suggest that only eastward-travelling barotropic modons will have realistic translation and particle speeds in the ocean. The stability of eastward-travelling oceanic modons cannot be inferred from the Fu(1983) spectrum. Arguments are presented suggesting that this conclusion should only be considered a very preliminary estimate of oceanic modon stability due to the limitations of the Fu(1983) spectrum.

The second aspect of modon dynamics examined in this thesis is contained in Chapter III, in which a perturbation theory is proposed to describe modon propagation in a slowly varying medium. The perturbation methods developed are two-dimensional generalizations of one-dimensional slowly varying solitary wave calculations (e.g., Luke(1966), Grimshaw(1970, 1971, 1977, 1979a,b, 1981), Zakharov and Rubenchik(1974) and Kodama and Ablowitz(1980,1981), among others). This calculation represents the first application of these methods to a fully two-dimensional solitary wave.

Two problems are posed and solved. In Section 3.1 a perturbation theory describing the propagation of an eastward-travelling modon over a weak Ekman bottom boundary layer is developed. This calculation was done in order to compare the

result of the leading order solution with the numerical solution of McWilliams et al.(1981).

The numerical solution suggested that the modon radius and translation speed decay exponentially and the modon wavenumber increases exponentially. Throughout the decay the modon parameters (to leading order) satisfied the modon dispersion relationship. In the final stages of the decay the modon dissolved into a field of westward-travelling planar Rossby waves. The leading order perturbation solution obtained here agrees with these results but is unable to describe the final degeneration into the Rossby waves. This calculation has been summarized in Swaters(1985).

In Section 3.2 a leading order perturbation theory is developed to describe modon propagation over slowly varying topography. As in previous work on the effects of variable topography on barotropic planetary waves (e.g., Veronis(1966), Rhines(1969a,b), Clarke(1971) and LeBlond and Mysak(1978; Sec. 20), among others) the theory is developed in the context of the rigid-lid shallow water equations on the β-plane.

Nonlinear hyperbolic equations are derived for the slow evolution of the leading order modon radius, translation speed and wavenumber. These equations are valid for arbitrary slowly varying finite-amplitude topography. In general they must be solved numerically. It is shown that to leading order the evolution of the modon is independent of the meridional (North-South) topographic structure. This result is interpreted in

terms of simple vorticity arguments.

Analytical perturbation solutions are obtained for small-amplitude topography (relative to the fluid depth, which is the case in many atmospheric and oceanic applications). The perturbations take the form of eastward and westward-travelling hyperbolic transients and a stationary component proportional to the topography. The general properties of the solution are described in Subsection 3.2.2. Subsections 3.2.3 and 3.2.4 describe the slowly varying modon for the specific examples of a topographic ridge and escarpment, respectively.

The work contained in this thesis is summarized in Chapter IV. In the Appendix details of the many integral calculations required in the topographic solution are given.

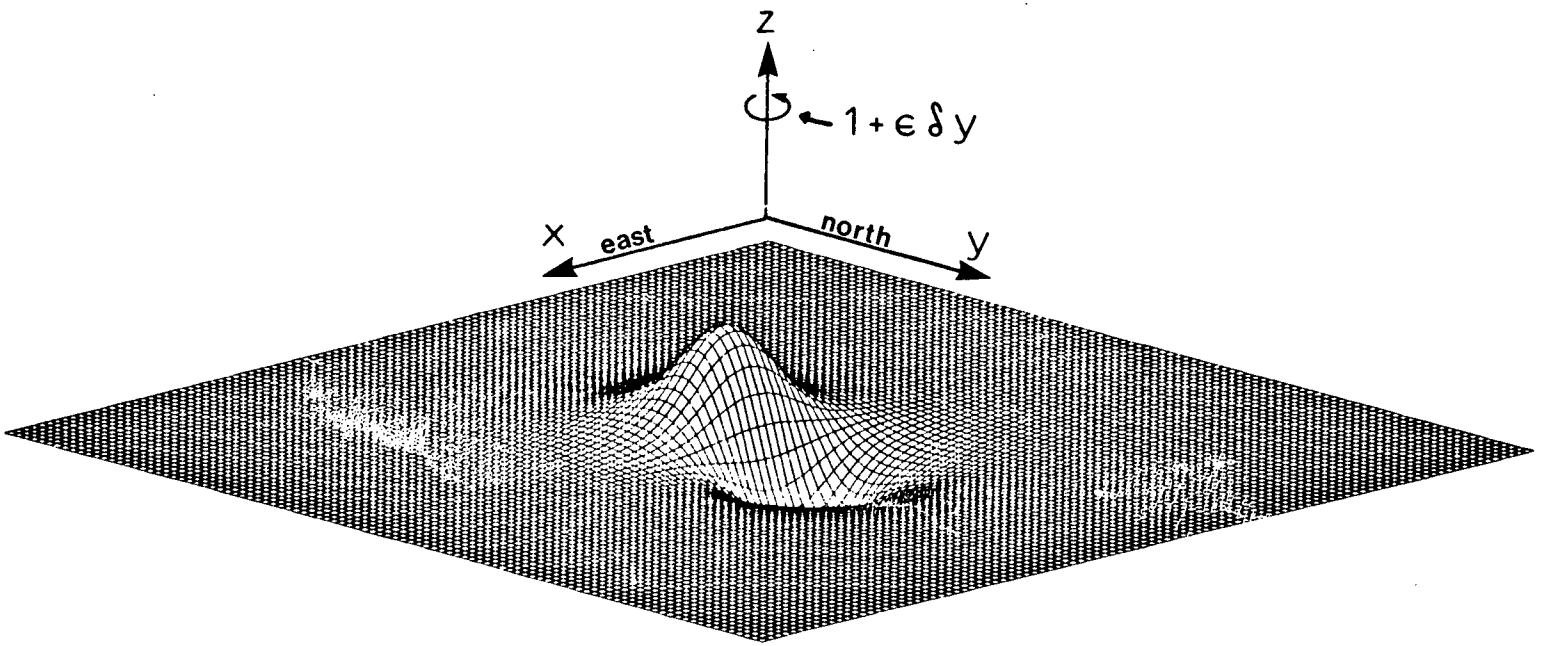

Figure 1. Three dimensional contour plot of the surface displacement associated with an eastward-travelling modon. For atmospheric scales, the horizontal distance between the maximum and minimum deflection is about 800 km with a deflection of the geopotential is on the order of 100 m. For oceanic scales, the horizontal distance between the the maximum and minimum deflection is about 80 km with a deflection on the order of 10 cm. The coordinate system is rotating with nondimensional angular velocity $1+\epsilon\delta y$ where ϵ is the Rossby number $c(fa)^{-1}$ and δ is the planetary vorticity factor $\beta a^2 c^{-1}$ with a, c, f and β the modon radius, modon translation speed, local Coriolis parameter and northward gradient in the Coriolis parameter, respectively.

II. STABILITY OF BAROTROPIC MODONS

McWilliams(1980) modelled an observed atmospheric blocking event with a barotropic modon. Among several questions posed was whether or not the modon solution is stable for typically observed atmospheric fluctuations. Subsequently, McWilliams et al.(1981) numerically examined the stability of eastward-travelling modons when perturbed by a random vorticity field. Their results indicate that for a given vorticity perturbation amplitude (ϵ), increasing the perturbation wavelength leads to instability; also, for a given perturbation wavelength, increasing ϵ leads to instability.

This chapter describes sufficient neutral stability conditions for westward and eastward-travelling modons. Modifications to the regime diagram proposed by McWilliams et al.(1981) are discussed in light of these results. The stability condition is calculated with typical atmospheric and oceanic energy spectra.

It is shown that atmospheric eastward-travelling barotropic modons are neutrally stable to the observed seasonally- and annually-averaged 300, 500 and 700 mb transient eddies. A similar stability calculation is unable to determine the stability of westward-travelling atmospheric modons. A neutral stability calculation is also done for an oceanic barotropic kinetic energy spectrum. On the basis of this calculation the stability or instability of oceanic modons cannot be inferred.

Charney and Flierl(1981) derived a stability theorem for

normal-mode infinitesimal perturbations of steady quasigeostrophic flow based on the conservation of energy and enstrophy (vorticity squared). This method gives stability conditions similar to the Blumen(1968) finite-amplitude result based on establishing sufficient conditions for which the mean flow is a stable extremum of a suitably constructed (Arnol'd, 1965) energy-enstrophy functional. Sufficient neutral stability conditions for barotropic modons are derived by similar methods.

Eastward-travelling modons are neutrally stable to perturbations solely composed of spectral components with wavenumbers $\eta = (\eta_1, \eta_2)$ satisfying $|\eta| < \kappa$ where κ is the modon wavenumber (i.e., the parameter describing the functional dependence of the pathlines on the potential vorticity in the modon interior). Westward-travelling modons are neutrally stable to perturbations solely composed with spectral components with wavenumbers satisfying $|\eta| > \kappa$.

For eastward-travelling modons, the neutral stability condition implies that when ϵ is finite (though possibly only 'small') and the dominant perturbation spectral component consists of scales $\kappa/|\eta| > 1$ the modon is neutrally stable. Thus when $\kappa/|\eta| > 1$ the slope of the neutral stability curve proposed by McWilliams et al.(1981) for eastward-travelling modons should begin to increase as $\kappa/|\eta|$ increases. This property in the neutral stability curve has been numerically determined for topographically-forced solitary planetary eddies (Malanotte-Rizzoli, 1982).

In reality, a modon would be subjected to perturbations described by a spectrum of wavenumbers. The derived stability condition suggests (for a modon radius on the order of the external deformation radius) that an atmospheric westward-travelling modon is neutrally stable when the eddy energy of the surrounding fluid is contained mainly in global wavenumbers[1] with magnitudes greater than approximately 16. However, eastward-travelling modons are neutrally stable in flow regimes in which the energy is contained mainly in wavenumbers with magnitudes less than approximately 16. Consequently eastward-travelling modons are neutrally stable for the observed mid-latitude eddy energetics because typical observations show $|\eta| \simeq 8$ (see Figure 3) (Eliasen and Machenhauer, 1965; Saltzman and Fleisher, 1962 and Tomatsu, 1979).

The only published barotropic wavenumber eddy energy spectrum available for the oceans is contained in Fu(1983). Simple scaling arguments are presented to suggest that only eastward-travelling barotropic modons will have realistic translation and particle speeds in the ocean. The neutral stability condition suggests that oceanic eastward-travelling modons will be stable if the eddy energy of the surrounding fluid is contained mainly in wavelengths greater than about 160 km. The neutral stability of eastward-travelling oceanic modons cannot be inferred from the Fu(1983) spectrum. It is

---

[1] The global wavenumber is defined so that a wavenumber magnitude of one corresponds to a wavelength equalling the circumference around a latitude circle.

noted that this calculation should only be considered a very preliminary estimate of oceanic modon stability due to the limitations of the Fu(1983) spectrum.

2.1 Integral Constraints For Perturbations Of Barotropic Modons

Consider the nondimensional barotropic potential vorticity equation (Pedlosky, 1979)

$$(\Delta - F)\psi_t + J(\psi + y, \Delta\psi - F\psi + \delta y) = 0 \qquad (2.1)$$

where ψ is the geostrophic pressure, $J(\cdot,*)$ is the Jacobian determinant $\partial(\cdot,*)/\partial(\xi,y)$ and $\Delta=\partial_{\xi\xi} + \partial_{yy}$ where ξ is the translated coordinate $\xi = x - t$ with x, y and t the usual east, north and time coordinates. The coefficients $\delta = \beta a^2/c$ and $F = f^2a^2/(gH)$ are the planetary vorticity factor and rotational Froude number respectively, with f, β, g, H, a and c the local Coriolis parameter, northward gradient of the Coriolis parameter, gravitational acceleration, fluid depth, modon radius and modon translation speed respectively. The length, time and speed scalings are a, a/c and c, respectively. We note that c may be positive or negative.

Steady solutions of (2.1) have the vorticity $\Delta\psi - F\psi + \delta y$ expressed as a function of the pathlines $\psi + y$, viz. $P(\psi + y)$. For the barotropic modon P is defined by (Flierl et al., 1980)

$$P(z) = \delta z \quad \text{for } r>1 \qquad (2.2a)$$

$$P(z) = -(\kappa^2 + F)z \quad \text{for } r<1, \tag{2.2b}$$

resulting in

$$\psi = -K_1[(\delta + F)^{1/2}r]\sin(\theta)/K_1[(\delta + F)^{1/2}] \quad r>1 \tag{2.3a}$$

$$\psi = (\delta + F)J_1(\kappa r)\sin(\theta)/(\kappa^2 J_1(\kappa)) - (\kappa^2 + F + \delta)\kappa^{-2}r\sin(\theta) \quad r<1 \tag{2.3b}$$

where $r^2 = \xi^2 + y^2$, $\tan(\theta) = y/\xi$ and where J_1 and K_1 are the ordinary and modified Bessel functions of order one respectively (see Figure 1). The parameter κ (henceforth called the modon wavenumber) is determined by requiring continuity of $\nabla\psi$ on $r=1$ and is the first nonzero solution of the modon 'dispersion' relation

$$-(\delta + F)^{1/2}J_2(\kappa)K_1[(\delta + F)^{1/2}] = \kappa J_1(\kappa)K_2[(\delta + F)^{1/2}]. \tag{2.3c}$$

It turns out (see Flierl et al., 1980) that κ is a slowly varying function of $\delta + F$ (in particular $\delta + F \simeq O(1) \rightarrow \kappa \simeq 4$).

To obtain the stability condition consider $\psi = \Psi + \exp(\sigma t)\psi'(x,y)$ with $|\psi'| << |\Psi|$ where Ψ is the modon solution (2.3). Substituting into (2.1), linearizing and exploiting (2.2) results in the eigenvalue problem

$$\sigma(\Delta - F)\psi + \underline{U}_0 \cdot \nabla[(\Delta - F - \dot{P})\psi] = 0 \tag{2.4}$$

where the prime has been dropped, $\dot{P} = dP(z)/dz$ and $\underline{U}_0 = (-\Psi_y - 1, \Psi_\xi)$. Equation (2.4) is defined on the disconnected open intervals $0<r<1$ and $1<r<\infty$ with $\dot{P}$ obtained from (2.2). On $r=1$ ψ and $\nabla\psi$ are assumed to be continuous. It follows from (2.4) that the spatially integrated energy and enstrophy equations are, respectively

$$(\sigma + \sigma^*) \int_{-\pi}^{\pi} \int_{0}^{\infty} |\nabla\psi|^2 + F|\psi|^2 \, r dr d\theta =$$

$$- \int_{-\pi}^{\pi} \int_{0}^{\infty} (\underline{U}_0 \cdot \nabla\psi^*)\Delta\psi + (\underline{U}_0 \cdot \nabla\psi)\Delta\psi^* \, r dr d\theta, \qquad (2.5)$$

$$(\sigma + \sigma^*) \int_{-\pi}^{\pi} \int_{0}^{\infty} |\Delta\psi - F\psi|^2/\dot{P} \, r dr d\theta =$$

$$\int_{-\pi}^{\pi} \int_{0}^{\infty} (\underline{U}_0 \cdot \nabla\psi^*)\Delta\psi + (\underline{U}_0 \cdot \nabla\psi)\Delta\psi^* \, r dr d\theta, \qquad (2.6)$$

where ψ^* is the complex conjugate of ψ.

Equations (2.5) and (2.6) have been derived by obtaining energy and enstrophy equations in the exterior ($r>1$) and interior ($r<1$) and adding the results together. In this derivation certain integration by parts are required which result in boundary integrals on $r=1$. These terms are either identically zero since $\underline{U}_0 \cdot \underline{n} = 0$ on $r=1$ where $\underline{n}$ is the unit normal on $r=1$ or sum to zero when the exterior and interior integrals

are added together (see Charney and Flierl(1981) and Malanotte-Rizzoli(1982)).

The addition of (2.5) and (2.6) gives

$$(\sigma + \sigma^*) \int_{-\pi}^{\pi} \int_{0}^{\infty} \{|\nabla\psi|^2 + F|\psi|^2 + |\Delta\psi - F\psi|^2/\dot{P}\}\, r dr d\theta = 0. \quad (2.7)$$

If the integral in (2.7) is nonzero then the $Re(\sigma)=0$ and the modon is neutrally stable (Drazin and Reid, 1981). Thus a sufficient condition for the neutral stability of barotropic modons is that the integral in (2.7) be nonzero. It is noted here that for instability or for asymptotic stability the integral must be identically zero (since in either case $Re(\sigma)$ is nonzero).

The condition that the integral in (2.7) is zero can be rearranged to give

$$\int_{-\pi}^{\pi} \int_{0}^{\infty} \{|\nabla\psi|^2 + F|\psi|^2 - |\Delta\psi - F\psi|^2/(\kappa^2 + F)\}\, r dr d\theta = -I_1/\delta \quad (2.8)$$

$$\int_{-\pi}^{\pi} \int_{0}^{\infty} \{|\nabla\psi|^2 + F|\psi|^2 + |\Delta\psi - F\psi|^2/\delta)\}\, r dr d\theta = I_2/\delta \quad (2.9)$$

with

$$I_1 = (\delta + F + \kappa^2)(\kappa^2 + F)^{-1} \int_{-\pi}^{\pi} \int_{1}^{\infty} |\nabla\psi - F\psi|^2\, r dr d\theta \geq 0$$

$$I_2 = (\delta + F + \kappa^2)(\kappa^2 + F)^{-1} \int_{-\pi}^{\pi} \int_{0}^{1} |\nabla\psi - F\psi|^2\, r dr d\theta \geq 0,$$

since $\delta + F>0$ for solutions of the form (2.3). Equations (2.8) and (2.9) can be rewritten

$$\int |\psi^T|^2(\kappa^2 - |\eta|^2)(|\eta|^2 + F)\, d\eta = -4\pi^2(\kappa^2 + F)I_1/\delta \qquad (2.10)$$

$$\int |\psi^T|^2(|\eta|^2 + F)(\delta + F + |\eta|^2)\, d\eta = 4\pi^2 I_2 \qquad (2.11)$$

due to Parseval's equality, where ψ^T is the Fourier transform of ψ, and η the wave number vector (η_1, η_2). Equation (2.10) forms the basis for the remaining analysis.

2.2 Discussion And Application To The Atmosphere And Ocean

The integral (2.10) provides sufficient conditions on the wavenumber spectrum of the perturbation field if the modon is to be neutrally stable. Consider the case $c < 0$ (i.e., a westward-travelling modon). It follows from (2.10) that if the perturbation is solely composed of wavenumbers satisfying $|\eta| > \kappa$ the LHS and RHS of (2.10) are of different sign (since $\delta<0$). Therefore the integral in (2.7) cannot be zero and the westward-travelling modon must be neutrally stable. Equation (2.11) places no constraint on the perturbation wavenumbers since both the LHS and RHS are nonnegative. This stability condition suggests that westward-travelling modons are neutrally stable when the perturbation field is dominanted by wavenumbers with magnitudes larger than the modon wavenumber.

Eastward-travelling modons ($c > 0$ hence $\delta > 0$) are neutrally stable if the perturbation is solely composed of

wavenumbers satisfying $|\eta| < \kappa$. As before, (2.11) places no restriction on the perturbation wavenumbers. This stability condition suggests that an eastward-travelling modon will be neutrally stable when the surrounding fluid is dominated by wavenumbers smaller than the modon wavenumber.

The sufficient stability conditions just described are in fact valid for finite-amplitude perturbations (Charney and Flierl, 1981, Benzi et al., 1982 and Purini and Salusti, 1984) although the analysis may be only valid for small-amplitude perturbations depending on the distribution of extremums to the Blumen(1968) energy-enstrophy functional (Drazin and Reid, 1981).

However this analysis is not a rigorous demonstration of full nonlinear stability. Ebin and Marsden(1970), Marsden and Abraham(1970) and Holm et al.(1983) have pointed out that the Arnol'd(1965) argument is not a proof of nonlinear stability due to inconsistencies between the topology of the Hilbert space of which ψ is a member and the topology of the second variation of the energy-enstrophy functional. A rigorous proof of a nonlinear stability theorem for plane curvilinear flows can be given using convexity arguments (see Arnol'd, 1969 and Holm et al., 1983).

McWilliams et al.(1981) proposed a regime diagram (see Figure 2; adapted from Figure 10 in McWilliams et al., 1981) for eastward-travelling modons. Their numerically determined neutral stability curve is shown as a solid line. The stability condition given above (for c>0) suggests that as $\kappa/|\eta|$ increases

for $\kappa/|\eta|>1$ (i.e., a disturbance dominated by wavenumbers smaller than the modon wavenumber) a region of stability should exist (at least for small-amplitude perturbations). Thus when $\kappa/|\eta|>1$ the slope of the neutral stability curve should begin to increase as $|\eta|$ decreases, allowing a region of stability adjacent to the wavenumber axis. This trend in the neutral stability curve is qualitatively shown by the dashed line in Figure 2 (where it is assumed that for $|\eta|\simeq\kappa$ the two curves should be close to each other). Similar neutral stability curve behaviour has been determined for topographically-forced planetary solitary eddies (Malanotte-Rizzoli, 1982).

In the LHS of (2.10), the only explicit reference to the modon is given by κ and F, both of which are spatially constant for a given translation speed (c) and modon radius (a). For atmospheric scales (see McWilliams, 1980) the modon radius is on the order of the deformation radius and $|c| \simeq 0(10)$ m/s. Thus $F \simeq 1$, $\delta \simeq 0(1)$[2] and consequently $\kappa \simeq 4$ (cf. (2.3c) see also Flierl et al.(1980)).

In mid-latitudes these parameter values imply that westward-travelling atmospheric modons will be neutrally stable if the energy in the transients in the surrounding fluid are contained mainly in scales with (global) wavenumber magnitudes greater than approximately 16 ($16 \simeq \kappa R\cos(\phi)/a$ where R and ϕ are the Earth radius and latitude, respectively). Eastward-

---

[2] The planetary vorticity factor must be 0(1) for phase dispersion to balance amplitude steeping in (2.1) (see Charney and Flierl, 1981).

travelling modons, on the other-hand, will be neutrally stable in flow regimes in which the energy is contained mainly in scales with wavenumbers less than approximately 16. However, the dominant contribution to the energy spectrum of eddies in the mid-latitude 300 mb, 500 mb and 700 mb atmosphere (which are representative of the barotropic flow) resides in zonal wavenumbers with magnitudes less than about 4-5 and meridional wavenumbers (see Figure 3) 6-8 giving a (global) wavenumber eddy energy peak at approximately 8 (calculated from Eliasen and Machenhauer, 1965; Saltzman and Fleisher, 1962 and Tomatsu, 1979). Consequently the LHS of (2.10) will be positive when evaluated for the observed 300 mb, 500 mb and 700 mb eddy energy spectra.

As an example, (2.10) can be evaluated for the Tomatsu(1979) seasonally- and annually-averaged 500 mb eddy kinetic energy spectrum. To calculate (2.10) we approximate $|\psi^T|^2$ by $2E(\eta_1,\eta_2)|\eta|^{-2}$ with E the nondimensional eddy kinetic energy spectrum. A mid-latitude north-south (cartesian) wavenumber was inferred with the approximation

$$\eta_2 \simeq a\{-D^2P_n^m(\phi)/P_n^m(\phi)\}^{1/2}/(R\cos(\phi))$$

evaluated at 45°N, where $P_n^m(\phi)$ is the associated Legendre function, $D^2P_n^m(\phi) = d^2P_n^m(\phi)/d\phi^2$ and $m = \eta_1 R\cos(\phi)/a$ the nondimensional zonal wavenumber. The contribution of the $P_n^m(\phi)$ harmonic to the Tomatsu(1979) mth zonal wavenumber spectra was inferred from the Eliasen and Machenhauer(1965) spectrum so that

the percentage contributions remained the same (see Figure 3) in both. These calculations imply a LHS of (2.10) of +35.57, +42.17 and +28.43 for the annual, winter and summer[3] eddy energy spectra, respectively; with expected standard deviations of approximately 14.88, 13.47 and 11.51, respectively based on percentage standard deviations consistent with Saltzman and Fleisher(1962). (These calculations are nondimensional.) Calculations based on the 300 mb and 700 mb eddy energy spectra are qualitatively similar.

Therefore the LHS and the RHS of (2.10) are of different sign (to two standard deviations) for $c>0$ and the conclusion is made that eastward-travelling modons are neutrally stable for typical (i.e., observed perturbation) mid-latitude energetics. A stability or instability inference cannot be made for westward-travelling modons since both sides of (2.10) are of the same sign and thus it is possible that the neutral stability condition is not satisfied.

The available data describing oceanic mesoscale wavenumber variability pales in comparison to the atmospheric record. To the author's knowledge, Fu(1983) contains the only published (barotropic) geostrophic kinetic energy wavenumber spectrum for the oceans. Fu's calculation is based on SEASAT altimeter measurements of the sea surface variability, for wavelengths between 100-1000 km. A calculation testing (2.10) using Fu's data should only be considered a preliminary estimate of modon

[3] The seasons are defined so that winter is September through to Feburary and summer is March through to August.

stability in the ocean.

Note that solutions of the form (2.3) require $\delta + F > 0$ (or else the modified Bessel functions have imaginary argument). The translation speed for westward-travelling modons therefore satisfies the constraint $c < -\beta a^2 F^{-1}$. Assuming $\beta \simeq 1.6 \cdot 10^{-11}$ $m^{-1}s^{-1}$, $a \simeq 10^5 m$, $f \simeq 10^{-4} s^{-1}$ and $H \simeq 5 \cdot 10^3$ m it follows that $F \simeq 10^{-2}$ and consequently that $c < -10$ ms^{-1}. This large (in absolute value) translation speed (and hence particle speeds) suggests that barotropic westward-travelling modons are not likely to be observed in the mid-ocean. Under the approximations $c>0$ and $F \to 0$ (2.10) reduces to

$$\int |\psi^T|^2 |\eta|^2 (\kappa^2 - |\eta|^2)\, d\eta \leq 0. \qquad (2.12)$$

As in the atmospheric calculation, $|\psi^T|^2$ is approximated by $2E(\eta_1, \eta_2)|\eta|^{-2}$ where $E(\eta_1, \eta_2)$ is the two dimensional kinetic energy spectrum. Since horizontal mesoscale variability in the oceans is nearly isotropic (Bernstein and White, 1974; Mode Group, 1978 and Richardson, 1983) it follows that (Fu, 1983)

$$E(\eta_1, \eta_2) = E_0(|\eta|)(2\pi|\eta|)^{-1}$$

where $E_0(|\eta|)$ is the scalar wavenumber spectrum for the geostrophic kinetic energy (see Figure 4, adapted from Figure 8 in Fu, 1983). Thus the inequality (2.12) takes the form

$$2 \int_0^\infty E_0(|\eta|)[\kappa^2 - |\eta|^2]\, d|\eta| \leq 0. \qquad (2.13)$$

Clearly if (2.13) is to be contradicted (i.e., a demonstration of neutral stability), the dominant contribution to the integral must come from $|\eta| < \kappa$. For $a \simeq 100$ km, $c \simeq 10$ cms^{-1} and $\beta \simeq 1.6 \cdot 10^{-11}$ it follows that $\kappa = 3.9616$, corresponding to a wavelength of about 160 km ($=200\pi/\kappa$ km). Thus oceanic barotropic modons will be neutrally stable to perturbations for which the energy is contained mainly in wavelengths greater than about 160 km.

The integral in (2.13) was calculated using the Fu(1983) spectrum (see Figure 4) with E_0 set identically zero for wavelengths outside the 100-1000 km band. For the high energy spectrum (see Figure 4), corresponding to data obtained near major current systems (see Fu, 1983), the LHS of (2.13) was computed to be -56.06. For the low energy spectrum (see Figure 4), corresponding to data obtained in regions remote from major current systems (see Fu, 1983), the LHS of (2.13) was computed to be -44.54. As a measure of the error, standard deviations of .6 and .5 were computed for the above estimates, respectively, based on the 95% confidence intervals for the high and low energy spectra in Fu(1983). (These results are nondimensional.) Based on these calculations, the neutral stability of barotropic modons in the oceans cannot be inferred.

There are, however, limitations to the Fu(1983) spectrum which may restrict its applicability here. For example, the data used to compute the spectra represents energy only at periods less than 24 days (Fu, 1983), whereas Wunsch(1981) has shown that the dominant energy containing eddies have periods

between 50 and 150 days. Also, Fu(1983) argued that because of the short duration of the data, the integrated kinetic energy observed is about 5 times less than that reported by Wyrtki et al.(1976). It is therefore conceivable that a wavenumber spectrum computed with longer records would be quite different from the Fu(1983) spectrum to the degree that the opposite conclusion given above may be reached. Clearly, further work on the mesoscale wavenumber spectrum of the ocean is required before the constraint (2.13) can be realistically tested.

Equation (2.1) can also be interpreted as a nonlinear reduced-gravity or 1-1/2 layer model (White and Saur, 1981 and Mysak, 1983) where ψ is the interfacial displacement and F is the internal Froude number. Consequently, $F \simeq 0(1)$ and westward-travelling modons will have realistic translation speeds ($c \simeq -10^{-1} ms^{-1}$). In this context, (2.10) could be calculated using a two dimensional baroclinic fluctuation energy wavenumber spectrum obtained from geostrophic velocity fields that are relative to a level of no motion (e.g., from isotherm deflection data collected from a spatial array of XBTs). A calculation of a low frequency energy wavenumber spectrum along these lines is currently in progress (K. A. Thomson, 1985; personal communication).

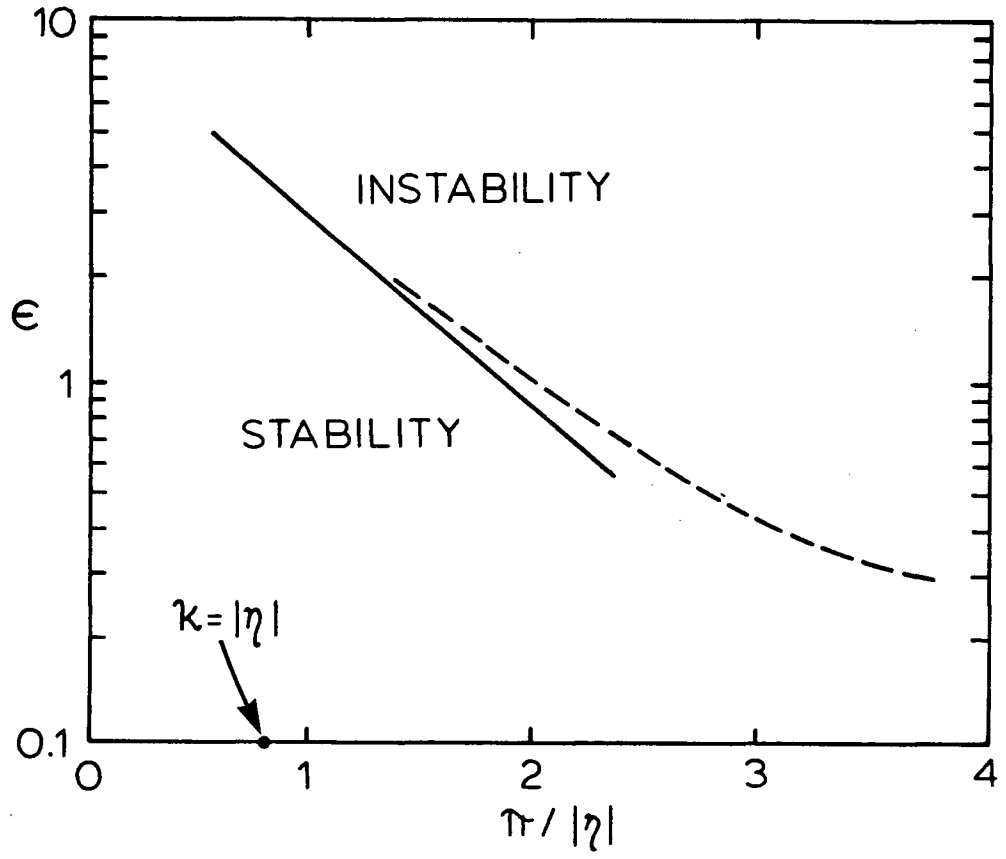

Figure 2. Stability regime diagram for an eastward-travelling modon. The vertical coordinate ϵ, is the area-averaged perturbation vorticity amplitude. The horizontal coordinate is scaled so that $|\eta| = \pi$ corresponds to a wavelength equalling one modon diameter (see Section 2.2). The solid line is the numerically determined neutral stability curve of McWilliams et al.(1981). The dashed line qualitatively illustrates the expected increasing slope in the neutral stability curve (cf. (2.10)) for $\pi/|\eta| >> \pi/\kappa \simeq 0.8$ under the assumption that when $|\eta| \simeq \kappa$ the two curves are similar.

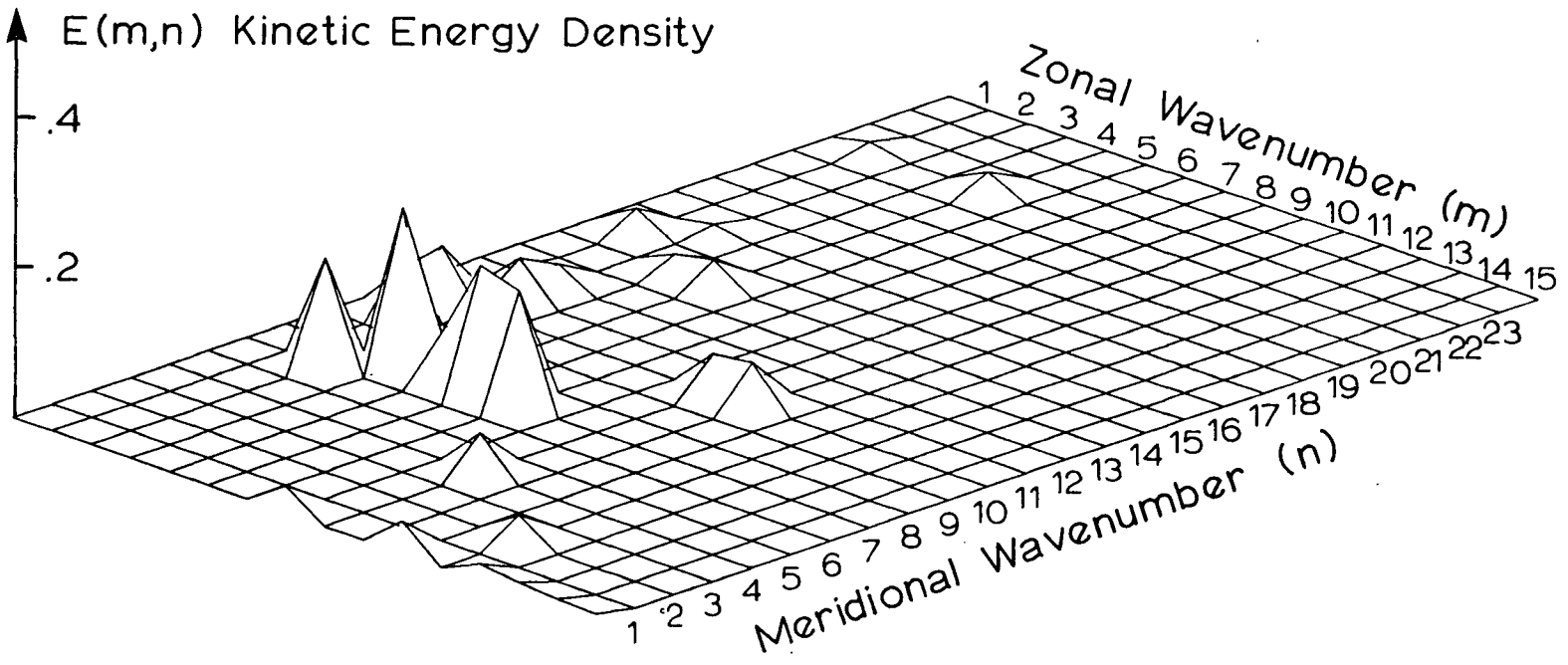

Figure 3. The two-dimensional atmospheric kinetic energy spectrum used to compute the LHS of (2.10) based on annually-averaged statistics. The zonal wavenumber m, is scaled so that m=1 corresponds to a wavelength equalling the circumference of a latitude circle. The (cartesian) meridional wave number n, is scaled so that n=1 corresponds to wavelength equalling the longitudinal circumference (i.e. geodesic circumference through the poles). The north-south wavenumber η_2 is related to n via η_2=an/R (see section 2.2). The energy density amplitude has been normalized so that $\int\int$ E(m,n) dndm = 1. The dominant contribution to the spectrum comes from m=1, 2, 3, 4, 5 and 6 and n=6, 7, 8 and 9, and accounts for 70% of the energy.

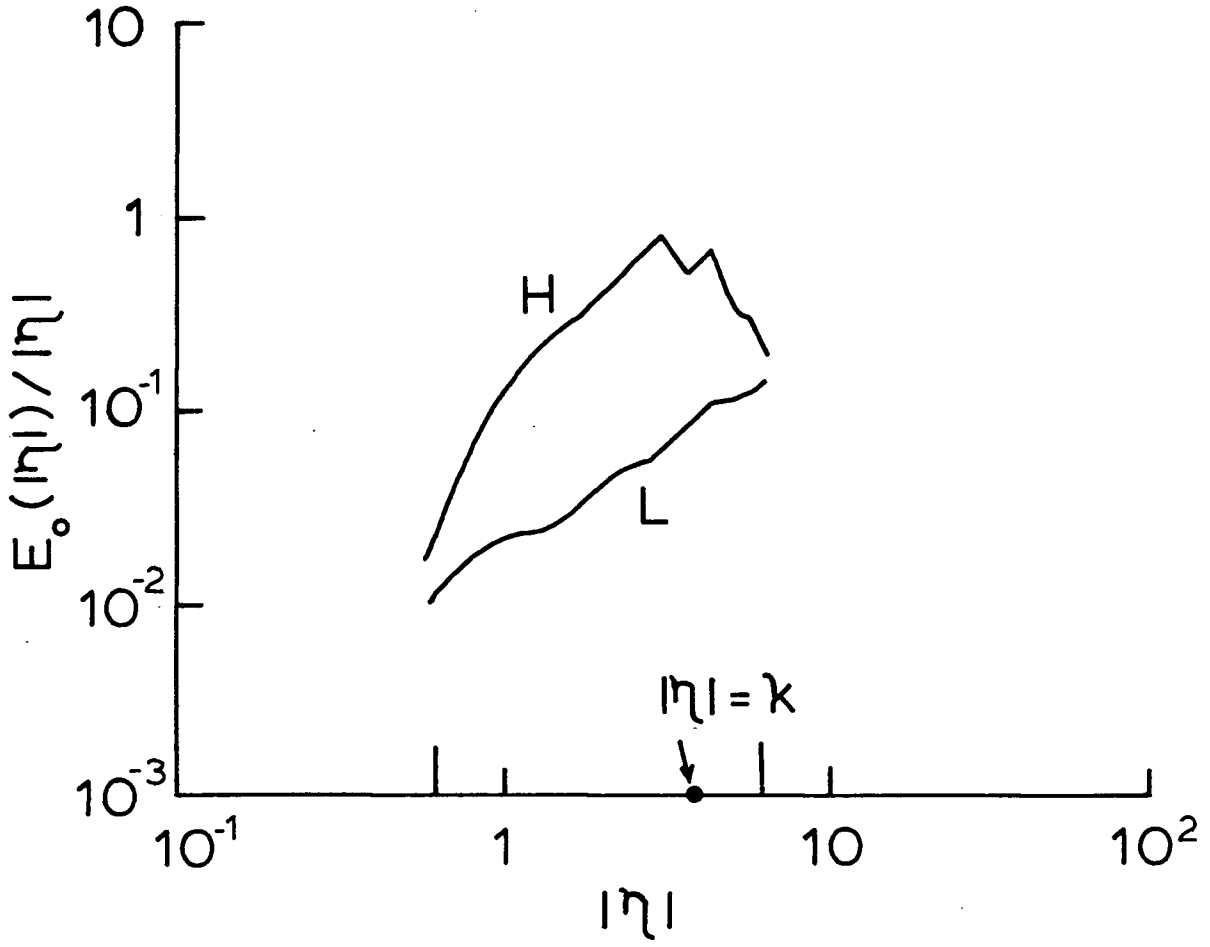

Figure 4. Scalar wavenumber spectrum of barotropic kinetic energy for the ocean used to compute the LHS of (2.13). The curve labelled H corresponds to data collected from high energy regions (eg. near major current systems). The curve labelled L corresponds to data collected from low energy regions (eg. away from major current systems). The two large vertical marks on the wavenumber axis correspond to 1000 km and 100 km from left to right, respectively. The point $|\eta|=\kappa$ is indicated with a dot on the wavenumber axis.

III. MODON PROPAGATION IN A SLOWLY VARYING MEDIUM

Whitham(1965) showed that the slow modulation of nonlinear waves in a dispersive medium could be described by the slow variation of the wave parameters (such as frequency, wavenumber and amplitude) within an averaged (over one wave period) Lagrangian formulation of the governing equations. Subsequent research developments in slowly varying nonlinear waves have generally tended to utilize perturbation methods (described below) or when possible an inverse scattering transformation (e.g., Kaup and Newell, 1978; and Karpman and Maslov 1979a,b). In this chapter a leading order perturbation theory is developed describing modon propagation in a slowly varying medium. The solutions presented here represent the first application of these methods to a fully two-dimensional solitary wave.

Two problems are posed and solved in this chapter. In Section 3.1 a perturbation method is developed to study the effect of an Ekman bottom boundary layer on an eastward-travelling modon. This problem was chosen in order that the analytical results obtained could be compared with a numerical solution for the same problem (McWilliams et al., 1981). (This provides a test for the perturbation method.) In Section 3.2 the perturbation method is used to describe the interaction between a barotropic modon and slowly varying topography.

Grimshaw(1970,1971) developed a perturbation method to describe the slow evolution of the Boussinesq solitary wave as it travels over slowly varying topography. Johnson(1973) and

Grimshaw(1977,1978,1979a,b,1981) developed similar perturbation theories to describe other slowly varying solitary waves in a variety of physical problems. Warn and Brasnett(1983) have applied these methods to model atmospheric blocking as the slow modulation of atmospheric solitons over variable topography.

In the usual fashion, the perturbation solution is obtained by introducing slow spatial and temporal variables (following Whitham, 1965 and Luke, 1966) reflecting the scaling of the slowly varying medium relative to a typical wavelength. The dependent variables and wave phase are expanded in a perturbation series in a small parameter characterizing the different scales associated with the wave and variable medium, with the O(1) solution taken to be the solitary wave.

In the Johnson and Grimshaw analysis, evolution equations for the wave parameters are determined by demanding that the coefficients of the inhomogeneities leading to higher order secularities vanish. Since these coefficients contain derivatives of the wave parameters with respect to the slow variables, differential equations are obtained describing the slow evolution of the solitary wave.

Luke(1966), Ablowitz(1971), Zakharov and Rubenchik(1974), Ko and Kuelh(1978), Ablowitz and Kodama(1979), Ablowitz and Segur(1981) and Kodama and Ablowitz(1980,1981) have developed an alternate perturbation method for describing various one-dimensional slowly varying solitary wave problems. The initial formulation of the two perturbation problems is identical; however, the differential equations describing the slow

modulation of the leading order wave parameters are obtained by exploiting a solvability condition on the first order perturbation equation.

The solvability condition is that the inhomogeneity in the perturbation equation be orthogonal to the homogeneous solution of the adjoint problem associated with the first order perturbation operator (i.e., the Fredholm alternative theorem). When the first order perturbation operator is self-adjoint, as in the nonlinear Klein-Gordon (Ablowitz, 1971), nonlinear Schroedinger and nonlinear sine-Gordon (Kodama and Ablowitz, 1980, 1981) equations, the two methods are formally the same. However, for the (regular and modified) Korteweg-de Vries (Kodama and Ablowitz, 1981), Kadomstev and Petviashvili (Ablowitz and Segur, 1981) and potential vorticity equations the perturbation operator is not self-adjoint.

In the Johnson and Grimshaw analysis the solution of the first order perturbation equations must be obtained in order to determine the secular terms. In the problem considered here this did not prove to be tractable. However, the homogeneous solution of the adjoint problem associated with the first order perturbation equations was easily seen to be the zeroth order solution. Thus the theory developed here follows the latter analysis.

3.1 Perturbation Solution For Modon Propagation Over A Bottom Ekman Boundary Layer

McWilliams et al.(1981) numerically calculated the effect of (linear, Newtonian and biharmonic) vorticity dissipation on an eastward-travelling modon and concluded that the decay was approximately exponential and shape preserving. The modon parameters (i.e., the radius, translation speed and wavenumber) evolved (to a first approximation) in such a manner as to preserve the modon dispersion relationship. In the final stages of the dissipation the modon degenerated into a field of westward-travelling planar Rossby waves. These observations suggest that the dissipation of a modon due to bottom friction can be theoretically viewed in the context of the slow evolution of solitary waves.

This Section describes a theory for analytically obtaining the leading order solution of an eastward-travelling modon in the presence of a bottom boundary layer. The solution we obtain agrees with the numerical calculation of McWilliams et al.(1981) for the dissipation of a modon although it is unable to describe the transition to westward-travelling Rossby waves in the final stages of the decay.

For typical oceanic and atmospheric modon scales (decribed in Subsection 3.1.1) the effect of bottom friction is an order of magnitude smaller than the inertial and dispersive terms in the potential vorticity equation. Thus the dissipation of a barotropic modon when the effects of a bottom Ekman layer are

included in the vorticity equation can be described by a slowly varying solitary wave calculation. The parameters which describe the modon solitary wave are allowed to be functions of a slow time and the solvability condition leads to initial-value problems for the leading order translation speed, radius and wavenumber. The method developed in this Section is used to describe modon propagation over slowly varying topography in Section 3.2.

3.1.1 Formulation And Solution Of The Dissipation Problem

The nondimensional barotropic potential vorticity equation in which the interior of the fluid is asymptotically matched to a bottom Ekman boundary layer is (Pedlosky, 1979)

$$\Delta\psi_t + J(\psi, \Delta\psi + \delta^2 y) = -\epsilon\Delta\psi \qquad (3.1.1)$$

where ψ is the geostrophic pressure field, $J(*,\cdot)$ is the Jacobian determinant $\partial(*,\cdot)/\partial(x,y)$ with x, y and t the usual (positive) eastward, (positive) northward and time coordinates and where Δ is the horizontal Laplacian. The parameters $\delta^2 = \beta a_0^2/c_0$ and $\epsilon = E^{1/2}/(2r_0)$ are the planetary vorticity factor and damping coefficient respectively, with E the vertical Ekman number $2\nu f^{-1}H^{-1}$ where ν, f and H are the vertical eddy viscosity, Coriolis parameter and fluid depth respectively, and where r_0 is the Rossby number $c_0 f^{-1}(a_0)^{-1}$ with a_0 and c_0 the undamped modon radius and translation speed respectively. The

space, time and velocity scalings have been chosen as a_0, a_0/c_0 and c_0 respectively. For typical oceanic (atmospheric) modon parameter values of β, a_0, c_0, ν, H and f of $1.6 \cdot 10^{-11}$ $m^{-1}s^{-1}$, 100 (1000) km, 10^{-1} (10) ms^{-1}, 10^{-2} (10) m^2s^{-1}, 4 (10) km and 10^{-4} s^{-1} respectively, it follows that $\epsilon \simeq 10^{-1}$. Thus for modon scales the RHS of (3.1.1) can be viewed as a small perturbation. The values of a_0 and c_0 were chosen to give an order unity planetary vorticity factor while satisfying quasigeostrophy. Equation (3.1.1) does not include the free surface effect, since for oceanic applications the length scale a_0 is much smaller than the external deformation radius $(gH/f)^{1/2} \simeq 2000$ km.

For a leading order solution the fast variables (Ko and Kuehl(1978), Grimshaw(1979,1981) and Kodama and Ablowitz(1981)) are given by

$$\xi = x - \epsilon^{-1} \int_0^T c(t')dt'$$

$$y = y$$

and a slow time is given by

$$T = \epsilon t.$$

Thus $\xi_t = -c(T)$ and $\xi_x = 1$. Substitution of these variables into (3.1.1) gives

$$J(\psi + cy,\ \Delta\psi + \delta^2 y) = -\epsilon\Delta\psi - \epsilon\Delta\psi_T \qquad (3.1.2)$$

where the Jacobian is taken with respect to ξ and y.

As in Grimshaw(1979a,b,1981) and Kodama and Ablowitz(1981) a perturbation solution to (3.1.2) is constructed in the form

$$\psi \simeq \psi^{(0)}(\xi,y;T) + \epsilon\psi^{(1)}(\xi,y;T) + \ldots .$$

The 0(1) problem is

$$J(\psi^{(0)} + cy,\ \Delta\psi^{(0)} + \delta^2 y) = 0,$$

the solution of which is taken to be the modon (Flierl et al., 1980)

$$\psi^{(0)} = -caK_1(\delta c^{-1/2} r)\sin(\theta)/K_1(\delta a c^{-1/2})$$

$$\Delta\psi^{(0)} = -\delta^2 aK_1(\delta c^{-1/2} r)\sin(\theta)/K_1(\delta a c^{-1/2})$$

$$\Delta\psi^{(0)} = (\delta^2/c)\psi^{(0)} \qquad r>a \qquad (3.1.3)$$

$$\psi^{(0)} = \delta^2\kappa^{-2} aJ_1(\kappa r)\sin(\theta)/J_1(\kappa a) - (\delta^2 + \kappa^2 c)\kappa^{-2} r\sin(\theta)$$

$$\Delta\psi^{(0)} = -\delta^2 aJ_1(\kappa r)\sin(\theta)/J_1(\kappa a)$$

$$\Delta\psi^{(0)} = -\kappa^2\psi^{(0)} - (\delta^2 + c\kappa^2)r\sin(\theta) \qquad r<a \qquad (3.1.4)$$

where J_1 and K_1 are the ordinary and modified Bessel functions of order one, with the polar coordinates r and θ defined by $r^2 = [\xi-\xi_0(T)]^2 + y^2$ and $\tan(\theta) = y/[\xi-\xi_0(T)]$.

The term $\xi_0(T)$ is an $0(\epsilon)$ phase shift (in comparison to the leading order phase ξ) and is determined by first order perturbation energy considerations (Ko and Kuelh, 1978, Grimshaw, 1979a,b and Kodama and Ablowitz, 1981). For the 0(1) analysis presented here it remains undetermined and is eventually chosen as a constant (the x-coordinate of the wave center at T=0). It is formally included as a slowly varying quantity at this stage because it appears in the $0(\epsilon)$ equations. The modon wavenumber κ in (3.1.4) is the first nonzero solution of the dispersion relation (obtained by requiring continuity of $\nabla\psi^{(0)}$ on r=a)

$$-\delta J_2(\kappa a)K_1(\delta a c^{-1/2}) = c^{1/2}\kappa J_1(\kappa a)K_2(\delta a c^{-1/2}). \qquad (3.1.5)$$

The modon radius, translation speed and wavenumber a, c and κ respectively, are allowed to be functions of the slow time (following the general theory of Grimshaw, 1979, Kodama and Ablowitz, 1981 and Ablowitz and Segur, 1981) with the initial conditions a(0)=1, c(0)=1 and $\kappa(0)=\kappa_0$ where κ_0 solves the modon dispersion relation for a=c=1 (κ_0 = 3.9226, based on δ=1).

The $0(\epsilon)$ problem associated with (3.1.2) is

$$J(\psi^{(0)} + cy, \Delta\psi^{(1)}) +$$

$$J(\psi^{(1)}, \Delta\psi^{(0)} + \delta^2 y) = -\Delta\psi^{(0)} - \Delta\psi^{(0)}_T,$$

which for r>a can be rewritten as (see (3.1.3))

$$J(\psi^{(0)} + cy, \Delta\psi^{(1)} - \delta^2 c^{-1}\psi^{(1)}) = -\Delta\psi^{(0)} - \Delta\psi^{(0)}_T. \qquad (3.1.6)$$

The homogeneous adjoint equation associated with (3.1.6) is

$$(\Delta - \delta^2 c^{-1})J(\psi^{(0)} + cy, u) = 0$$

for which $u = \psi^{(0)}(r>a)$ is a solution. The solvability condition on $\psi^{(0)}$ for r>a is therefore (see the Luke and Ablowitz citations given above)

$$\int_{-\pi}^{\pi}\int_{a}^{\infty} \psi^{(0)}(\Delta\psi^{(0)} + \Delta\psi^{(0)}_T)\, r dr d\theta = 0. \qquad (3.1.7)$$

The $0(\epsilon)$ problem for r<a can be written as (see (3.1.4))

$$J(\psi^{(0)} + cy, \Delta\psi^{(1)} + \kappa^2\psi^{(1)}) = -\Delta\psi^{(0)} - \Delta\psi^{(0)}_T, \qquad (3.1.8)$$

with the related homogeneous adjoint equation

$$(\Delta + \kappa^2)J(\psi^{(0)} + cy, u) = 0$$

for which $u = \psi^{(0)}(r<a)$ is a solution. The solvability

condition on $\psi^{(0)}$ for r<a is therefore

$$\int_{-\pi}^{\pi}\int_{0}^{a} \psi^{(0)}(\Delta\psi^{(0)} + \Delta\psi^{(0)}_{T})\, r dr d\theta = 0. \qquad (3.1.9)$$

It is noted here that

$$\Delta\psi^{(0)}_{T} = \{ a^{-1}a_{T} - [DK_1(\delta a c^{-1/2})/K_1(\delta a c^{-1/2})]\delta a c^{-1/2}[a^{-1}a_{T} - (2c)^{-1}c_{T}]\}\Delta\psi^{(0)} + c^{1/2}(rc^{-1/2})_{T}\,\Delta\psi^{(0)}_{r} - \cos(\theta)\xi_{0T}\,\Delta\psi^{(0)}_{r} + r^{-1}\sin(\theta)\xi_{0T}\,\Delta\psi^{(0)}_{\theta}, \quad r>a$$

$$\Delta\psi^{(0)}_{T} = \{ a^{-1}a_{T} - [DJ_1(\kappa a)/J_1(\kappa a)]\kappa a[a^{-1}a_{T} + \kappa^{-1}\kappa_{T}]\}\Delta\psi^{(0)} + \kappa^{-1}(\kappa r)_{T}\,\Delta\psi^{(0)}_{r} - \cos(\theta)\xi_{0T}\,\Delta\psi^{(0)}_{r} + r^{-1}\sin(\theta)\xi_{0T}\,\Delta\psi^{(0)}_{\theta}, \quad r<a$$

where $DK_1(\delta a c^{-1/2})$ and $DJ_1(\kappa a)$ are the derivatives of $K_1(\delta a c^{-1/2})$ and $J_1(\kappa a)$ with respect to their arguments $\delta a c^{-1/2}$ and κa, respectively. The fast variable r is retained in the terms $(rc^{-1/2})_{T}$ and $(\kappa r)_{T}$ because of the slowly varying a(T) in the integration limits in (3.1.7) and (3.1.9). Note that the last two terms in both equations express the slow evolution of the phase shift term. It turns out that these terms integrate to zero in the solvability conditions due to the periodicity in θ.

After some algebra it can be shown that (3.1.7) and (3.1.9) imply respectively

$$A\, a^{-1} a_T - [A - 1]\, (2c)^{-1} c_T = -1 \qquad (3.1.10)$$

$$B\, a^{-1} a_T + [B - 1]\, \kappa^{-1} \kappa_T = -1 \qquad (3.1.11)$$

where

$$A = \gamma K_2(\gamma)/K_1(\gamma) - 1 - K_1^2(\gamma)/D_1$$

$$D_1 = -\gamma^{-1}\{\gamma K_1^2(\gamma) - 2K_0(\gamma)K_1(\gamma) - \gamma K_0^2(\gamma)\}$$

$$B = 1 - \{kJ_0(k)D_2/J_1^3(k) -$$

$$2(kJ_0(k)/J_1(k) + 2)(1 + k^2\gamma^{-2})J_2(k)/(kJ_1(k)) + 1 + 2k^2\gamma^{-2}\}/$$

$$\{D_2/J_1^2(\gamma) - 2(1 + k^2\gamma^{-2})J_2(k)/(kJ_1(k))\}$$

$$D_2 = k^{-1}\{kJ_2^2(k) - 2J_2(k)J_1(k) + kJ_1^2(k)\}$$

where

$$\gamma = (\delta^2 a^2/c)^{1/2} \qquad k = \kappa a.$$

Equations (3.1.10) and (3.1.11) are two eqautions in three unknowns. A third equation is obtained by differentiating (3.1.5) with respect to T yielding

$$\kappa^{-1}\kappa_T = N[a^{-1}a_T - (2c)^{-1}c_T] - (2c)^{-1}c_T \qquad (3.1.12)$$

where $N = -\{\gamma R + k^2R/\gamma\}/\{4 + \gamma/R + k^2R/\gamma\}$ and $R=K_2(\gamma)/K_1(\gamma)$. Eliminating $\kappa^{-1}\kappa_T$ between (3.1.11) and (3.1.12) gives

$$M\, a^{-1}a_T - [M - 1]\,(2c)^{-1}c_T = -1 \qquad (3.1.13)$$

where $M = BN+B-N$. Provided $M\neq A$ the unique solutions (3.1.10), (3.1.11) and (3.1.13) are easily seen to be

$$a_T = -a \qquad c_T = -2c \qquad \kappa_T = \kappa \quad \text{i.e.,}$$

$$a = \exp(-\epsilon t) \qquad c = \exp(-2\epsilon t) \qquad \kappa = \kappa_0\exp(\epsilon t). \qquad (3.1.14)$$

The solutions (3.1.14) are the principal result of our calculation in this Section. Concomitant with the intuitive expectation that the RHS of (3.1.3) must result in a exponential-like decay in the modon, (3.1.14) implies that the vorticity and streamfunction amplitudes decay as exp(-T) and exp(-3T) respectively.

The exponential decay that the solutions (3.1.14) predict can be seen as the result of the energy and enstrophy equations associated with (3.1.1). It follows from (3.1.1) that

$$\partial_t \int_{-\pi}^{\pi}\int_0^{\infty} \nabla\psi\cdot\nabla\psi \; r\,dr\,d\theta = -2\epsilon \int_{-\pi}^{\pi}\int_0^{\infty} \nabla\psi\cdot\nabla\psi \; r\,dr\,d\theta$$

$$\partial_t \int_{-\pi}^{\pi}\int_{0}^{\infty} |\Delta\psi|^2 \, r dr d\theta = -2\epsilon \int_{-\pi}^{\pi}\int_{0}^{\infty} |\Delta\psi|^2 \, r dr d\theta.$$

Thus the spatially integrated energy and vorticity equations predict exponential decay as implied by (3.1.14).

The solutions (3.1.14) appear non-unique when M=A, since when this occurs there are only two independent equations for three unknowns (i.e., (3.1.10) and (3.1.13) are identical). However, numerical calculations showed that γ=5.776 and k=4.4835 were the only values which could satisfy the dispersion relation (3.1.5) and M=A(=.5073). The following argument shows that the discreteness of these values and the continuity of a, c and κ imply the uniqueness of (3.1.14) irrespective of A and M.

Suppose A=M at $T=\tau$ and there exist solutions a, c and κ such that $\gamma_T(T=\tau)\neq 0$ (recall $\gamma^2=\delta^2 a^2/c$; the proof works equally well exploiting $k=\kappa a$). It follows that there exists $\alpha>0$ for which $\gamma(T)\neq\gamma(\tau)$ for the interval $\tau<T<\tau+\alpha$. Hence M≠A in this interval and thus (3.1.14) are the solutions in this interval. Suppose the same hypotheses but that $\gamma_T(T=\tau)=0$. But then either $\gamma_T=0$ in some nonzero interval $(\tau,\tau+\alpha)$ or not. If not, the previous result applies on this interval. If true, from the definition of γ and from (3.1.10) and (3.1.11) it follows $a_T^{-1}a_T = (2c)_T^{-1}c_T = -\kappa_T^{-1}\kappa_T = -1$ are the solutions on this interval. However τ is arbitrary so the proof is complete.

3.1.2 Discussion Of The Dissipation Solution

The solutions for a, c and κ satisfy $(\kappa a)_T = 0$, $(ac^{-1/2})_T = 0$ and $(\kappa c^{1/2})_T = 0$. Therefore (3.1.5) reduces to

$$-\delta J_2(\kappa_0)K_1(\delta) = \kappa_0 J_1(\kappa_0)K_2(\delta)$$

for all T implying that the dispersion relationship is invariant during the decay. Thus the modon remains dynamically equivalent to its initial state, at least initially and to 0(1), as any WKB-like theory must predict. The exponential decay of the streamfunction and vorticity and the invariance of the dispersion relation which we have obtained is in agreement with the numerical solution of (3.1.1) (McWilliams et al., 1981) for a modon initial state.

The compatibility conditions (3.1.7) and (3.1.9) are in fact sufficient to eliminate the secularity in $\psi^{(1)}$ (note that $\Delta\psi^{(0)}$ is a homogeneous solution to (3.1.6) and (3.1.8)) since $\Delta\psi^{(0)} + \Delta\psi^{(0)}_T$ is indentically zero as a consequence of (3.1.14) (introduce the change of variable $r \rightarrow a(T)r$ in (3.1.3) and (3.1.4)).

Figure 5 is a sequence of contour plots of the pathlines $\psi^{(0)} + c(T)y$ as T increases. The observer is in the reference frame of the modon so that as dissipation occurs the surrounding fluid appears to slow down, as indicated by the increasing separation of the contours. Figure 6 is a sequence of contour plots showing the decay in the vorticity field as T increases.

The observer is fixed with respect to the fluid at infinity. The modon moves to the right with speed c(T).

An upper bound on the distance over which the dissipating modon travels as a modon can be obtained from the characteristic equation

$$dx/dt = c(T)$$

which integrates to

$$x(t) = \xi_0 + (1 - \exp(-2\epsilon t))/(2\epsilon)$$

so that the modon travels a maximum distance $(2\epsilon)^{-1}$ (about 5 modon radii) before breaking up into a field of Rossby waves.

McWilliams et al.(1981) estimate that for $t < 15$ the modon decays as a modon (based on similar parameter values for δ^2 and r) and when $t \simeq 15$ a modon Rossby wave transition occurs. Based on the scaling in this Section, the transition takes place when $T \simeq 1.5$ (note that Figure 5 only goes up to T=1.39). At this stage the amplitudes of $\psi^{(0)}$ and $\Delta\psi^{(0)}$ are very small (see Figures 5 and 6) and thus the above solution qualitatively describes the principal decay mechanism. For oceanic scales of a_0 and c_0 of 100 km and 0.1 m s^{-1} respectively the above perturbation solution will be asymptotically valid for a time scale of 100 days, whereas for atmospheric scales of a_0 and c_0 of 1000 km and 10 m s^{-1}, respectively (see McWilliams, 1980) the perturbation solution will be asymptotically valid on a time

scale of 10 days.

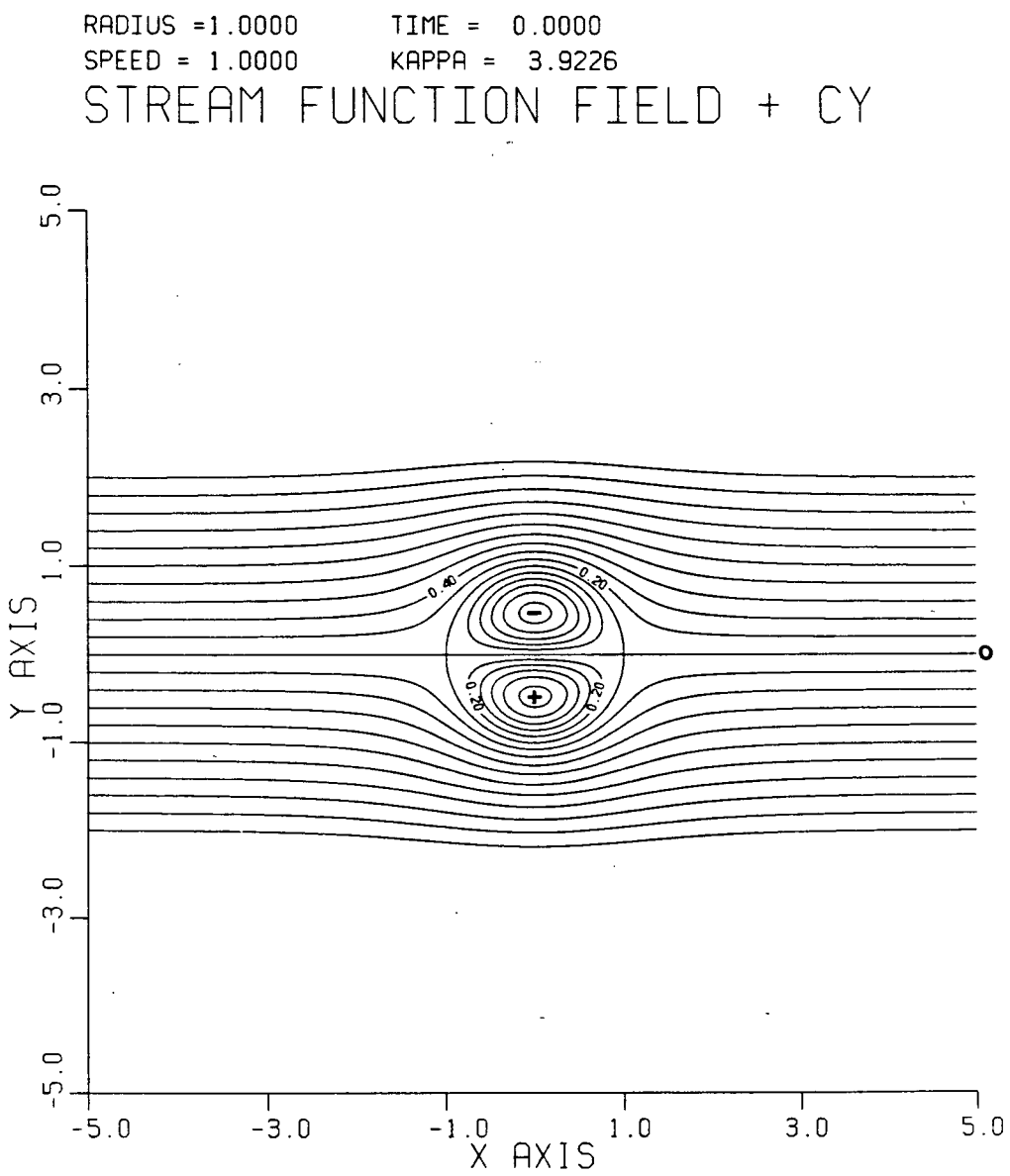

Figure 5a. Sequence of contour plots of the pathlines $\psi^{(0)}$ + c(T)y for the Ekman dissipation problem. The observer is fixed with respect to a coordinate system attached to the modon. The contour intervals are ±0.2. The zero contour is marked with a 0. The values of a, c and κ at each slow time T are listed in the upper left hand corner.

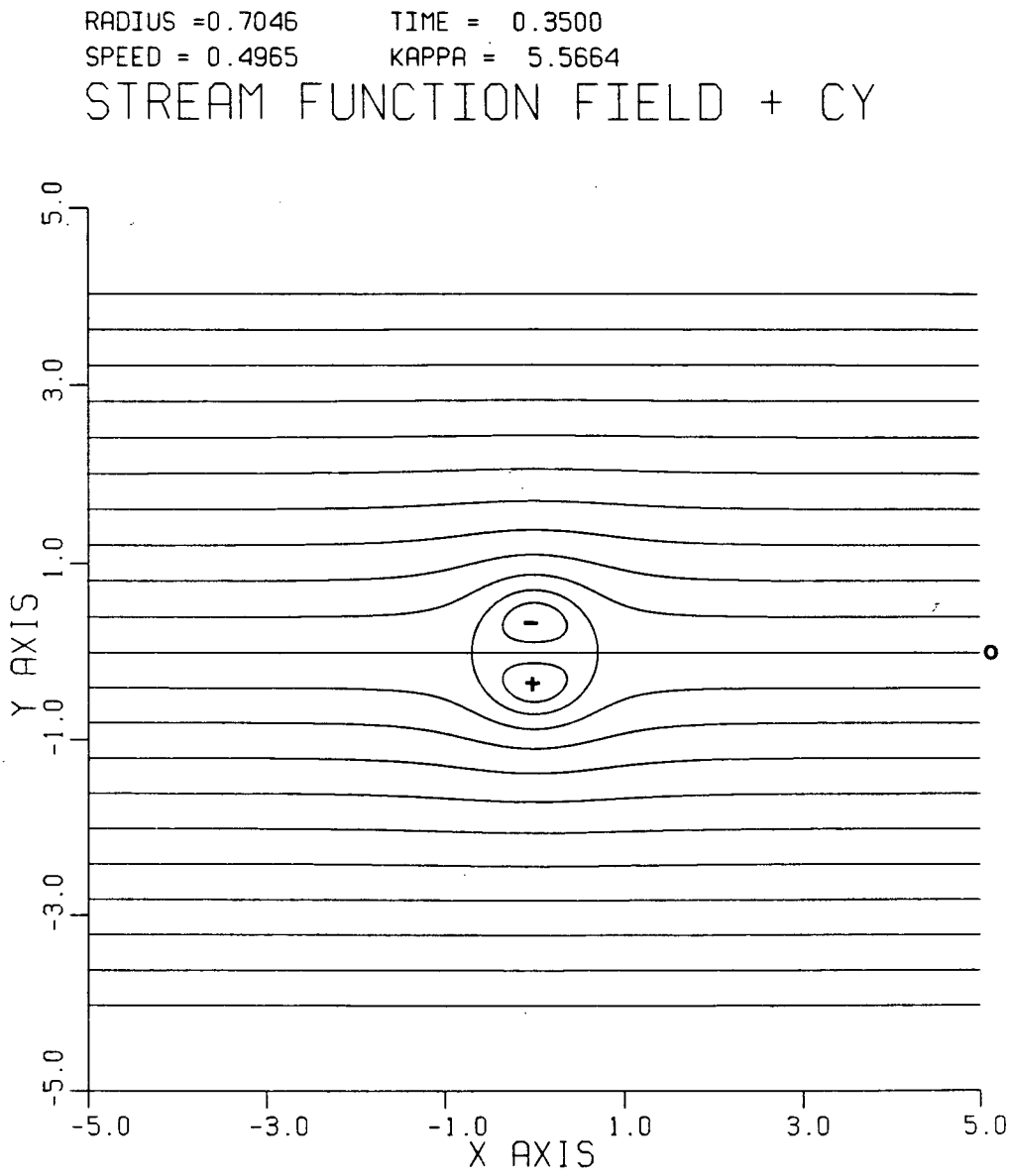

Figure 5b. Modon pathlines at T=0.35 under Ekman dissipation.

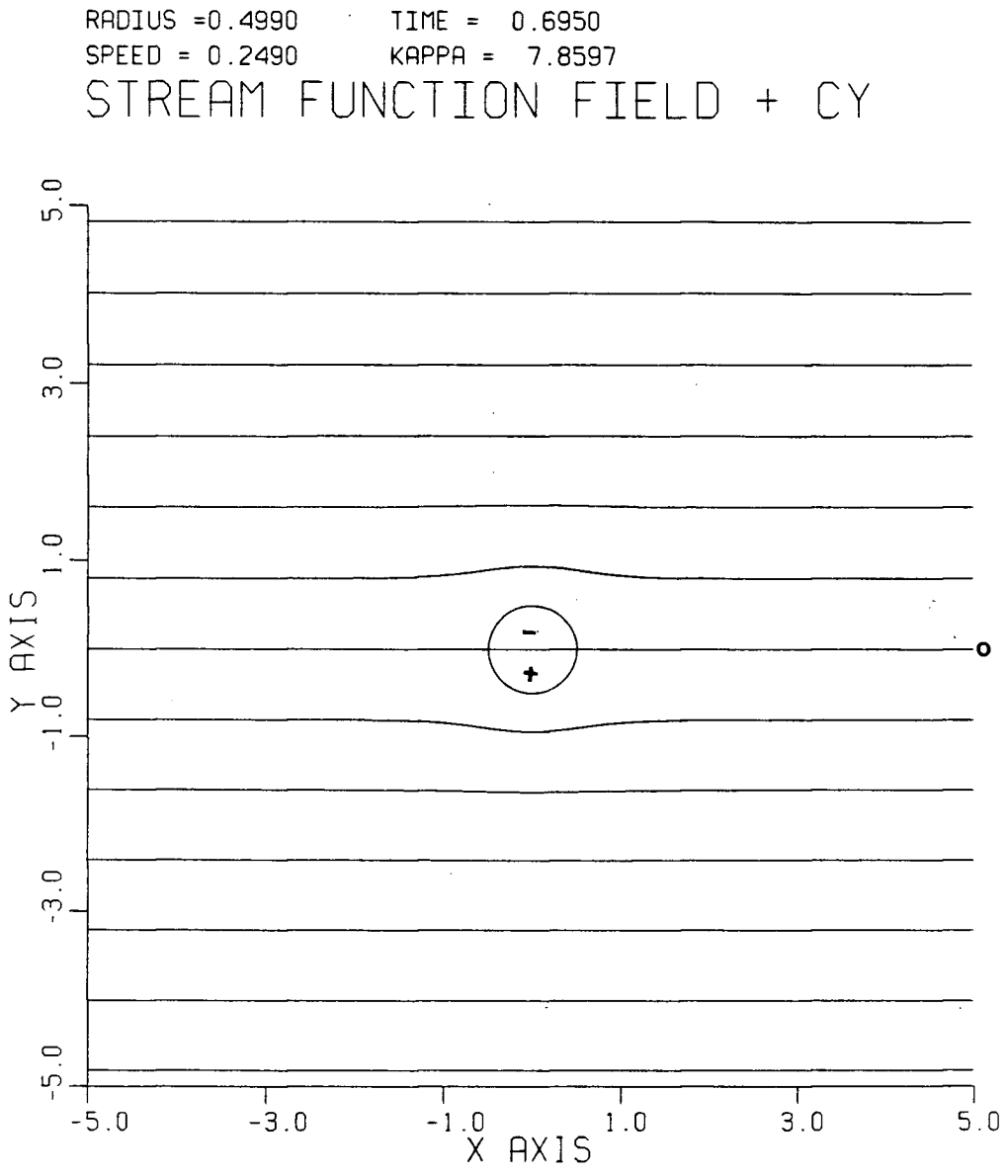

Figure 5c. Modon pathlines at T=0.695 under Ekman dissipation.

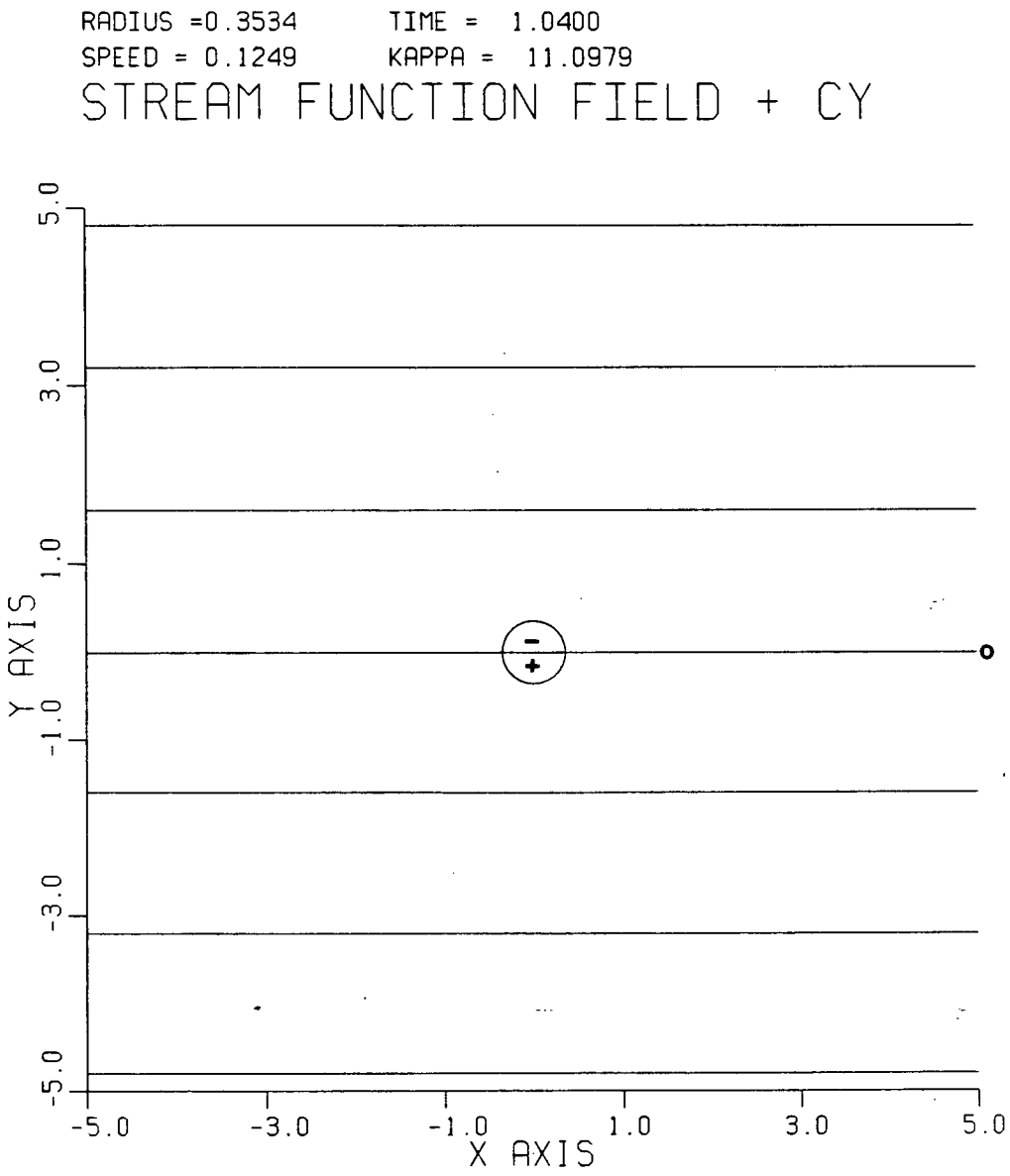

Figure 5d. Modon pathlines at T=1.04 under Ekman dissipation.

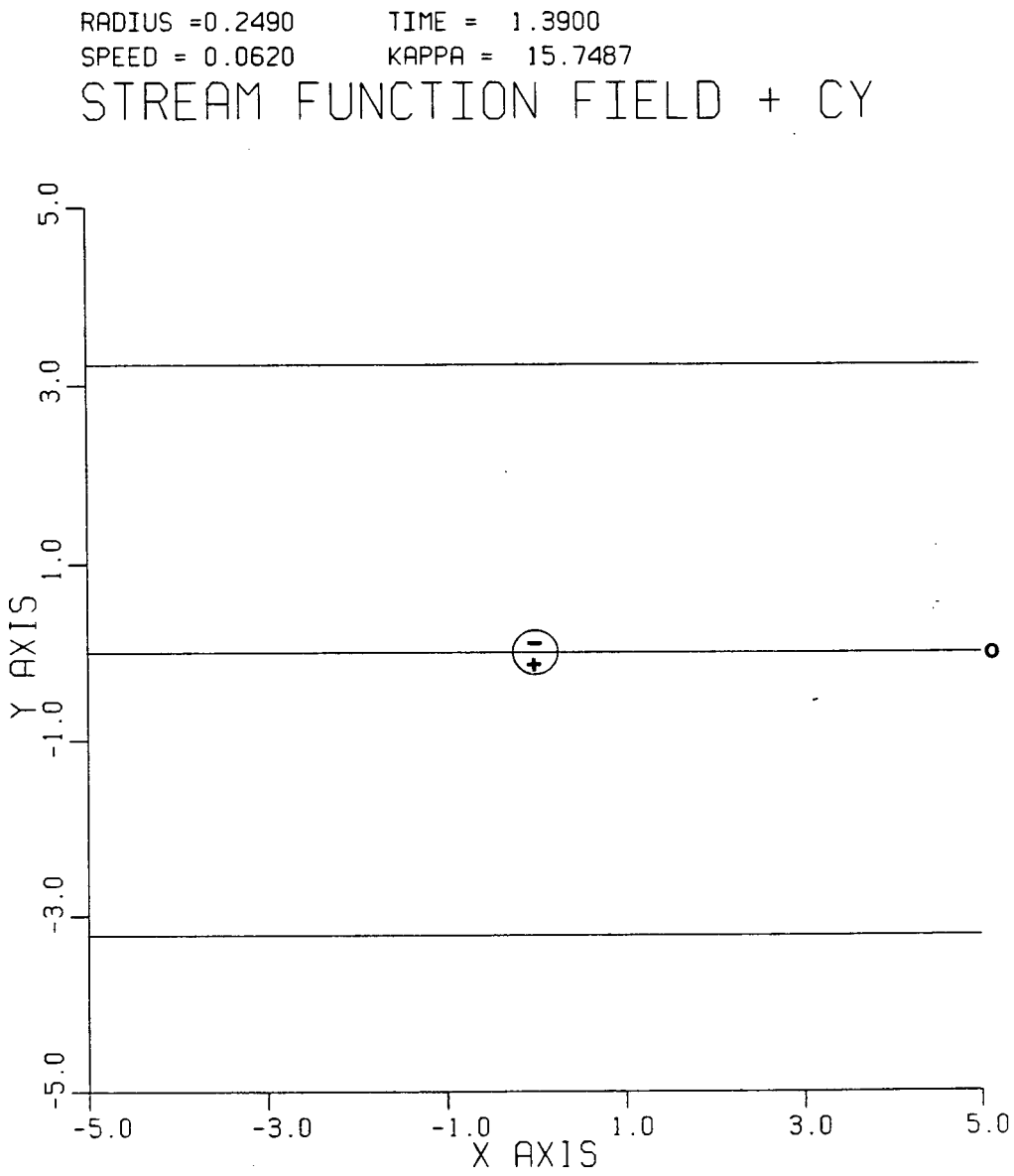

Figure 5e. Modon pathlines at T=1.39 under Ekman dissipation.

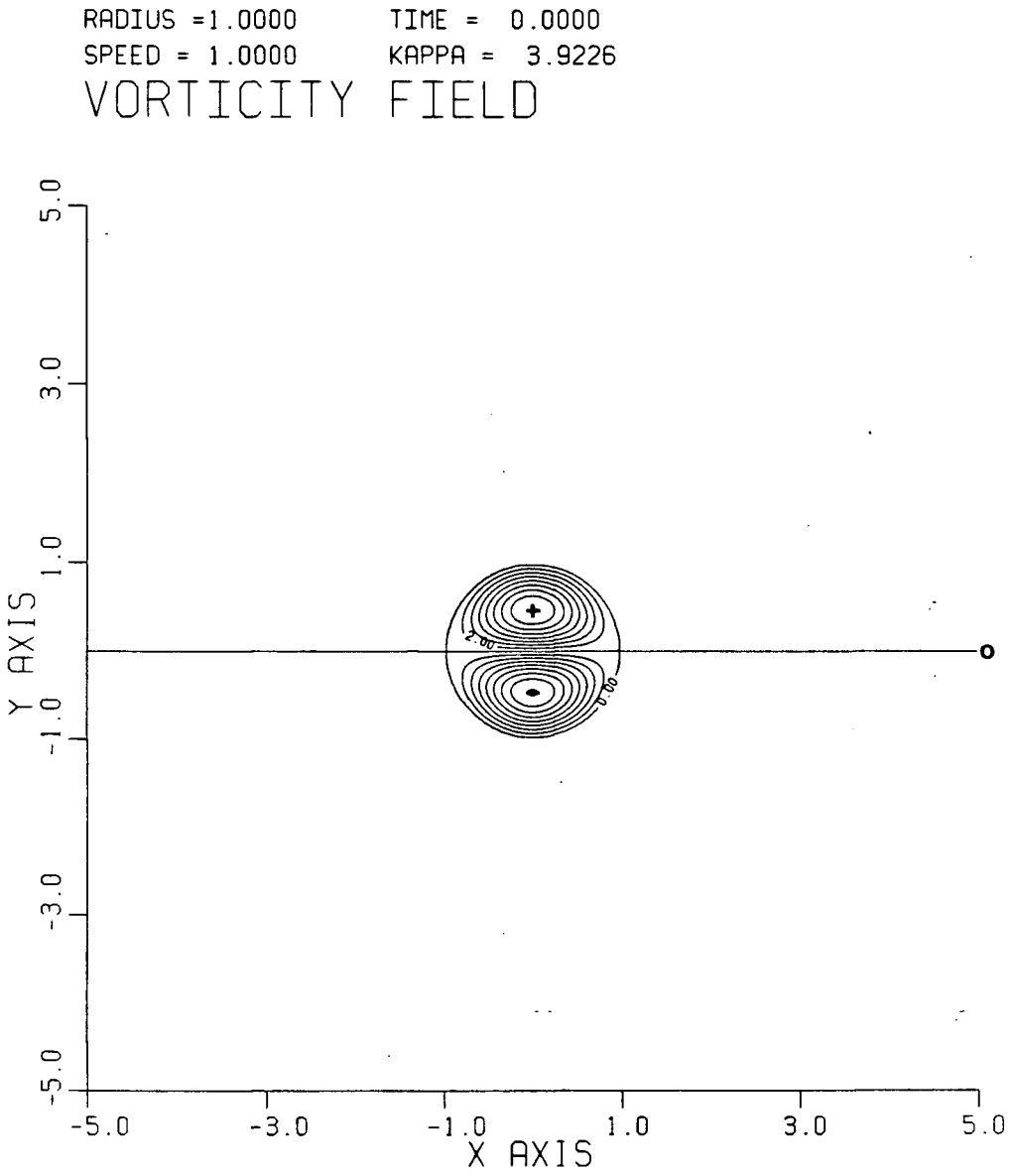

Figure 6a. Sequence of contour plots of the vorticity $\Delta\psi^{(0)}$ for the Ekman dissipation problem. The observer is fixed with respect to the fluid at infinity. The contour intervals are ±2.0. The zero contour is marked with a 0. The values of a, c and κ at each slow time T are listed in the upper left hand corner.

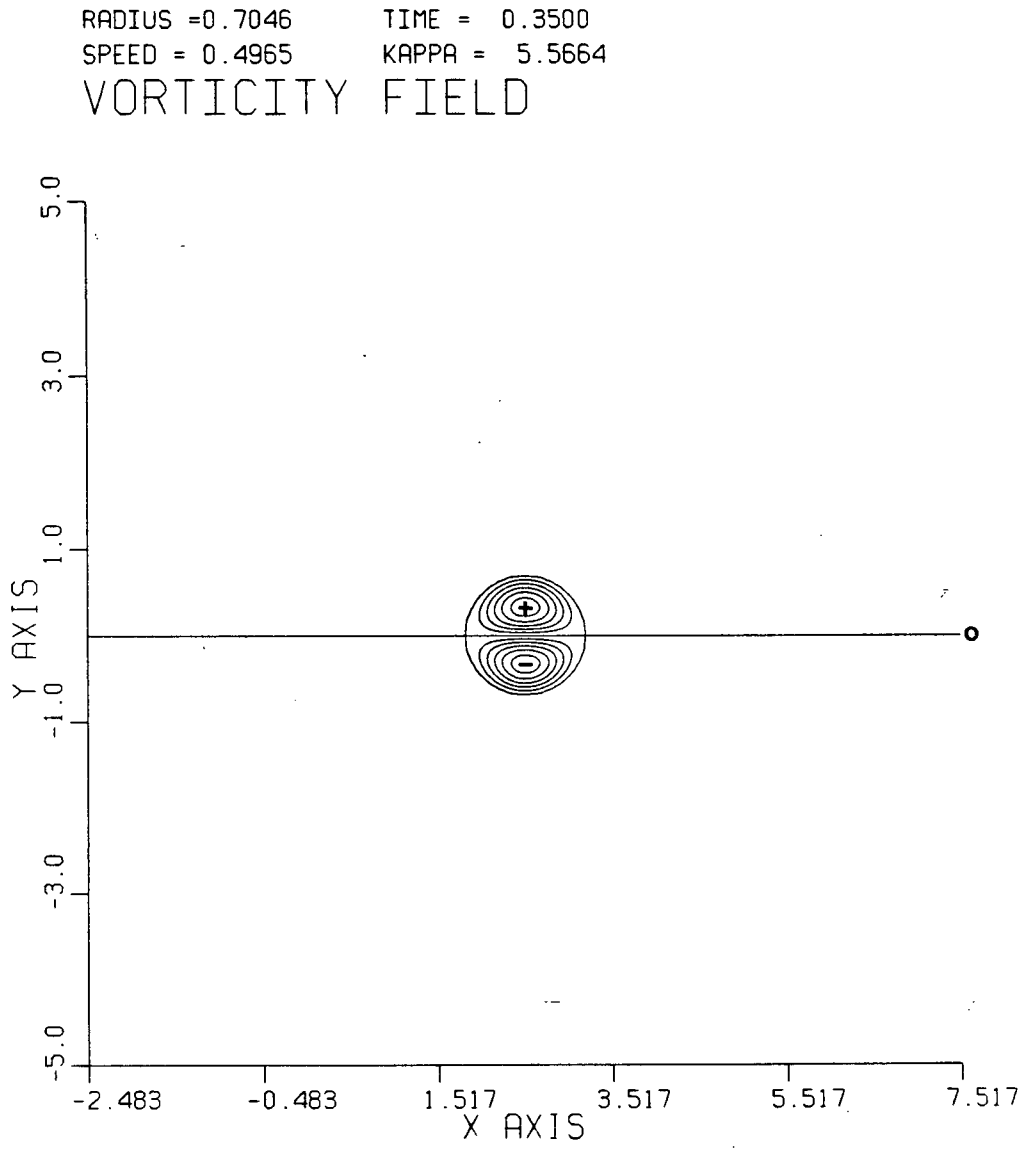

Figure 6b. Modon vorticity at T=0.35 under Ekman dissipation.

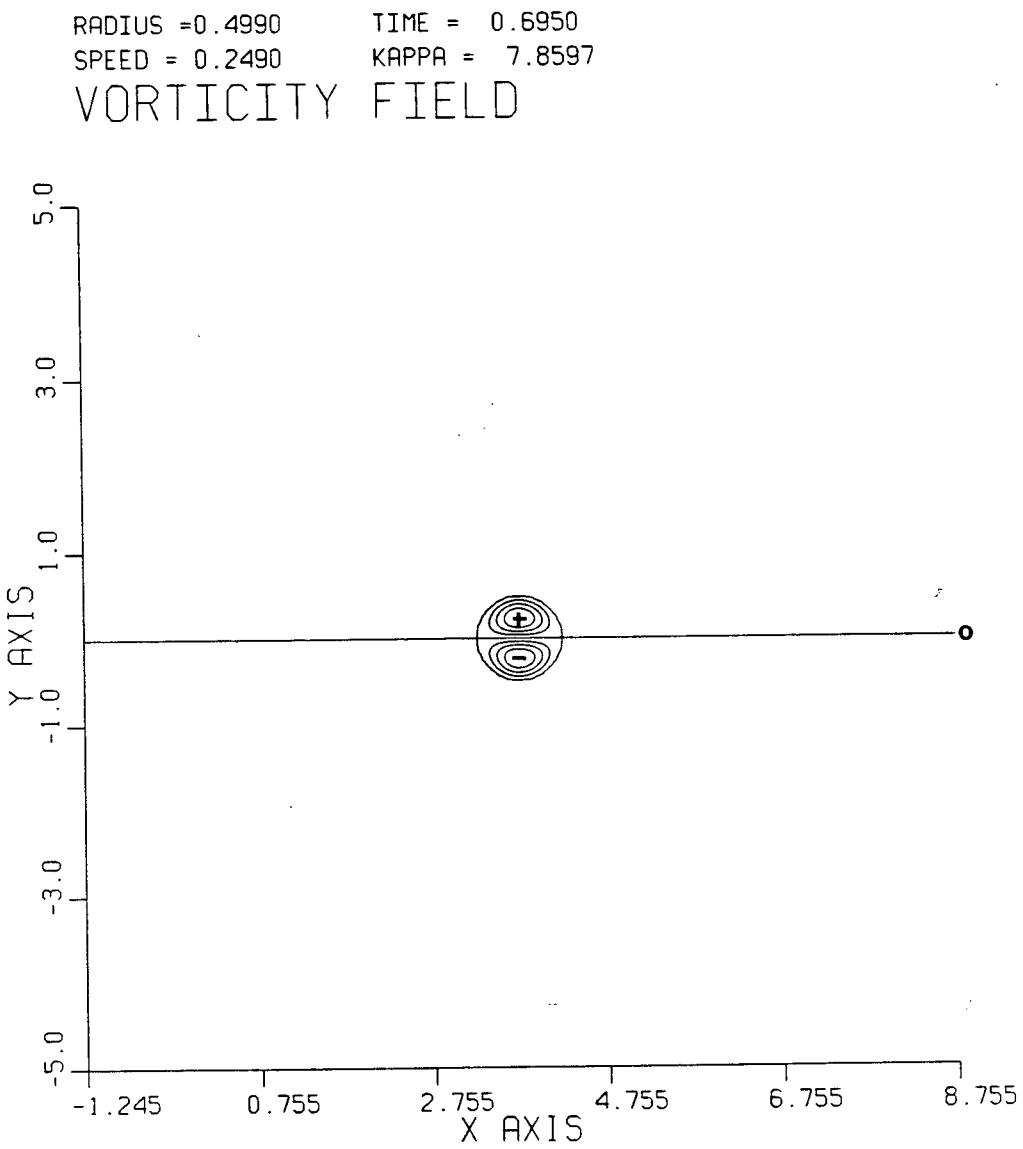

Figure 6c. Modon vorticity at T=0.695 under Ekman dissipation.

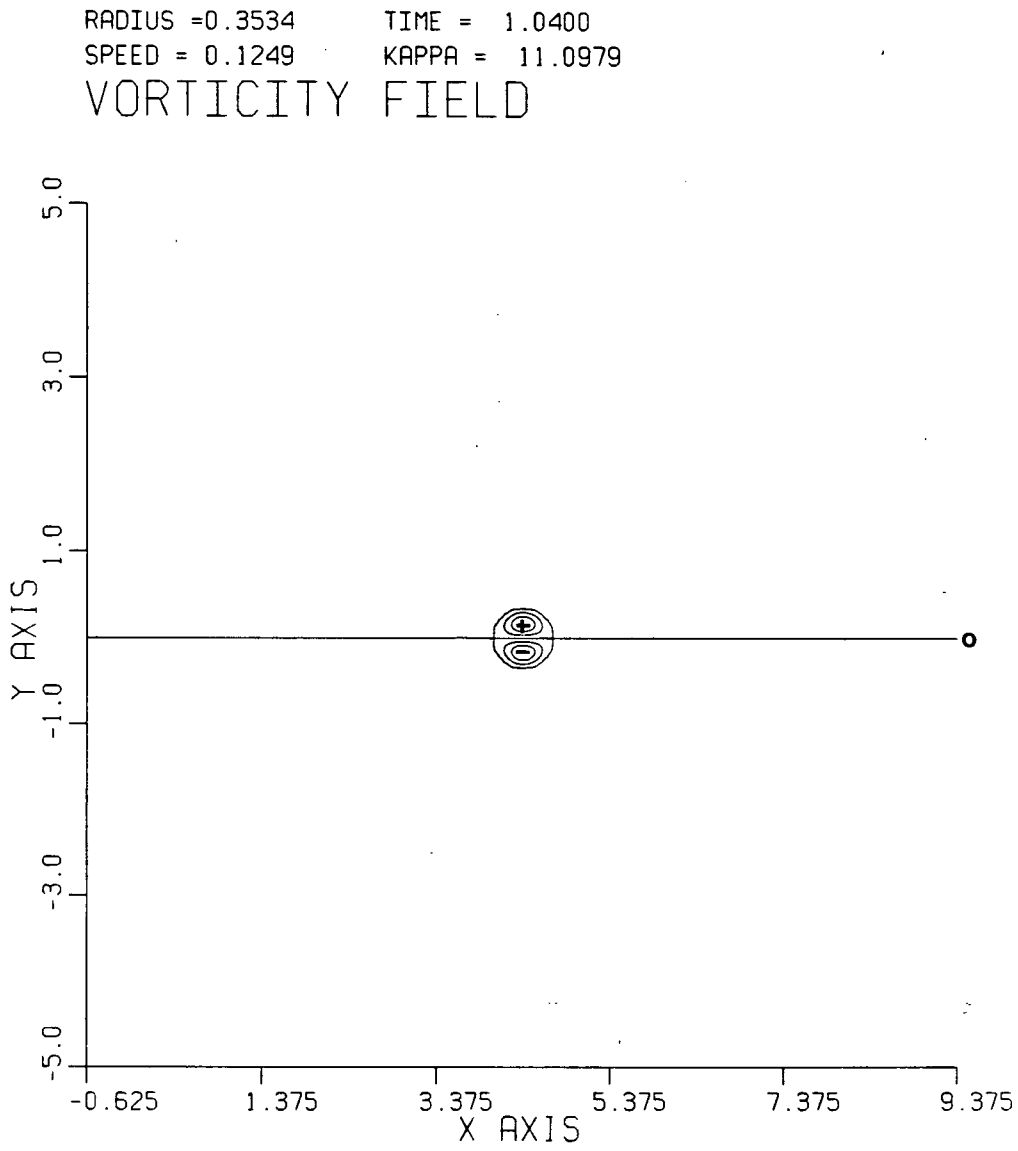

Figure 6d. Modon vorticity at T=1.04 under Ekman dissipation.

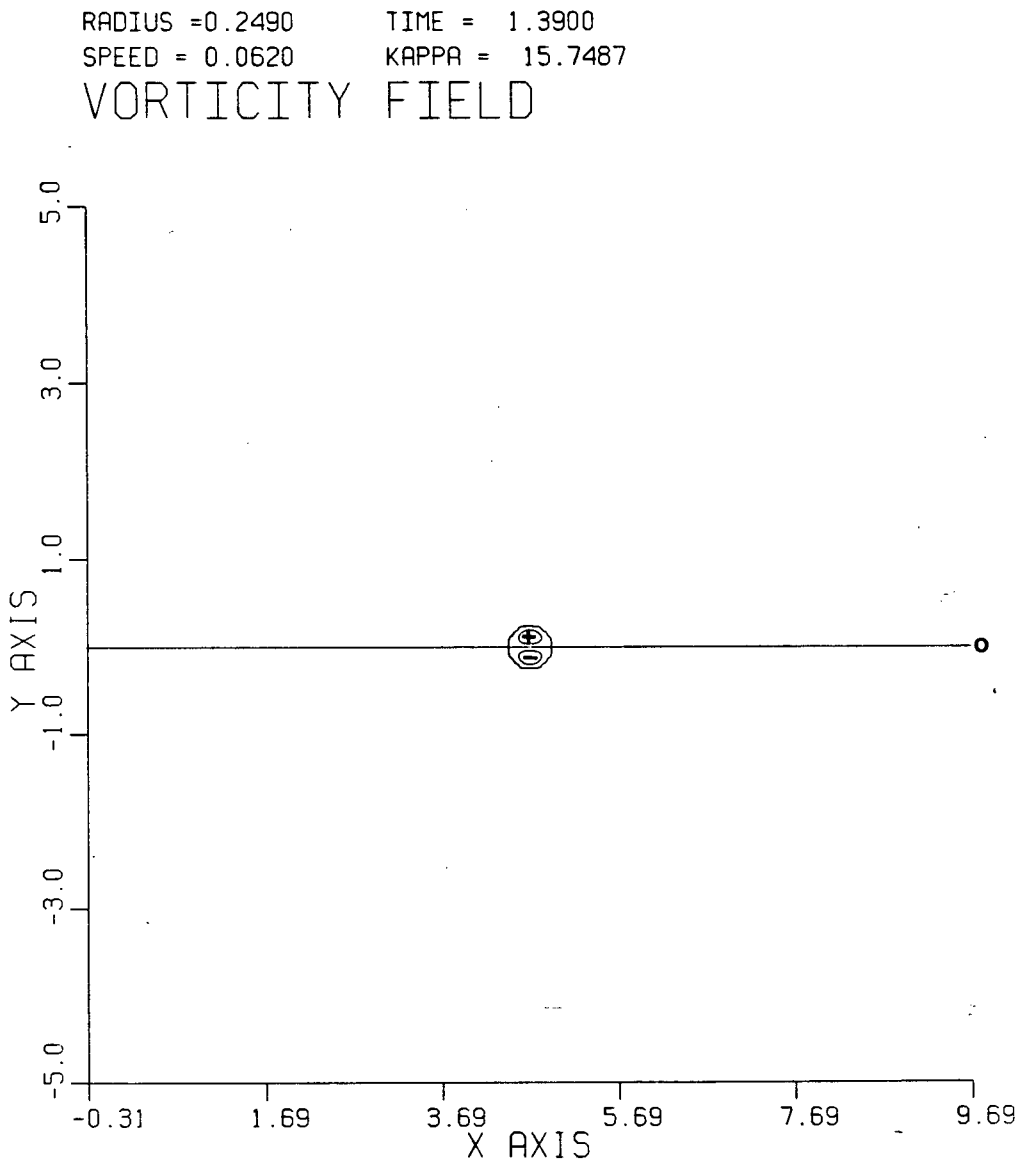

Figure 6e. Modon vorticity at T=1.39 under Ekman dissipation.

3.2 Modon Propagation Over Slowly Varying Topography

In this Section a leading order perturbation theory for modon propagation over slowly varying topography is developed. This solution, which is independent of any functional form of the topography, is applied to two specific topographic configurations.

In Subsection 3.2.1 the general theory is developed which is valid for finite-amplitude slowly varying topography (i.e., topographic amplitudes on the order of the depth of the fluid). Also in Subsection 3.2.1, analytical perturbation solutions for the modon radius, translation speed and wavenumber are obtained for small-amplitude topography. These analytical solutions are described in Subsection 3.2.2. Subsections 3.2.3 and 3.2.4 apply the small-amplitude solutions to a modon travelling over a meridional ridge (modelled as a gaussian in the x-coordinate direction) and an escarpment (modelled as a hyperbolic tangent in the x-coordinate direction), respectively.

3.2.1 Perturbation Solution For Modon Propagation Over Slowly Varying Topography

As in Veronis(1966), Rhines(1969a,b), Clarke(1971), LeBlond and Mysak(1978; Sec. 20), Malanotte-Rizzoli and Hendershott(1980), Matsuura and Yamagata(1982) and Yamagata(1982) the effects of variable topography on planetary waves are modelled with the shallow water equations on the β-plane. The nondimensional rigid-lid shallow water potential vorticity equation can be

written as (LeBlond and Mysak, 1978; Sec. 20)

$$\nabla\cdot(H^{-1}\nabla\psi_t) + J[\psi, H^{-1}\nabla\cdot(H^{-1}\nabla\psi) + fH^{-1}] = 0. \qquad (3.2.1)$$

All symbols are defined as in Section 3.1 with the following exceptions; ψ is the transport streamfunction

$$-Hu = \psi_y \qquad Hv = \psi_x ,$$

where u and v are the (positive) eastward and (positive) northward velocity components respectively, and where $H(\epsilon x,\epsilon y) = 1 - \mu h(\epsilon x,\epsilon y)$ is the slowly varying topography with $\epsilon = a_0/(\text{length scale of topography}) << 1$ and μ is the topographic amplitude parameter.[4] In this Subsection it is assumed that $0<\epsilon<<\mu\leq 1$. The leading order solution will be valid for finite-amplitude topography (i.e., $\mu\simeq O(1)$), although the smallness of μ will be eventually demanded (i.e., $0<\epsilon<<\mu<<1$) in order to obtain analytical solutions.

The Coriolis parameter is $f = (r_0)^{-1} + \delta^2 y$. The effects of planetary vorticity dominate topographic steering if $(\delta^2 r_0)^{-1} O(\nabla H/H) \simeq \epsilon(\delta^2 r_0)^{-1} < 1$ (LeBlond and Mysak, 1978; Sec. 20). Typical slopes of the ocean floor away from mid-ocean ridges, large seamounts and escarpment breaks give $\epsilon \simeq 10^{-3}$,

[4] The topographic parameter is the maximum absolute value of the height of the topography divided by the mean depth. The theory applies to topographic depressions (e.g., trenchs) as well as to topographic protrusions (e.g., ridges).

thus $\epsilon(\delta^2 r_0)^{-1} \simeq 10^{-1}$ (for scalings described in Section 3.1). We note that larger bottom slopes can be considered as r_0 is allowed to increase (e.g., atmospheric applications or in equatorial regions).

As in Luke(1966), Grimshaw(1970,1971,1979a,b,1981), Kodama and Ablowitz(1980) and the work in Section 3.1 a solution to (3.2.1) is found in the form

$$\psi = H(X,Y)\{ A(X,Y,T) + \psi^{(0)}(\xi,y;X,Y,T) + \epsilon\psi^{(1)}(\xi,y;X,Y,T) + \ldots \}, \qquad (3.2.2a)$$

with the related perturbation velocity field

$$u = u^{(0)}(\xi,y;X,Y,T) + \epsilon u^{(1)}(\xi,y;X,Y,T) + \ldots , \qquad (3.2.2b)$$

$$v = v^{(0)}(\xi,y;X,Y,T) + \epsilon v^{(1)}(\xi,y;X,Y,T) + \ldots , \qquad (3.2.2c)$$

where $\xi_t = -c(X,Y,T)$ and $\xi_x = 1$ and where the slow variables X, Y and T are defined by

$$X=\epsilon x, \quad Y=\epsilon y \quad \text{and} \quad T=\epsilon t.$$

Substitution of these variables into (3.2.1) yields

$$-cH^{-1}\Delta\psi_\xi + \delta^2 H^{-1}\psi_\xi + H^{-2}J(\psi, \Delta\psi) = \epsilon\{ -H^{-1}\Delta\psi_T + 2cH^{-1}\psi_{\xi\xi X} +$$

$$2cH^{-1}\psi_{\xi yY} - \delta^2 H^{-1}\psi_X - H^{-2}J_X(\psi, \Delta\psi) - H^{-2}J_Y(\psi, \Delta\psi) -$$

$$2H^{-2}J(\psi,\ \psi_{\xi X}) - 2H^{-2}J(\psi,\ \psi_{yY}) - cH^{-2}H_X\psi_{\xi\xi} - cH^{-2}H_Y\psi_{\xi y} +$$

$$2H^{-3}(\Delta\psi)J_X(\psi,\ H) + 2H^{-3}(\Delta\psi)J_Y(\psi,\ H) + fH^{-2}J_X(\psi,\ H) +$$

$$fH^{-2}J_Y(\psi,\ H) + H^{-3}H_X J(\psi,\ \psi_\xi) + H^{-3}H_Y J(\psi,\ \psi_y)\} + O(\epsilon^2), \quad (3.2.3)$$

where $J(\cdot,*) = \partial(\cdot,*)/\partial(\xi,y)$, $J_X(\cdot,*) = \partial(\cdot,*)/\partial(X,y)$ and $J_Y(\cdot,*) = \partial(\cdot,*)/\partial(\xi,Y)$.

The formulation of the phase variable ξ does not include a x-direction wavenumber, say k. It can shown that if one defines ξ such that $\xi_t = -ck$ and $\xi_x = k$ the leading order results presented here are not changed since the x-direction wavenumber factors out of the governing equations and only c remains. Therefore, at least to this order such a parameter is free and one can set it equal to unity. Moreover, we argue that the role played by a slowly varying wavenumber in the definition of the phase variable is played by the slowly varying modon radius and wavenumber. Also, it would be incorrect to attempt to incorporate the y variable into the phase variable ξ since it would no longer be possible to define the polar coordinates required to write the modon solution.

The 0(1) problem is

$$J(\psi^{(0)} + cy,\ \Delta\psi^{(0)} + \delta^2 y) = 0,$$

the solution of which is taken to be the modon (3.1.3), (3.1.4)

and (3.1.5). The comments regarding the phase shift term $\xi_0(X,Y,T)$ made in Section 3.1 apply here and thus eventually ξ_0 will be chosen to be the x-coordinate of the wave center at T=0, allowing the topography to be centered at X=0. The wave parameters a, c and κ are slowly varying functions of X, Y and T that satisfy the dispersion relationship (3.1.5). For the initial value problem, $a(X,Y,0)=1$, $c(X,Y,0)=1$ and $\kappa(X,Y,0)=\kappa_0$, where (as in Section 3.1) κ_0 is obtained from the dispersion relation (3.1.5) when T=0 ($\kappa_0=3.9226$ when $\delta=1$).

The $0(\epsilon)$ problem can be written as

$$J(\psi^{(0)} + cy, \Delta\psi^{(1)}) + J(\psi^{(1)}, \Delta\psi^{(0)} + \delta^2 y) = -\delta^2 A_X -$$

$$\delta^2 H^{-1} AH_X - H^{-1} J_X(HA, \Delta\psi^{(0)}) - H^{-1} J_Y(HA, \Delta\psi^{(0)}) - \Delta\psi^{(0)}_T +$$

$$2c\psi^{(0)}_{\xi\xi X} - \delta^2 \psi^{(0)}_X - J_X(\psi^{(0)}, \Delta\psi^{(0)}) - 2J(\psi^{(0)}, \psi^{(0)}_{\xi X}) +$$

$$2c\psi^{(0)}_{\xi yY} - J_Y(\psi^{(0)}, \Delta\psi^{(0)}) - 2J(\psi^{(0)}, \psi^{(0)}_{yY}) +$$

$$c(H^{-1}H_X)\psi^{(0)}_{\xi\xi} - \delta^2 (H^{-1}H_X)\psi^{(0)}_X - (H^{-1}H_X) J(\psi^{(0)}, \psi^{(0)}_\xi) -$$

$$(\Delta\psi^{(0)} + f)(H^{-1}H_X)\psi^{(0)}_y - (H^{-1}H_X)\psi^{(0)}\Delta\psi^{(0)}_y +$$

$$c(H^{-1}H_Y)\psi^{(0)}_{\xi y} - (H^{-1}H_Y) J(\psi^{(0)}, \psi^{(0)}_y) +$$

$$(\Delta\psi^{(0)} + f)(H^{-1}H_Y)\psi^{(0)}_\xi + (H^{-1}H_Y)\psi^{(0)}\Delta\psi^{(0)}_\xi. \qquad (3.2.4)$$

As in Luke(1966), Grimshaw(1970,1971,1979a,b,1981) and Kodama and Ablowitz(1981), $\psi^{(1)}$ is assumed to have the property $\nabla\psi^{(1)} \to 0$ as $r \to \infty$. Consequently, in the limit as $r \to \infty$ (3.2.4) reduces to

$$A_X + (H^{-1}H_X)A = 0, \qquad (3.2.5)$$

(recall $\psi^{(0)} \to 0$ as $r \to \infty$). The general solution of (3.2.5) is

$$A = g(Y,T)H^{-1}$$

for some function $g(Y,T)$. Thus the first term in the perturbation expansion (3.2.2a) (i.e., AH) is simply $g(Y,T)$ which will be left undetermined in the leading order analysis developed here.

Note that since $AH = g(Y,T)$, $J_X(HA, \Delta\psi^{(0)})=0$ and $J_Y(HA, ,\Delta\psi^{(0)})=-g_Y \Delta\psi^{(0)}_\xi$. It turns out this last remaining term integrates to zero in the imposed solvability conditions due to the periodicity in θ (see the Appendix). Also, note that $g(Y,T)$ will not contribute to the 0(1) velocity field since

$$u^{(0)} = -\psi^{(0)}_y \qquad v^{(0)} = \psi^{(0)}_\xi.$$

Therefore, with no loss of generality, $g(Y,T)$ can be set equal to zero in this leading order analysis. It is formally retained at this stage because of its appearance in the $0(\epsilon)$ problems.

For r>a, (3.2.4) can be rewritten as (see (3.1.3))

$$J(\psi^{(0)}, \Delta\psi^{(1)} - \delta^2 c^{-1}\psi^{(1)}) = (\delta^2/c)H^{-1}g_Y \psi^{(0)}_\xi - \Delta\psi^{(0)}_T +$$

$$2c\psi^{(0)}_{\xi\xi X} - \delta^2\psi^{(0)}_X + (\delta^2/c)\, \psi^{(0)}_X \psi^{(0)}_y - 2J(\psi^{(0)}, \psi^{(0)}_{\xi X}) +$$

$$c(H^{-1}H)_X\psi^{(0)}_{\xi\xi} - \delta^2(H^{-1}H)_X\psi^{(0)} - (H^{-1}H)_X J(\psi^{(0)}, \psi^{(0)}_\xi) -$$

$$[(r_0)^{-1} + \delta^2 y](H^{-1}H)_X\psi^{(0)}_y - (2\delta^2/c)(H^{-1}H)_X\psi^{(0)}\psi^{(0)}_y +$$

$$2c\psi^{(0)}_{\xi yY} - (\delta^2/c)\,\psi^{(0)}_Y\psi^{(0)}_\xi - 2J(\psi^{(0)}, \psi^{(0)}_{yY}) +$$

$$c(H^{-1}H)_Y\psi^{(0)}_{\xi y} - (H^{-1}H)_Y J(\psi^{(0)}, \psi^{(0)}_y) +$$

$$[(r_0)^{-1} + \delta^2 y](H^{-1}H)_Y\psi^{(0)}_\xi + 2(\delta^2/c)(H^{-1}H)_Y\psi^{(0)}\psi^{(0)}_\xi. \qquad (3.2.6)$$

The homogeneous adjoint equation associated with (3.2.6) is

$$(\Delta - \delta^2 c^{-1})J(\psi^{(0)} + cy, u) = 0$$

for which $u = \psi^{(0)}(r>a)$ is a solution. The solvability condition on $\psi^{(0)}$ for $r>a$ is therefore (see the Luke and Ablowitz citations)

$$\int_{-\pi}^{\pi}\int_a^\infty \psi^{(0)}\{\text{RHS}(3.2.6)\}\, r dr d\theta = 0. \qquad (3.2.7)$$

For $r<a$, (3.2.4) can be rewritten as (see (3.1.4))

$$J(\psi^{(0)}, \Delta\psi^{(1)} + \kappa^2\psi^{(1)}) = -\kappa^2 H^{-1}g_Y\psi^{(0)}_\xi - \Delta\psi^{(0)}_T +$$

$$2c\psi^{(0)}_{\xi\xi X} + \kappa^2 c\psi^{(0)}_X - (\kappa^2)\,\psi^{(0)}_X\psi^{(0)}_y - 2J(\psi^{(0)}, \psi^{(0)}_{\xi X}) +$$

$$c(H^{-1}H)_X\psi^{(0)}_{\xi\xi} + \kappa^2 c(H^{-1}H)_X\psi^{(0)} - (H^{-1}H)_X J(\psi^{(0)}, \psi^{(0)}_\xi) -$$

$$[(r_0)^{-1} - \kappa^2 cy](H^{-1}H)_X\psi^{(0)}_y + 2\kappa^2(H^{-1}H)_X\psi^{(0)}\psi^{(0)}_y +$$

$$2c\psi^{(0)}_{\xi yY} + (\kappa^2)\,\psi^{(0)}_{Y}\psi^{(0)}_{\xi} + [r\sin(\theta)(\delta^2 + \kappa^2 c)]\,\psi^{(0)}_{Y\,\xi} -$$

$$2J(\psi^{(0)}_{yY}, \psi^{(0)}) + c(H^{-1}H_{Y})\psi^{(0)}_{\xi y} - (H^{-1}H_{Y})J(\psi^{(0)}_{Y}, \psi^{(0)}_{y}) +$$

$$[(r_0)^{-1} - \kappa^2 cy](H^{-1}H_{Y})\psi^{(0)}_{\xi} - 2\kappa^2(H^{-1}H_{Y})\psi^{(0)}\psi^{(0)}_{\xi}. \qquad (3.2.8)$$

The homogeneous adjoint equation associated with (3.2.8) is

$$(\Delta + \kappa^2)J(\psi^{(0)} + cy,\ u) = 0$$

for which $u = \psi^{(0)}(r<a)$ is a solution. The solvability condition on $\psi^{(0)}$ for $r<a$ is therefore

$$\int_{-\pi}^{\pi}\int_{0}^{a} \psi^{(0)}\{\text{RHS}(3.2.8)\}\, r\,dr\,d\theta = 0. \qquad (3.2.9)$$

The calculation of the compatibility conditions (3.2.7) and (3.2.9) is tedious but entirely straightforward. These computations are described in the Appendix.

Four observations are made here about these calculations. It has been noted that the first term in the RHS of (3.2.6) and (3.2.8) (containing g(Y,T)) integrates to zero due to the periodicity in θ (see the Appendix). Also, all terms that contain derivatives of the phase shift term $\xi_0(X,Y,T)$ with respect to X,Y and T integrate to zero for the same reason (see the Appendix). In addition, terms which contain the Rossby number as a coefficient in (3.2.6) and (3.2.8) also integrate to zero due to the periodicity in θ (see the Appendix). Thus the

equations we derive to describe the slow variation of the modon parameters are independent of the Rossby number, $\xi_0(X,Y,T)$ and $g(Y,T)$.

Of physical interest is the observation that each individual term in the RHS's of (3.2.6) and (3.2.7) that contains a derivative with respect to the slow variable Y integrates to identically zero due to the periodicity in θ (see the Appendix). Therefore the meridional structure of the slowly varying topography appears in parametric form in the leading order solution and the leading order evolution of the modon parameters is solely determined by the east-west topographic structure.

However, only the leading order solution has a parametric dependence on the meridional topographic structure. It is easy to check that higher order derivatives with respect to Y do not satisfy this orthogonality property. (Such terms are $O(\epsilon^2)$ and have been ignored in (3.2.3).) Meridional gradients in the topography therefore give rise to $O(\epsilon^2)$ modulations in the modon parameters.

A physical explanation for this leading order parameteric dependence on the meridional topographic structure can be given based on the following vorticity arguments. Equation (3.2.1) states that the potential vorticity $(v_x - u_y + f)/H$ is a conserved quantity. Consider a particle of fluid displaced parallel to the x-axis. If H_x is non-zero then the relative vorticity must change in response to changes in H (f being constant when y is

constant). Thus the leading order relative vorticity adjustment to zonal displacements occurs in response to zonal topographic variations.

However, the leading order vorticity adjustment is not due to topographic variations in meridional displacements. The scaling of (3.2.1) (see also (3.2.3)) has assumed that changes in planetary vorticity dominate topographic variations. Thus the leading order vorticity adjustment to meridional displacements occurs in response to changes in the planetary vorticity (i.e., the y-coordinate) and topographic variations are second order in comparison.

After considerable algebra (see the Appendix), (3.2.7) and (3.2.9) result in the following two differential equations for a(X,Y,T) and c(X,Y,T)

$$A_1 a^{-1} a_T - (A_1 - 1)(2c)^{-1} c_T + (c/2)[A_1 a^{-1} a_X - (A_1 - 1)(2c)^{-1} c_X] + cA_2 (2c)^{-1} c_X + cA_3 a^{-1} a_X = -cE_1 H^{-1} H_X \qquad (3.2.10)$$

$$B_1 a^{-1} a_T - (B_1 - 1)(2c)^{-1} c_T + (c/2)[B_1 a^{-1} a_X - (B_1 - 1)(2c)^{-1} c_X] + cB_2 (2c)^{-1} c_X + cB_3 a^{-1} a_X = -cE_2 H^{-1} H_X \qquad (3.2.11)$$

respectively, where A_1, A_2, A_3, E_1, B_1, B_2, B_3 and E_2 are

nondimensional functions of γ and k (recall $\gamma^2=\delta^2a^2/c$ and $k=\kappa a$) which are derived in the Appendix. The system (3.2.10) and (3.2.11) can be rewritten as

$$a^{-1}a_T + c(A_{11} + 1/2)a^{-1}a_X + cA_{12}(2c)^{-1}c_X = -cF_1H^{-1}H_X \quad (3.2.12)$$

$$(2c)^{-1}c_T + cA_{21}a^{-1}a_X +$$

$$c(A_{22} + 1/2)(2c)^{-1}c_X = -cF_2H^{-1}H_X , \quad (3.2.13)$$

where

$$A_{11} = [(1 - B_1)A_3 + (A_1 - 1)B_3]/(A_1 - B_1)$$

$$A_{12} = [(1 - B_1)A_2 + (A_1 - 1)B_2]/(A_1 - B_1)$$

$$A_{21} = (-B_1A_3 + A_1B_3)/(A_1 - B_1)$$

$$A_{22} = (-B_1A_2 + A_1B_2)/(A_1 - B_1)$$

$$F_1 = [(1 - B_1)E_1 + (A_1 - 1)E_2]/(A_1 - B_1)$$

$$F_2 = (-B_1E_1 + A_1E_2)/(A_1 - B_1).$$

The evolution of $\kappa(X,Y,T)$ is determined by solving (3.1.5) at each space-time coordinate given $a(X,Y,T)$ and $c(X,Y,T)$, the solutions of (3.2.12) and (3.2.13).

Whitham(1965) argued that hyperbolic differential equations ought to govern the evolution of the slowly varying wave so that the parameter modulations could propagate in space-time. The eigenvalues of the matrix $[M_{ij}]$ with entries $M_{11}=A_{11}+1/2$, $M_{12}=A_{12}$, $M_{21}=A_{21}$ and $M_{22}=A_{22}+1/2$ (denoted with the usual convention) were numerically determined to be real and distinct for all values of γ and k (consistent with the dispersion relation (3.1.5)) except for when $A_1=B_1$ (in which case the matrix $[M_{ij}]$ is not defined). $A_1=B_1$ only when $\gamma=5.776$ and $k=4.4835$ (A_1 and B_1 are in fact identical to the functions A and M defined in Section 3.1, respectively). Similar arguments to those presented in Section 3.1 can show that if there exists a solution to the initial-value problem associated with (3.2.10) and (3.2.11) then the continuity of a, c and κ and the discreteness of the γ and κ for which $A_1=B_1$ imply that the solutions satisfy (3.2.12) and (3.2.13) (except at the set of discrete space-time coordinates for which the singularity occurs). The equations (3.2.12) and (3.2.13) therefore form a nonlinear hyperbolic system which is valid for finite-amplitude topography. In practice, the problem must be solved numerically.

Analytical solutions can be obtained for a, c and κ by demanding the smallness of the topographic amplitude parameter μ. When $0<\epsilon<<\mu<<1$ (which is the case in many oceanic and atmospheric applications), solutions to (3.2.12), (3.2.13) and (3.1.5) can be obtained in the form

$$a = 1 + \mu a^{(1)}(X,Y,T) + 0(\mu^2)$$

$$c = 1 + \mu c^{(1)}(X,Y,Y) + 0(\mu^2)$$

$$\kappa = \kappa_0[1 + \mu\kappa^{(1)}(X,Y,T) + 0(\mu^2)].$$

Note that $a^{(1)}$, $c^{(1)}$ and $\kappa^{(1)}$ are μ-perturbations and are not to be confused with the role played by $\psi^{(1)}$, $u^{(1)}$ and $v^{(1)}$ in the ϵ-perturbation expansion (3.2.2).

Since $H(X,Y) = 1-\mu h(X,Y)$ it follows

$$H^{-1}H_X = -\mu h_X + 0(\mu^2).$$

The $0(\mu)$ terms in (3.2.12) and (3.2.13) are

$$a^{(1)}_T + (A_{011} + 1/2)a^{(1)}_X + A_{012}c^{(1)}_X/2 = F_{01}h_X \qquad (3.2.14)$$

$$c^{(1)}_T/2 + A_{021}a^{(1)}_X + (A_{022} + 1/2)c^{(1)}_X/2 = F_{02}h_X, \qquad (3.2.15)$$

where A_{011}, A_{012}, A_{021}, A_{022}, F_{01} and F_{02} are the values of A_{11}, A_{12}, A_{21}, A_{22}, F_1 and F_2 respectively, evaluated for $\gamma = \delta$ and $k=\kappa_0$. Expanding the dispersion relationship (3.1.5) in a Taylor series about $\mu=0$ gives at $0(\mu)$

$$\kappa^{(1)} = N_0[a^{(1)} - c^{(1)}/2] - c^{(1)}/2, \qquad (3.2.16)$$

where $N_0 = -\{\delta R + (\kappa_0)^2 R/\delta\}/\{4 + \delta/R + (\kappa_0)^2 R/\delta\}$ with $R=K_2(\delta)/K_1(\delta)$.

From (3.2.14) and (3.2.15) it follows that

$$a^{(1)}_{TT} + \rho_1 a^{(1)}_{XT} + \rho_2 a^{(1)}_{XX} = \nu_1 h_{XX} \tag{3.2.17}$$

$$c^{(1)}_{TT} + \rho_1 c^{(1)}_{XT} + \rho_2 c^{(1)}_{XX} = 2\nu_2 h_{XX}, \tag{3.2.18}$$

where

$$\rho_1 = A_{011} + A_{022} + 1$$

$$\rho_2 = (A_{022} + 1/2)(A_{011} + 1/2) - A_{012}A_{021}$$

$$\nu_1 = (A_{022} + 1/2)F_{01} - A_{012}F_{02}$$

$$\nu_2 = (A_{011} + 1/2)F_{02} - A_{021}F_{01}.$$

The solutions to (3.2.17) and (3.2.18) subject to the initial conditions

$$a^{(1)}(X,Y,0) = 0, \quad a^{(1)}_T(X,Y,0) = F_{01}h_X \tag{3.2.19a}$$

$$c^{(1)}(X,Y,0) = 0, \quad c^{(1)}_T(X,Y,0) = 2F_{02}h_X \tag{3.2.19b}$$

are given by

$$a^{(1)}(X,Y,T) = \lambda_1 h(X,Y) + \lambda_2 h(X-\sigma_1 T,Y) + \lambda_3 h(X-\sigma_2 T,Y), \quad (3.2.20)$$

$$c^{(1)}(X,Y,T) = \lambda_4 h(X,Y) + \lambda_5 h(X-\sigma_1 T,Y) + \lambda_6 h(X-\sigma_2 T,Y), \quad (3.2.21)$$

where the coefficients are defined as

$$\lambda_1 = \nu_1(\sigma_1\sigma_2)^{-1}$$

$$\lambda_2 = (F_{01}\sigma_1 - \nu_1)[\sigma_1(\sigma_2 - \sigma_1)]^{-1}$$

$$\lambda_3 = (\nu_1 - F_{01}\sigma_2)[\sigma_2(\sigma_2 - \sigma_1)]^{-1}$$

$$\lambda_4 = 2\nu_2(\sigma_1\sigma_2)^{-1}$$

$$\lambda_5 = 2(F_{02}\sigma_1 - \nu_2)[\sigma_1(\sigma_2 - \sigma_1)]^{-1}$$

$$\lambda_6 = 2(\nu_2 - F_{02}\sigma_2)[\sigma_2(\sigma_2 - \sigma_1)]^{-1},$$

and where the characteristic speeds σ_1 and σ_2 are given by

$$\sigma_1 = \{\rho_1 - [(\rho_1)^2 - 4\rho_2]^{1/2}\}/2$$

$$\sigma_2 = \{\rho_1 + [(\rho_1)^2 - 4\rho_2]^{1/2}\}/2.$$

The initial conditions on $a^{(1)}_T$ and $c^{(1)}_T$ (see (3.2.19)) are obtained by evaluating (3.2.14) and (3.2.15) at T=0, respectively. The solution for $\kappa^{(1)}(X,Y,T)$ is determined by

(3.2.16), (3.2.20) and (3.2.21) yielding

$$\kappa^{(1)}(X,Y,T) = \lambda_7 h(X,Y) + \lambda_8 h(X-\sigma_1 T,Y) + \lambda_9 h(X-\sigma_2 T,Y), \quad (3.2.22)$$

with λ_7, λ_8 and λ_9 given by

$$\lambda_7 = N_0(\lambda_1 - \lambda_4/2) - \lambda_4/2$$

$$\lambda_8 = N_0(\lambda_2 - \lambda_5/2) - \lambda_5/2$$

$$\lambda_9 = N_0(\lambda_3 - \lambda_6/2) - \lambda_6/2.$$

3.2.2 Discussion Of The Small-Amplitude Topographic Solution

The slowly varying modon will be described (to leading order) by (3.1.3) and (3.1.4) with a, c and κ given by

$$a = 1 + \mu a^{(1)}(X,Y,T) \quad (3.2.23)$$

$$c = 1 + \mu c^{(1)}(X,Y,T) \quad (3.2.24)$$

$$\kappa = \kappa_0[1 + \mu\kappa^{(1)}(X,Y,T)], \quad (3.2.25)$$

where $a^{(1)}$, $c^{(1)}$ and $\kappa^{(1)}$ are given by (3.2.20), (3.2.21) and (3.2.22) respectively, evaluated at the modon center X at time T. The position of the modon center as a function of time is obtained from the characteristic equation

$$dX/dT = c(X,0,T), \tag{3.2.26}$$

written in slow variables. (Note that the modon center to lead order occurs on Y=0; see (3.1.3) and (3.1.4).) In general, (3.2.26) is not separable so X(T) is defined implicitly and must be obtained numerically. Formally, the solution of (3.2.26) is written

$$X(T) = \epsilon\xi_0 + \int_0^T c[X(T),0,T]dT \tag{3.2.27}$$

where $X(0)=\epsilon\xi_0$ (see Subsection 3.1.1).

However if attention is restricted to $T<<1$ (i.e., $t<<\epsilon^{-1}$) then

$$c(X,0,T) \simeq c(\epsilon\xi_0,0,0) + c_T(\epsilon\xi_0,0,0)T + 0(T^2).$$

Consequently, (3.2.27) and (3.2.15) implies that the modon center will be approximately given by

$$X = \epsilon\xi_0 + T + \mu F_{02} h_X(\epsilon\xi_0,0)T^2 + 0(T^3). \tag{3.2.28}$$

Using (3.2.28) the space variable X can be eliminated from the solutions (3.2.23), (3.2.24) and (3.2.25) to obtain analytic asymptotic (i.e., $T<<1$) solutions in the single slow time variable T.

As a typical calculation of the solution parameters let δ=1.0, hence: κ_0=3.9226 (from 3.1.5), N_0=-0.9636, ρ_1=-7.39, ρ_2=-39.44, ν_1=2.00, ν_2=-9.20, σ_1=-10.98, σ_2=3.59, F_{01}=4.04 and F_{02}=-0.63 from which it follows λ_1=-0.05, λ_2=0.29, λ_3=-0.24, λ_4=0.46, λ_5=-0.20, λ_6=-0.26, λ_7=0.04, λ_8=-0.28 and λ_9=0.24. Other values of δ give qualitatively similar results (except near the singular value δ=5.776). The initial-value solution therefore takes the form of eastward and westward-travelling hyperbolic waves and a stationary component proportional to the topography. Note that in consequence of the initial conditions (3.2.19), the parameters satisfy

$$\lambda_1 + \lambda_2 + \lambda_3 = 0 \qquad (3.2.29a)$$

$$\lambda_4 + \lambda_5 + \lambda_6 = 0 \qquad (3.2.29b)$$

$$\lambda_7 + \lambda_8 + \lambda_9 = 0. \qquad (3.2.29c)$$

These relations are clearly required if h = constant is to result in only the trivial solution (i.e., $a^{(1)}$, $c^{(1)}$ and $\kappa^{(1)}$ are all zero).

Consider the solution for $a^{(1)}(X,Y,T)$ given by (3.2.20). Since $\lambda_3<0$, the radius-perturbation associated with the eastward-travelling wave (i.e., $h(X-\sigma_2 T,Y)$) acts to decrease the modon radius. Since $\lambda_2>0$, the radius-perturbation associated with the westward-travelling wave (i.e., $h(X-\sigma_1 T,Y)$) acts to increase the radius. Since $\lambda_1<0$, the radius-perturbation associated with the stationary component (i.e., $h(X,Y)$) acts to decrease the modon radius. These results have

implicitly assumed a positive topography (i.e., $h(X,Y)\geq 0$). If one considers a topographic depression (i.e., $h(X,Y)\leq 0$), the results are simply reversed.

Similar reasoning applies to the translation speed $c(X,Y,T)$ solution (3.2.21). Since $\lambda_5<0$ and $\lambda_6<0$, the speed-perturbations associated with the westward-travelling wave and eastward-travelling wave act to decrease the translation speed. Since $\lambda_4>0$, the speed-perturbation associated with the stationary component of the solution acts to increase the translation speed. As before, if one considers a topographic depression these results are reversed.

The qualitative behaviour of the wavenumber-perturbations associated with the individual solution components in (3.2.22) is opposite to that of the radius-perturbations. Since $\lambda_7>0$ and $\lambda_9>0$, the wavenumber-perturbations associated with the stationary and eastward-travelling wave components act to increase the modon wavenumber. Since $\lambda_8<0$ the wavenumber-perturbation associated with the westward-travelling wave acts to increase the modon wavenumber. As before, if one considers a topographic depression these results are reversed.

When the topography satisfies $h(X,Y)\rightarrow A^{+}(Y)$ and $A^{-}(Y)$ for $X\rightarrow+\infty$ and $X\rightarrow-\infty$ respectively, it is meaningful to speak of a 'local' (i.e., in a neighbourhood of $X=0$) steady-state solution (i.e., $T\rightarrow\infty$) for $a(X,Y,T)$, $c(X,Y,T)$ and $\kappa(X,Y,T)$. Note that if one defines $h(X,Y)=A^{-}(Y)+h'(X,Y)$, the terms containing $A^{-}(Y)$ in (3.2.20), (3.2.21) and (3.2.22) sum to zero due to (3.2.29). Thus with no loss of generality we set $A^{-}=0$ and assume $h(X,Y)$ is

relative to the upstream topography (which may depend on Y but is asymptotically constant in X). Under these conditions (3.2.20), (3.2.21) and (3.2.22) will imply local steady-state solutions of the form

$$a \simeq 1 + \mu\{\lambda_2[A^+ - h(X,Y)] - \lambda_3 h(X,Y)\} \qquad (3.2.30)$$

$$c \simeq 1 + \mu\{\lambda_5[A^+ - h(X,Y)] - \lambda_6 h(X,Y)\} \qquad (3.2.31)$$

$$\kappa \simeq \kappa_0 + \kappa_0\mu\{\lambda_8[A^+ - h(X,Y)] - \lambda_9 h(X,Y)\} \qquad (3.2.32)$$

(in a neighbourhood of X=0 for sufficiently large time).

Two cases are of interest. Consider the structure of the approximate local steady-state solutions for isolated (or compact) topography (i.e., $A^+=0$). Then (3.2.30), (3.2.31) and (3.2.32) further reduce to

$$a \simeq 1 + \mu\lambda_1 h(X,Y) \qquad (3.2.33)$$

$$c \simeq 1 + \mu\lambda_4 h(X,Y) \qquad (3.2.34)$$

$$\kappa \simeq \kappa_0 + \mu\kappa_0\lambda_7 h(X,Y) \qquad (3.2.35)$$

where (3.2.29) has been used. Since $\lambda_1<0$, (3.2.33) implies that $a\leq 1$. Therefore the radius of the modon decreases as it travels over isolated positive topography (ignoring the transient waves since $T\gg 1$ is assumed). If the modon were travelling over an

isolated depression, say a trench, its radius would increase (i.e., $a \geq 1$) since $h(X,Y) \leq 0$.

From (3.2.34), $c>1$ over positive isolated topography and $c<1$ over isolated depressions since $\lambda_4>0$. Modon particle speeds are on the same order as the translation speed so the fluid accelerates over isolated positive topography and deaccelerates over isolated depressions, in line with intuitive continuity arguments.

The modon wavenumber adjusts to isolated topography in just the reverse manner as the modon radius (as might be expected since a wavenumber is dimensionally the inverse of a length). From (3.2.35), the modon wavenumber will satisfy $\kappa>\kappa_0$ over positive isolated topography and satisfies $\kappa<\kappa_0$ over isolated depressions since $\lambda_7>0$.

In summary, the following qualitative structure develops as the modon travels over isolated slowly varying topography (ignoring the transient waves). If the topography is positive, the modon translation speed increases and hence the particle speeds increase, the radius decreases and the wavenumber increases. The modon therefore contracts and accelerates over positive topography. Over isolated depressions the reverse happens. The modon dilates and deaccelerates. Subsection 3.2.3 illustrates the evolution of the modon over positive isolated topography by considering a meridional ridge modelled with a gaussian in the x-coordinate direction as an example.

When $A^+(Y)$ is not zero the approximate solutions (3.2.30), (3.2.31) and (3.2.32) depend on the far field (i.e., $X>>1$)

topographic structure. The terms with A^+ represent the transmission of this far field information into the X=0 neighbourhood by way of the westward-travelling hyperbolic wave.

In general, of course, the analysis will be different for each assumed form for $A^+(Y)$. To illustrate the differences and similarities between isolated and nonisolated topography consider A^+ as a nonzero constant. Allowing a meridional dependence does not complicate the essential ideas as the solutions depend only parametrically on Y.

Consider the case $0 \le h \le A^+ < \infty$ (henceforth called increasing topography). It follows from (3.2.30) that $a>1$ for all X since $\lambda_2>0$ and $\lambda_3<0$. As X increases, $h \to A^+$ so $a \to 1-\mu\lambda_3 A^+ \ge 1$. As X decreases, $h \to 0$ so $a \to 1+\mu\lambda_2 A^+ \ge 1$. However, since $|\lambda_2|>|\lambda_3|$ it follows that there will be a relative decrease in the modon radius from $X<<0$ to $X>>0$ for sufficiently large T.

From (3.2.31), $c>1$ for $X>0$ since $\lambda_6<0$, and $c<1$ for $X<0$ since $\lambda_5<0$. Because $|\lambda_6|>|\lambda_5|$ the increase in the translation speed for $X>0$ is larger than the decrease in the translation speed for $X<0$. The particle speeds will also have this property.

The behaviour of the modon wavenumber is again reversed to that of the modon radius. There is a global decrease in the wavenumber since all terms in (3.2.32) are negative. However, similar reasoning to that given for the modon radius shows there is a relative increase in the modon wavenumber from $X<0$ to $X>0$ since $|\lambda_8|<|\lambda_9|$. In Subsection 3.2.4 the solutions for a topographic escarpment modelled as a hyperbolic tangent in the

x-coordinate direction are presented as an example of a topographic configuration displaying the above properties.

The behaviour of the solutions for a decreasing topographic configuration ($-\infty<A^{+}\leq h\leq 0$, i.e., a topographic depression) gives the opposite results to those stated above. The modon radius decreases for all X with a relative increase from $X<0$ to $X>0$. The translation speed will satisfy $c>1$ for $X<0$ and $c<1$ for $X>0$ with the decrease in c for $X<0$ larger than the increase in c for $X>0$. The particle speeds will also have this property. The modon wavenumber will increase for all X with a relative decrease from $X<0$ to $X>0$.

The leading order solution $\psi^{(0)}(\xi,y;X,Y,T)$ is not expected to be uniformly valid as $\xi\to\pm\infty$. It is easily seen that $\Delta\psi^{(0)}$ is a homogeneous solution to the $O(\epsilon)$ problem (3.2.4) and that certain terms in the RHS's of (3.2.4) and (3.2.6) are proportional to $\Delta\psi^{(0)}$. Thus resonance will in general occur and the expansion (3.2.2) is not expected to be valid for all ξ.

In one dimensional solitary waves this nonuniformity manifests itself as a 'shelf' ahead and behind of the solitary wave (e.g., Ko and Kuelh; 1978 and Grimshaw; 1979a,b and Kodama and Ablowitz; 1980). The shelf appears as a consequence of $\psi^{(1)}\to B^{+}$ and B^{-} as $\xi\to+\infty$ and $-\infty$ respectively, where B^{+} and B^{-} are constants. In general, it is assumed that ahead of the solitary wave the fluid (to leading order) is undisturbed, thus $B^{+}=0$ (e.g., Grimshaw, 1979a,b). The shelf region behind the wave is removed by the introduction of an outer expansion valid for $\xi\simeq O(\epsilon^{-n})$ (the power n is determined in the problem) (e.g.,

Grimshaw; 1979a,b and Kodama and Ablowtiz, 1980). However, since it is the term $\nabla\psi^{(1)}$ that determines part of the $O(\epsilon)$ velocity field, this constant does not contribute to $(u^{(1)},v^{(1)})$, consequently a nonuniformity of this type does not seem to be relevant here.

3.2.3 Gaussian-ridge Topography

In this Subsection the solution for modon propagation over a slowly varying ridge is described. The topography is given by

$$H(X,Y) = 1 - \mu\exp(-X^2), \qquad (3.2.36)$$

hence $h(X,Y) = \exp(-X^2)$. Since $h\to 0$ as $|X|\to\infty$ the qualitative behaviour of the solutions for a, c and κ will follow the analysis given in Subsection 3.2.3 for the case $A^+=0$.

Figures 7, 8 and 9 illustrate the spatial structure of the modon translation speed $c=1+\mu c^{(1)}$, modon radius $a=1+\mu a^{(1)}$ and modon wavenumber $\kappa=\kappa_0 + \mu\kappa_0\kappa^{(1)}$ respectively, with $\mu=0.2$ for the sequence of slow times T=0.0, 0.2, 0.6, 1.4 and 4.0. These figures represent space-like slices (i.e., T held constant) of the modon parameters in space-time. The particular value of a, c and κ that a particular modon experiences at a given time is, of course, determined by the characteristic in space-time the modon is propagating on. This characteristic is the unique solution of (3.2.26), which is approximately (3.2.28) (for $T\ll 1$), with the given h(X) in (3.2.36).

Figure 7a shows the initial condition on the translation

speed (i.e., c(X,0,0)=1). Figure 7b shows the spatial structure of c at T=0.2. The westward-travelling and eastward-travelling wave transients are just becoming distinguishable from the stationary component in (3.2.21). In Figure 7c the separation is more apparent. The westward-travelling wave is further removed from X=0 than is the eastward-travelling wave since $|\sigma_1|>|\sigma_2|$. The amplitude of the eastward-travelling wave is larger than the westward-travelling wave since $|\lambda_6|>|\lambda_5|$. By the time T=1.4 (Figure 7d) the westward-travelling wave has left the displayed space domain (i.e., $-10\leq X\leq 10$). The more slowly moving eastward-travelling wave has completely separated from the stationary component. Figure 7e shows the stationary component of the solution (3.2.21). This is the local steady-state solution for c(X,Y,T) described last Section for isolated topography.

Figures 8a, 8b, 8c, 8d and 8e show the space-like structure in the modon radius. Since the translation speeds for the westward-travelling and eastward-travelling transient waves in (3.2.20) are the same as in the solutions for $c^{(1)}$ (see (3.2.21)), the separation behaviour in the transients is the same as that given above. The eastward-travelling wave (see Figures 8c and 8d) acts to decrease the modon wavenumber (if the modon had an initial positive X position) since $\lambda_3<0$. The westward-travelling transient (see Figures 8b and 8c) acts to increase the modon radius since $\lambda_2>0$. The stationary component of the modon radius solution (see Figure 8e) acts to reduce the modon radius over the topography since $\lambda_1<0$.

Figures 9a, 9b, 9c, 9d and 9e show the space-like structure of the modon wavenumber. The initial condition is shown in Figure 11a. The separation behaviour is the same as in the above comments since the translation speeds are the same. The westward-travelling transient (see Figures 9b and 9c) acts to decrease the wavenumber since $\lambda_s<0$. The eastward-travelling transient (see Figures 9c and 9d) acts to increase the modon wavenumber since $\lambda_s>0$. The stationary component (see Figure 9e) acts to increase the modon wavenumber over the topography.

In summary, consider the following qualitative behaviour of the modon if its initial position is, say, $\epsilon\xi_0=-10$. The modon will initially propagate eastward unaffected by the topography (see Figures 7b, 8b and 9b). When the characteristic associated with the westward-travelling transient intersects the modon characteristic, the modon translation speed is reduced, its radius is increased and its wavenumber decreases. The modon continues to propagate eastward since $c>0$ (see Figure 7) throughout this initial interaction. After sufficient time the westward-travelling wave propagates completely through the modon characteristic and subsequently does not contribute to the solution.

Some time later the modon characteristic intersects the space-time region containing the characteristics associated with the stationary component of the solution. The modon translation speed increases, the radius decreases and the wavenumber increases (see Figures 7e, 8e and 9e). Subsequent to this interaction there is no further interaction with the topography

or the transient waves. The eastward-travelling transient propagates with speed σ_2=3.59 which is greater than the modon translation speed (see Figure 7) and thus the two characteristics (i.e., of the modon and the eastward-travelling wave) never intersect for T>0 if ξ_0<0.

This analysis has assumed that h(X)>0. If the 'ridge' was a depression (i.e., h(X)<0) the above results would be reversed. If $\xi_0 \geq 0$ (say $\epsilon\xi_0$=10), the qualitative analysis is similar to the above except that the effects of the eastward-travelling transient must taken into account. Clearly in this scenario the westward-travelling wave does not affect the modon since for spatial coordinates greater than the current location of the modon center the topography is identically zero. Hence characteristics orginating from spatial coordinates positive of the modon center at any given time have zero amplitude and therefore do not affect the modon.

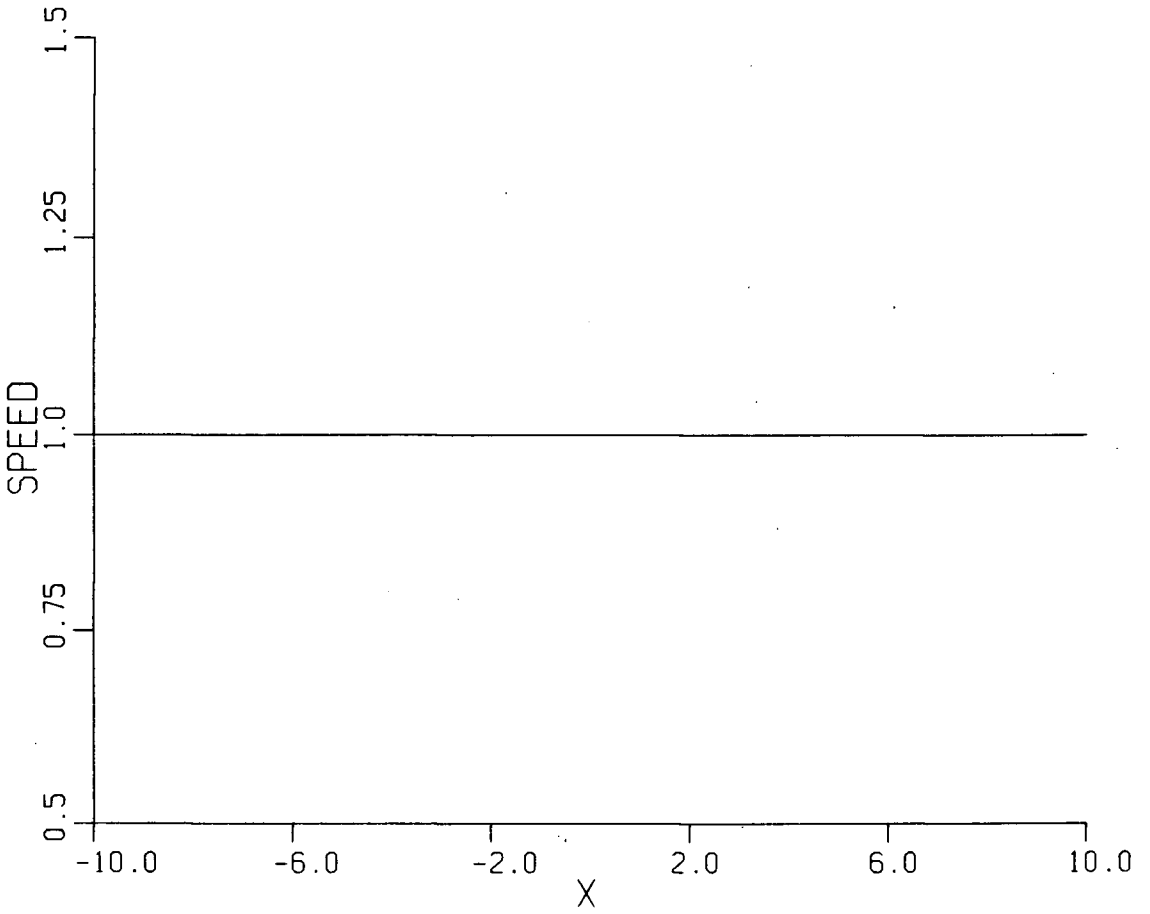

Figure 7a. Sequence of space-like slices showing the space-time evolution of the modon translation speed for modon propagation over a slowly varying gaussian ridge centered at X=0. This plot shows the initial condition (i.e. at T=0.0) on the translation speed (i.e. c(X,Y,0)=1).

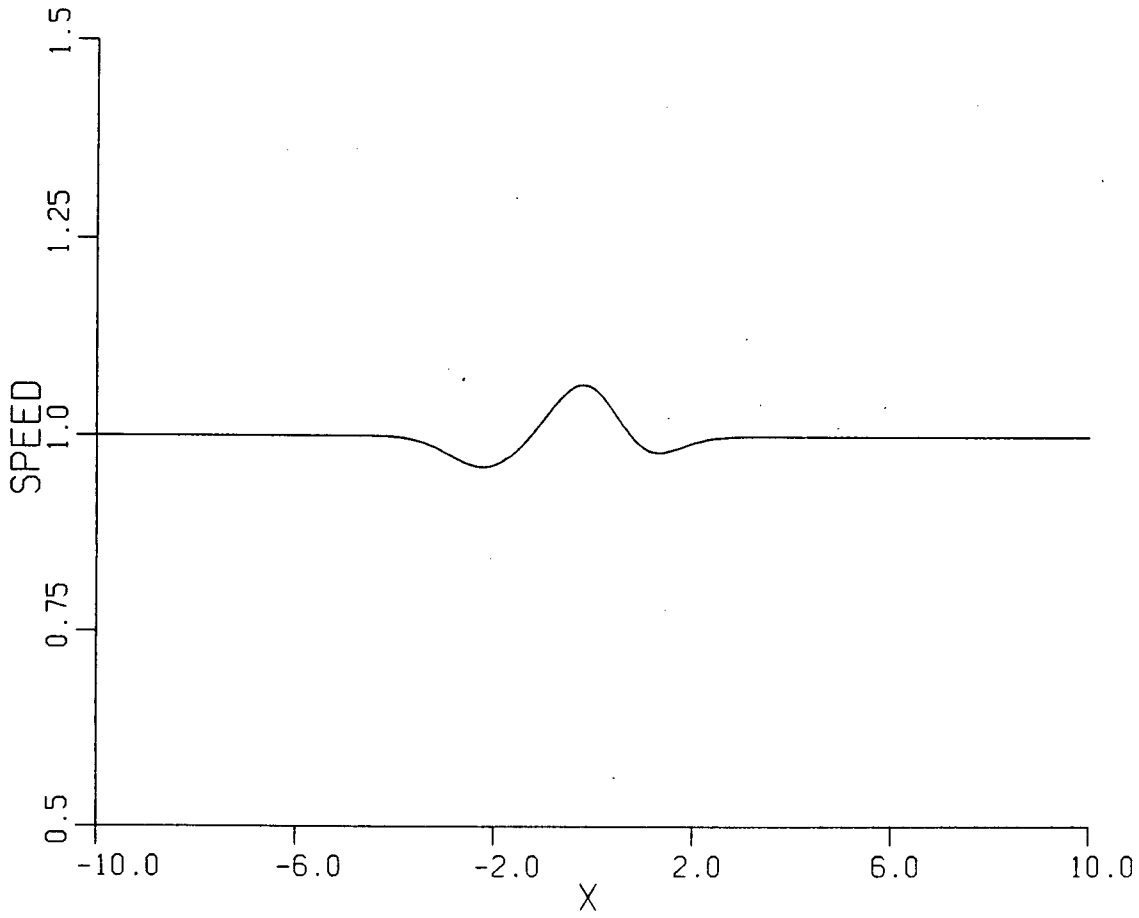

Figure 7b. Space-like structure of the modon translation speed induced by a gaussian ridge at T=0.2.

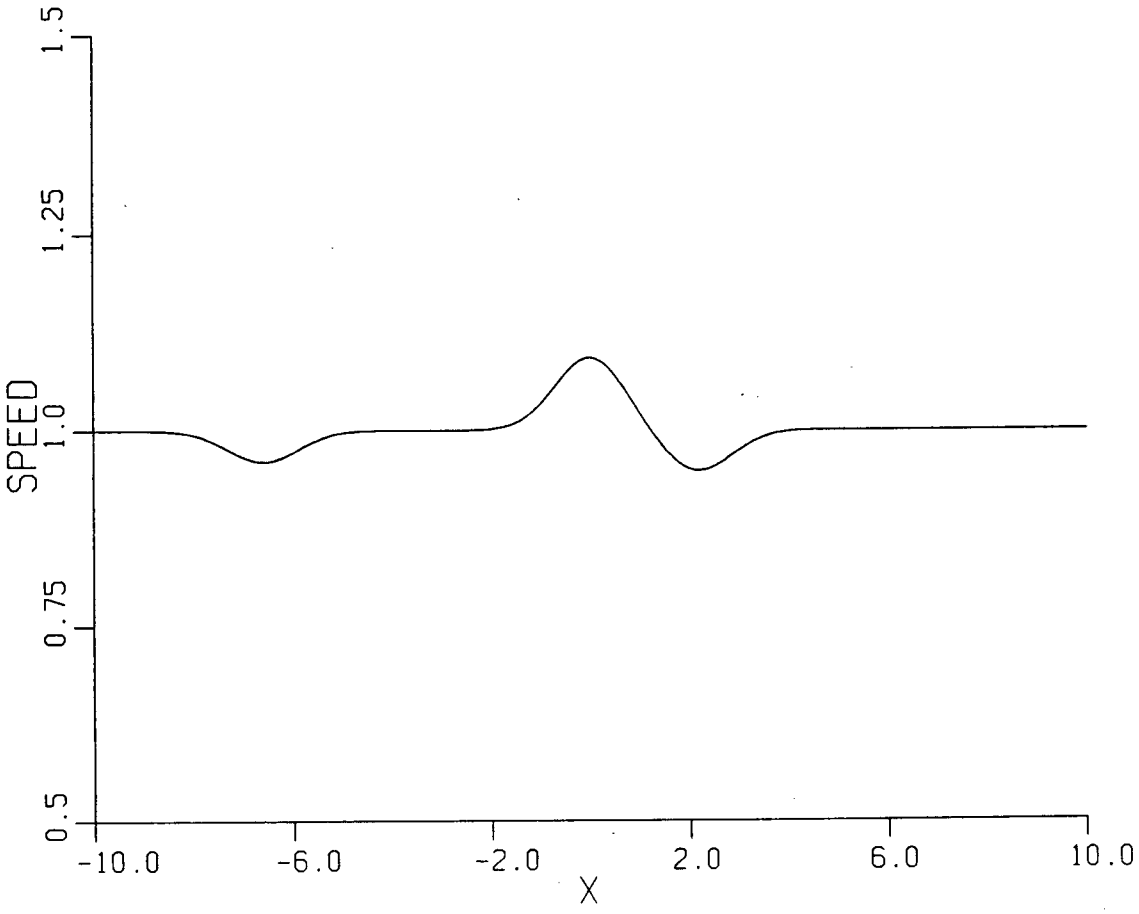

Figure 7c. Space-like structure of the modon translation speed induced by a gaussian ridge at T=0.6.

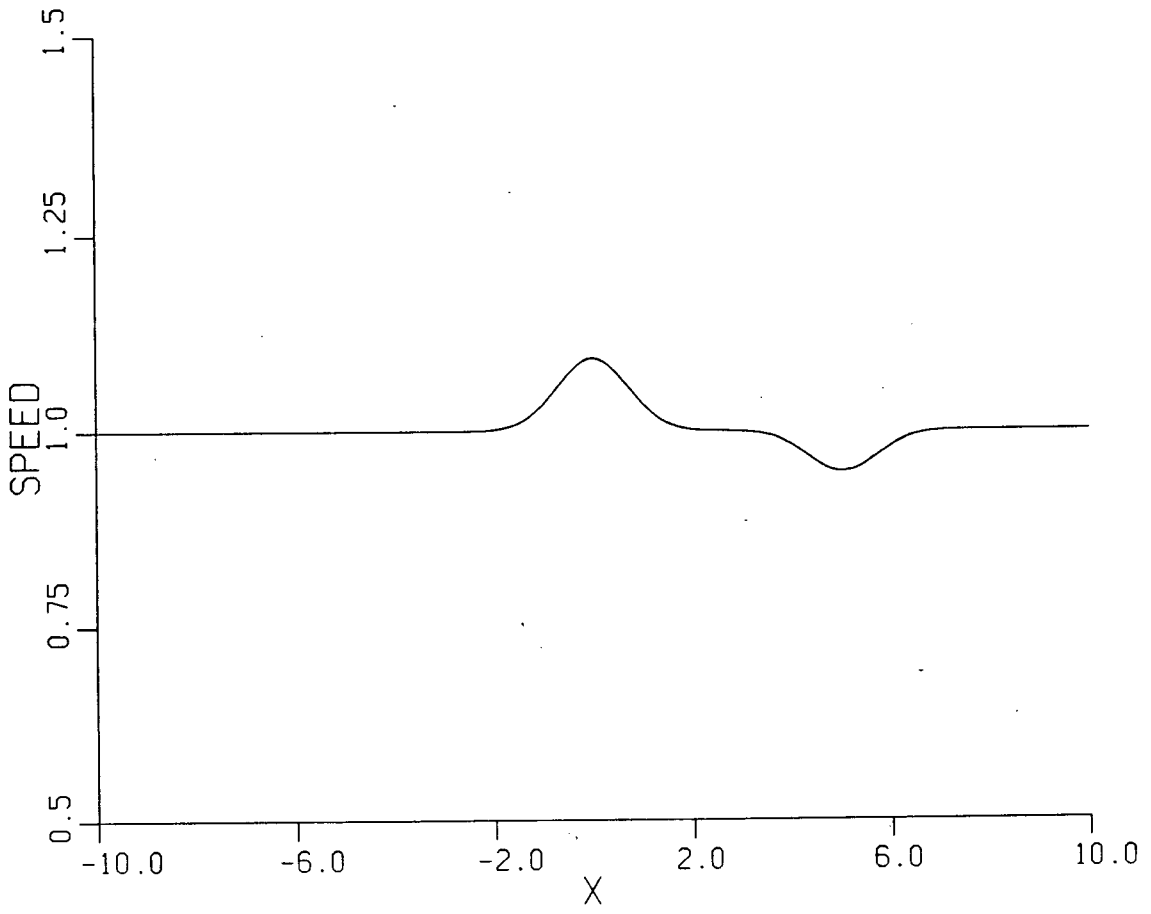

Figure 7d. Space-like structure of the modon translation speed induced by a gaussian ridge at T=1.4.

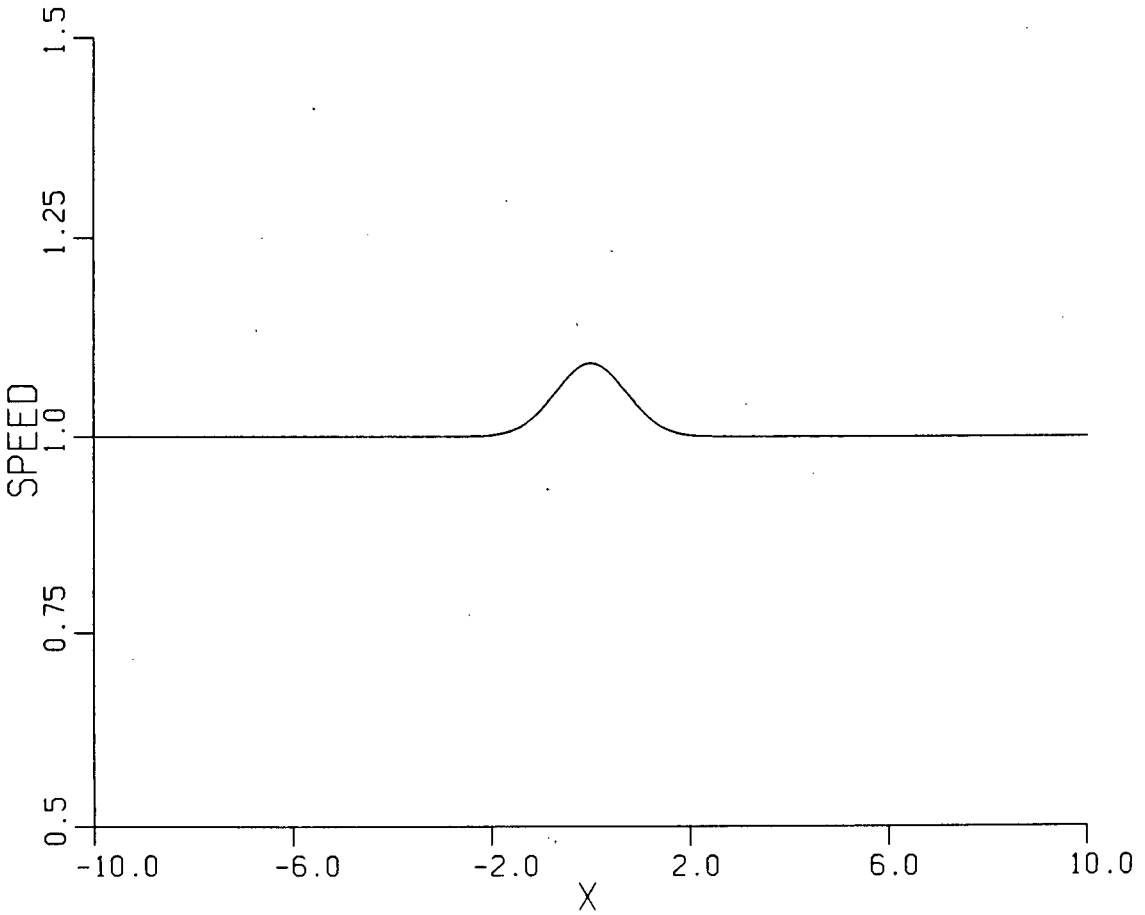

Figure 7e. Space-like structure of the modon translation speed induced by a gaussian ridge at T=4.0.

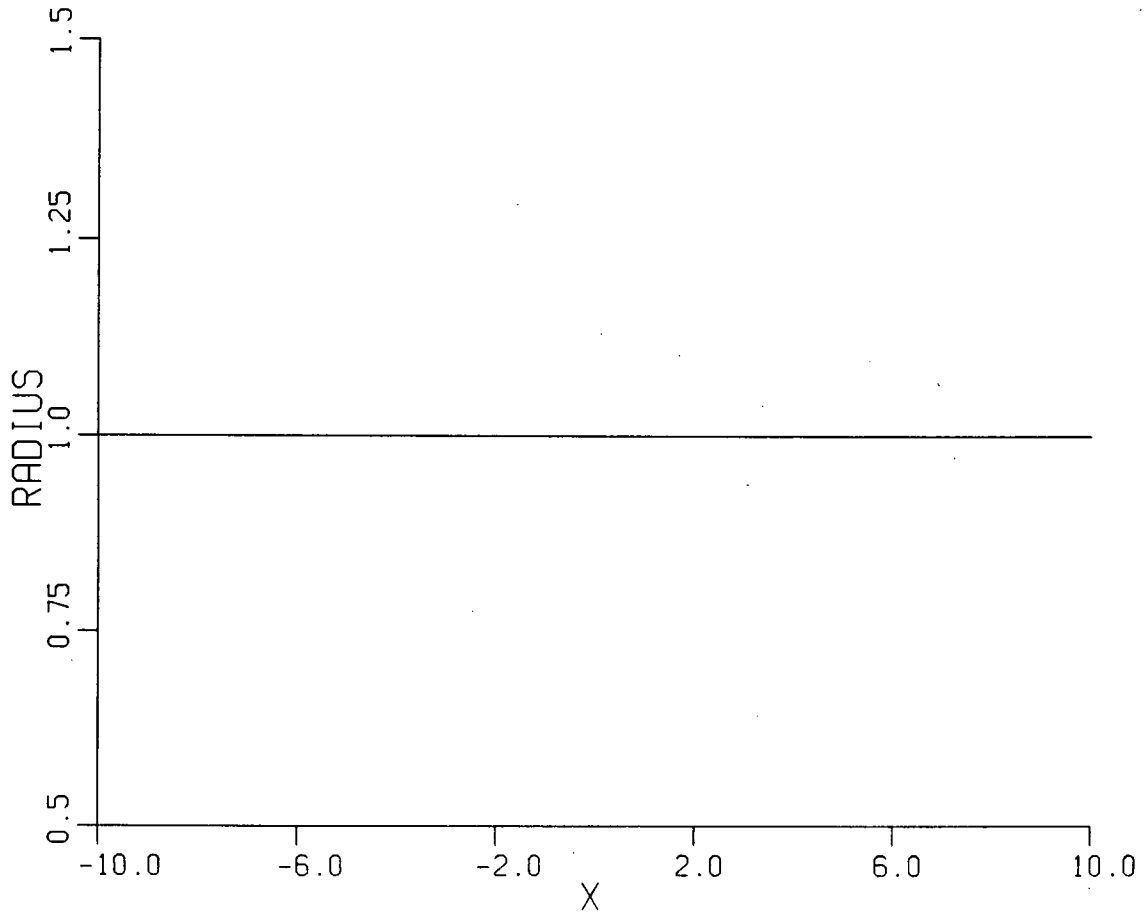

Figure 8a. Sequence of space-like slices showing the space-time evolution of the modon radius for modon propagation over a slowly varying gaussian ridge centered at X=0. This plot shows the initial condition (i.e. at T=0.0) on the radius (i.e. a(X,Y,0)=1).

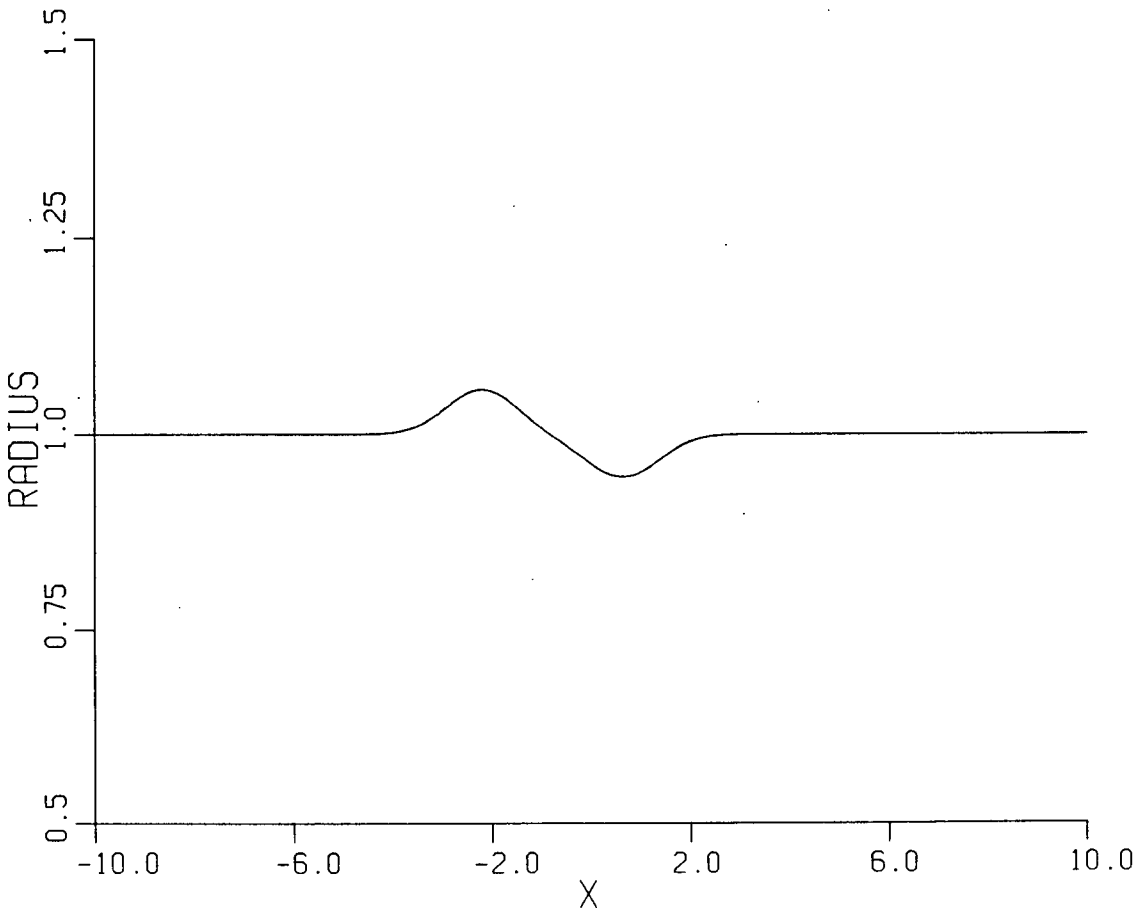

Figure 8b. Space-like structure of the modon radius induced by a gaussian ridge at T=0.2.

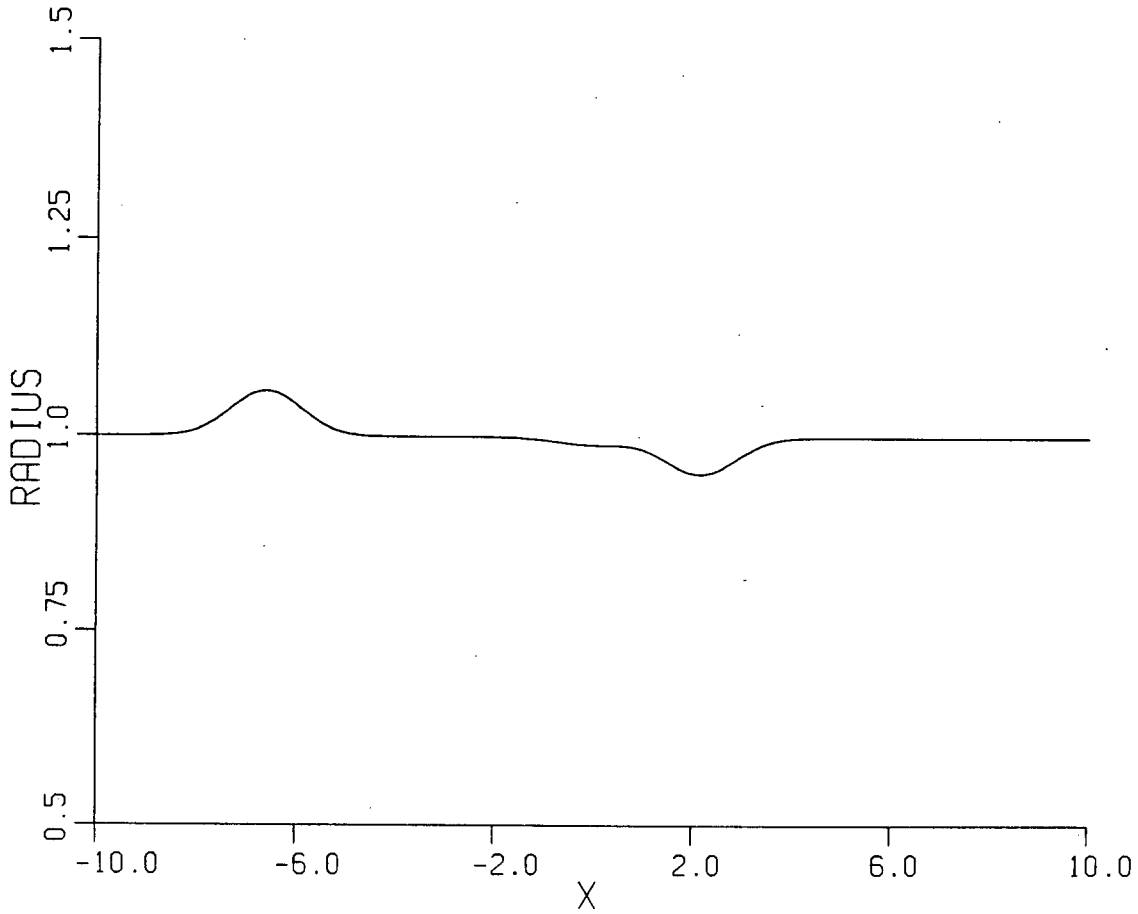

Figure 8c. Space-like structure of the modon radius induced by a gaussian ridge at T=0.6.

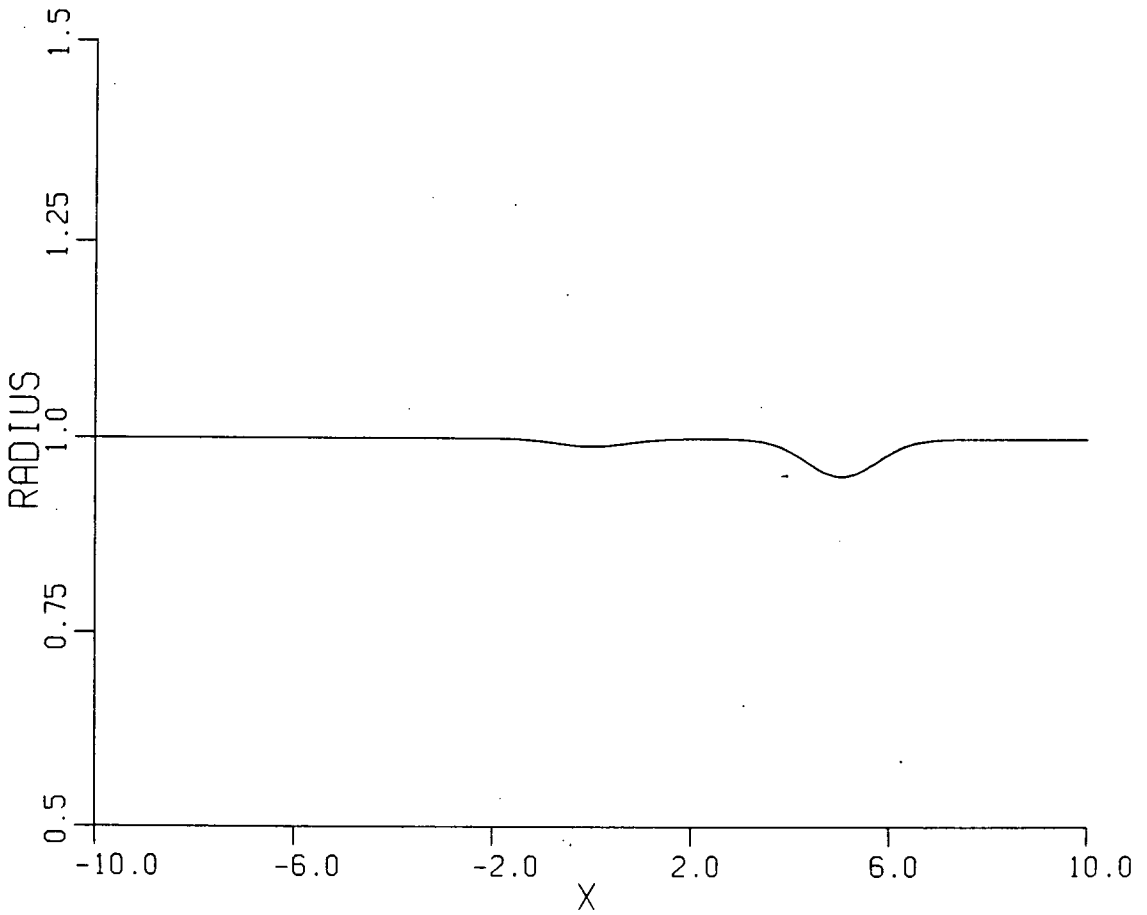

Figure 8d. Space-like structure of the modon radius induced by a gaussian ridge at T=1.4.

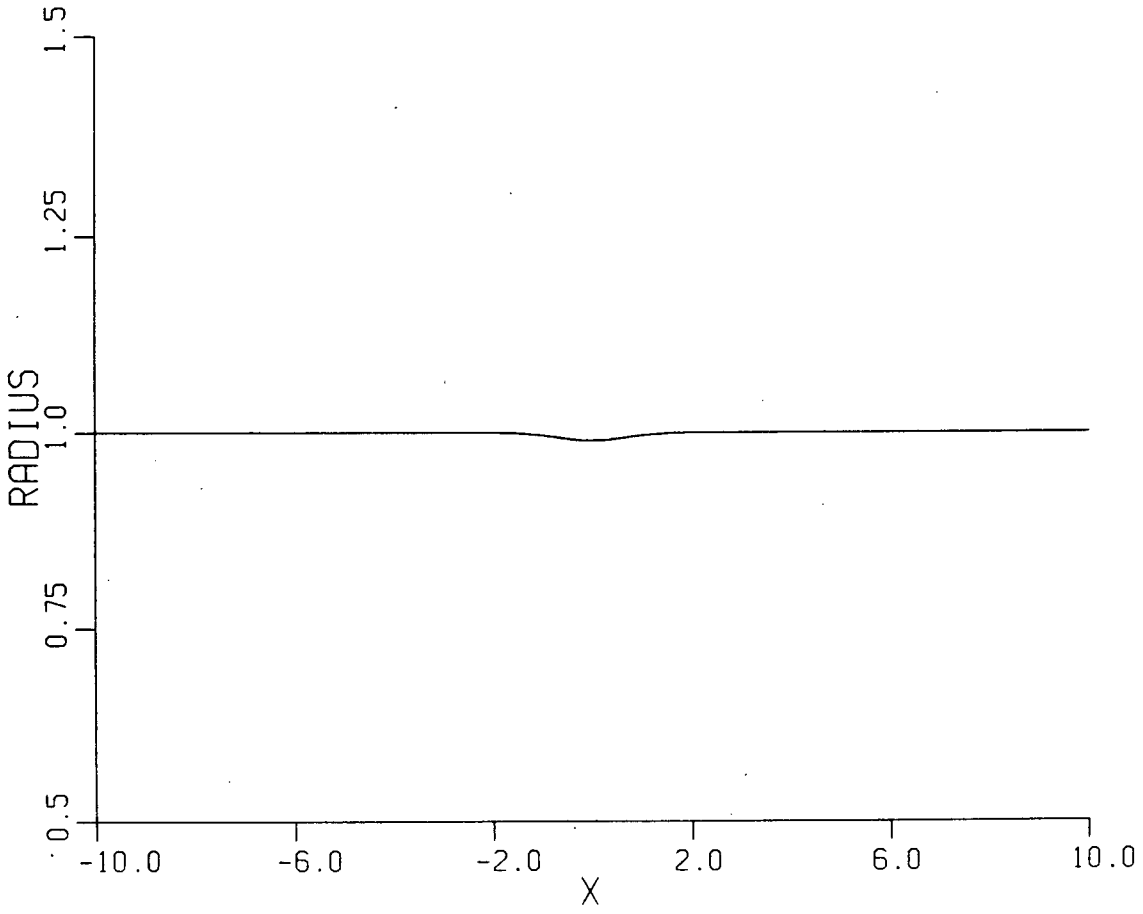

Figure 8e. Space-like structure of the modon radius induced by a gaussian ridge at T=4.0.

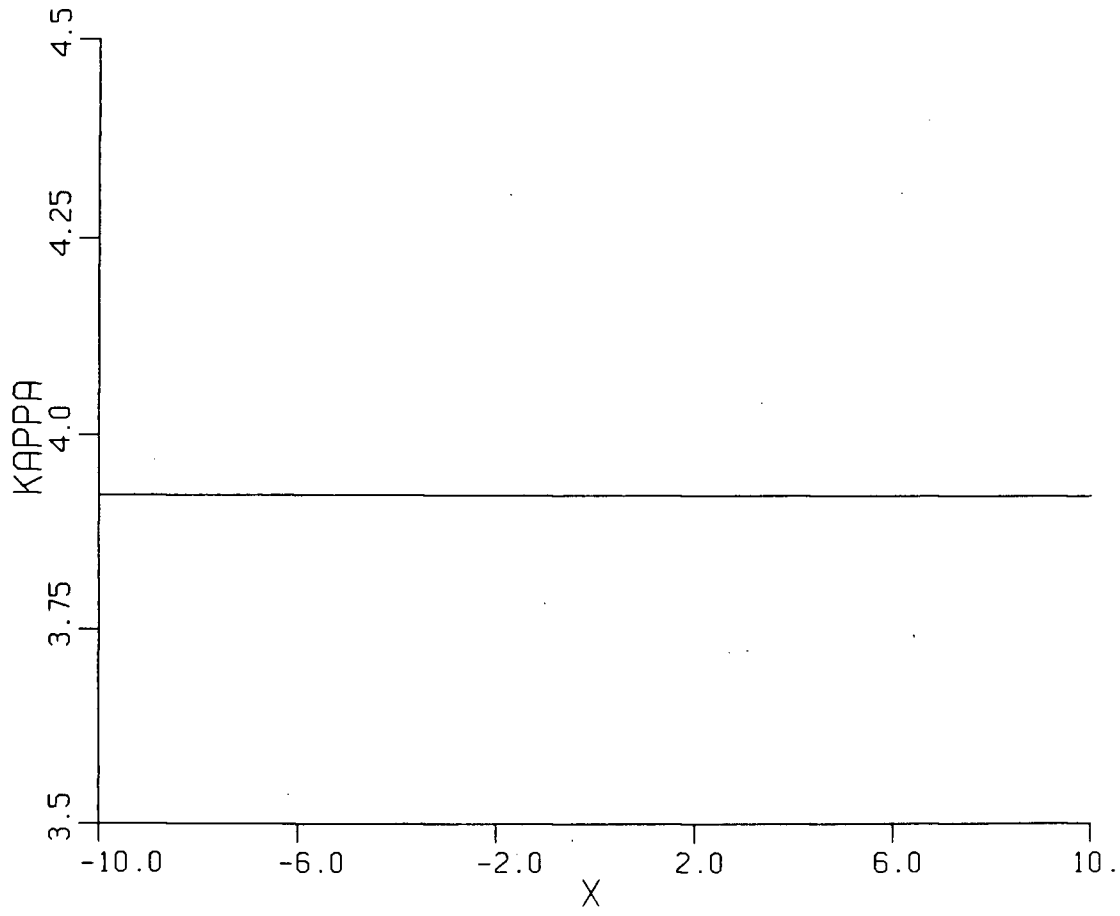

Figure 9a. Sequence of space-like slices showing the space-time evolution of the modon wavenumber for modon propagation over a slowly varying gaussian ridge centered at X=0. This plot shows the initial condition (i.e. at T=0.0) on the wavenumber (i.e. $\kappa(X,Y,0)=\kappa_0$).

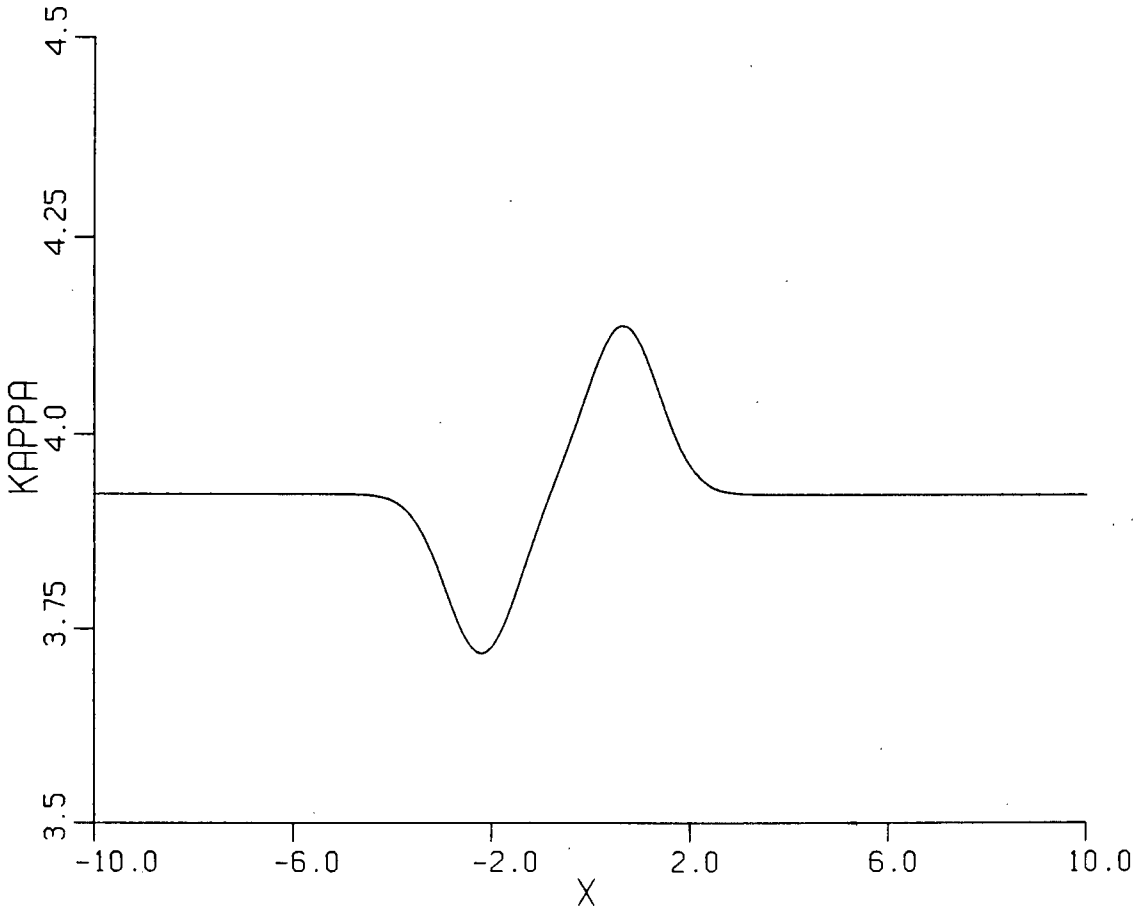

Figure 9b. Space-like structure of the modon wavenumber induced by a gaussian ridge at T=0.2.

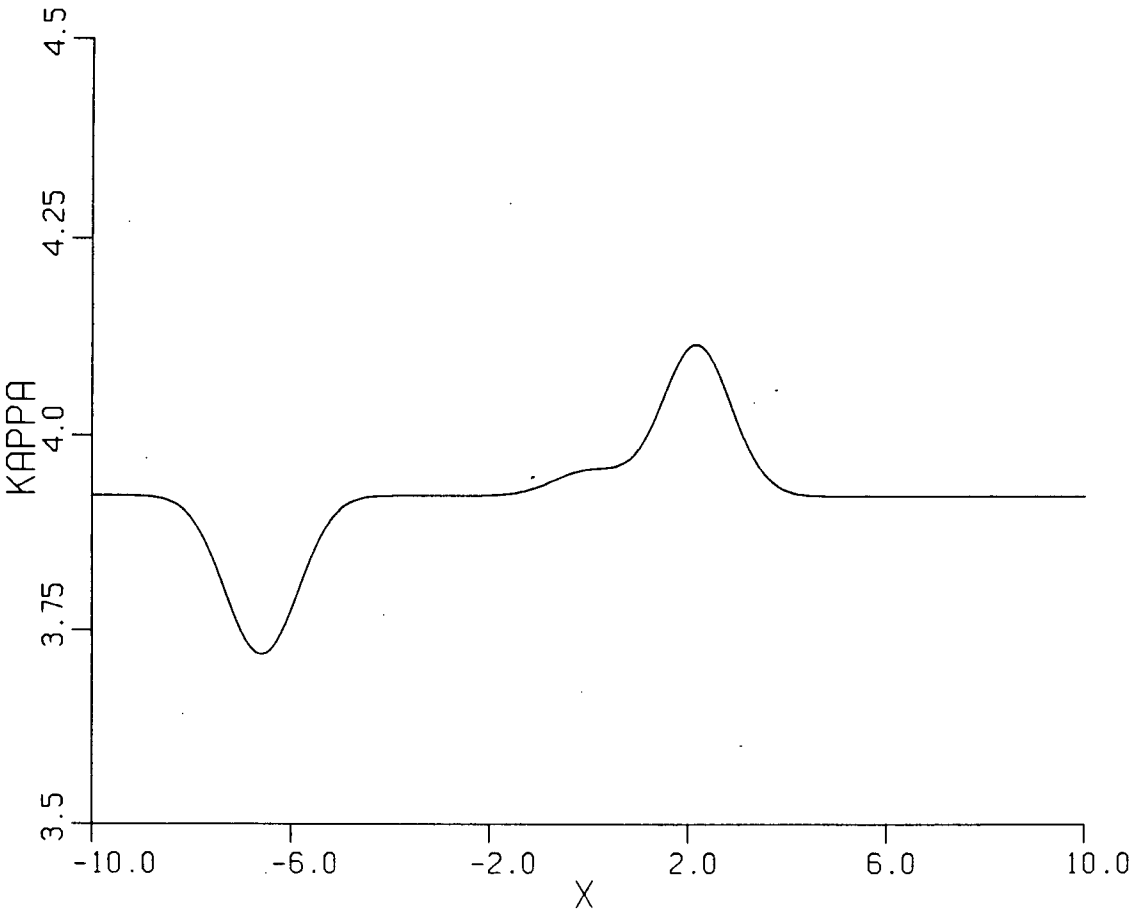

Figure 9c. Space-like structure of the modon wavenumber induced by a gaussian ridge at T=0.6.

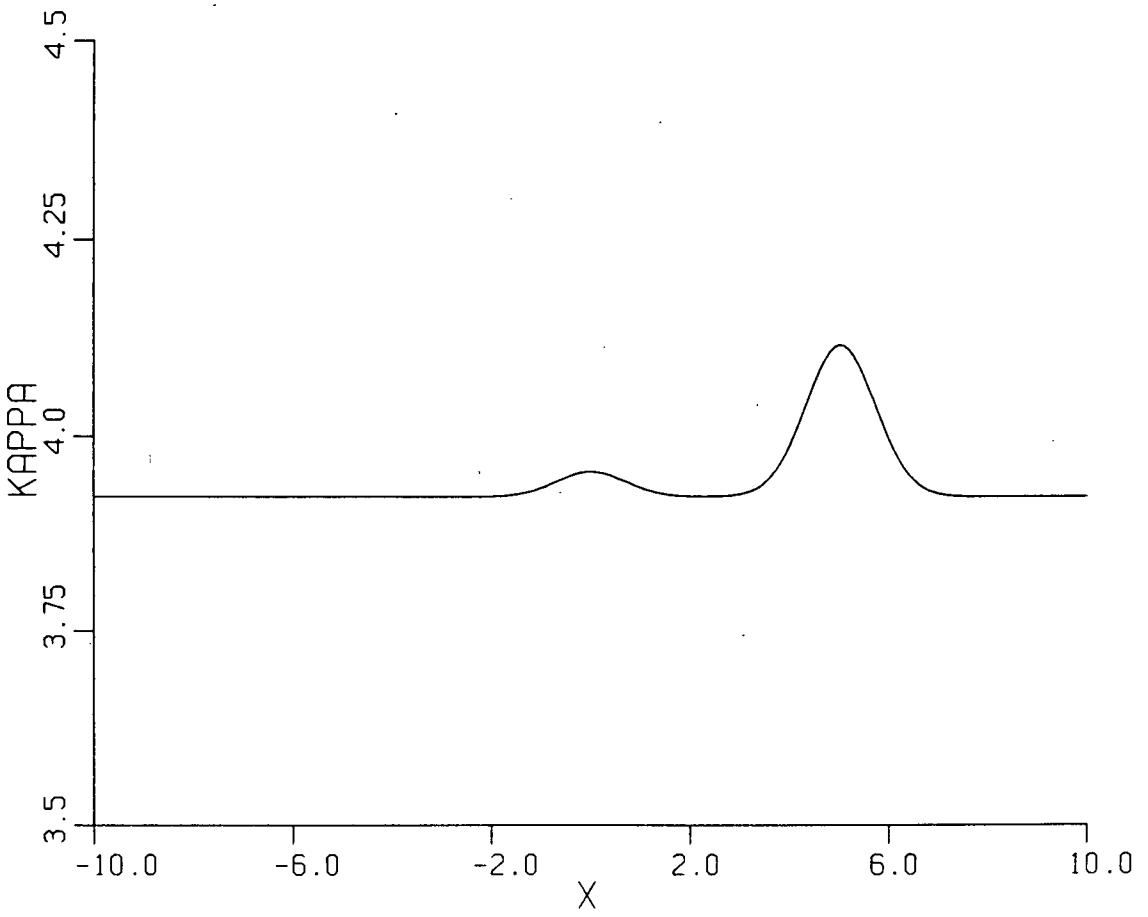

Figure 9d. Space-like structure of the modon wavenumber induced by a gaussian ridge at T=1.4.

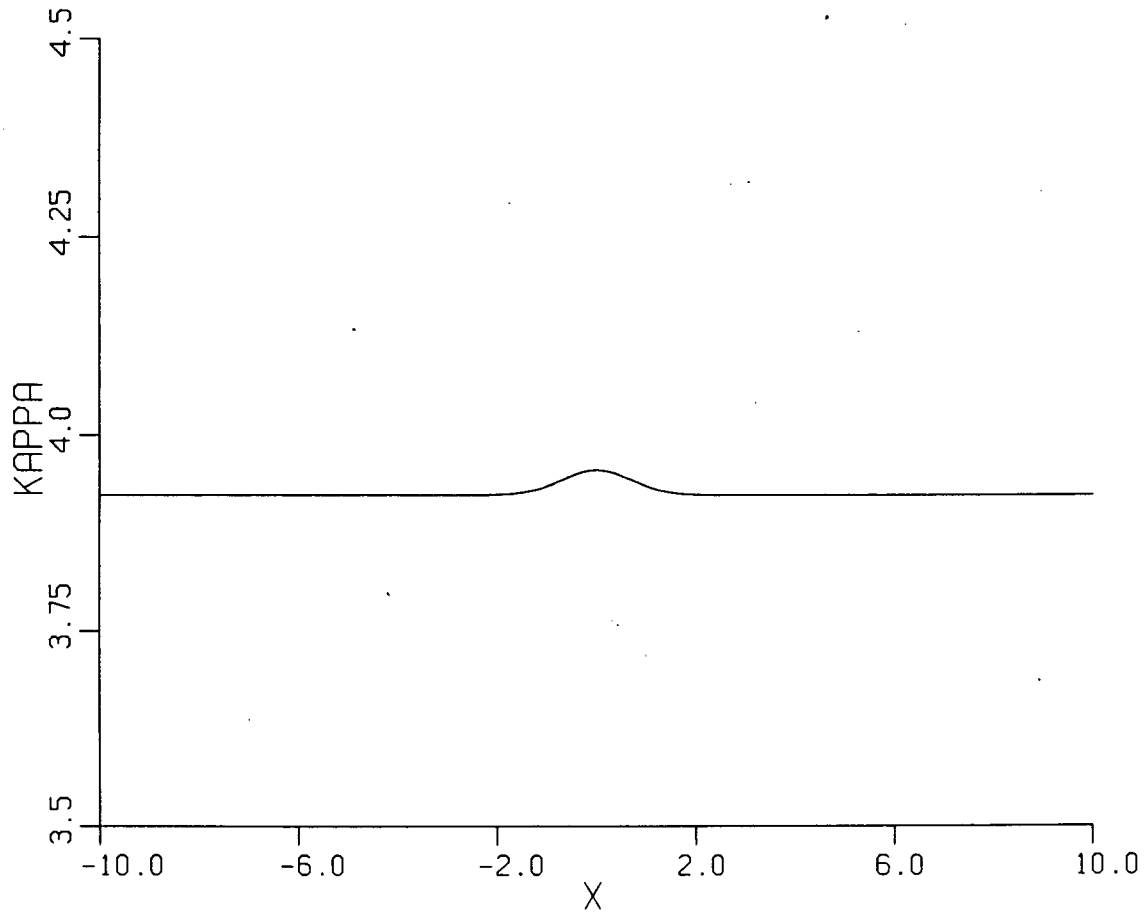

Figure 9e. Space-like structure of the modon wavenumber induced by a gaussian ridge at T=4.0.

3.2.4 Tanh-escarpment Topography

In this Subsection the solution for modon propagation over a slowly varying escarpment is described. The topography is given by

$$H(X,Y) = 1 - \mu\{1 + \tanh(X)\}/2, \qquad (3.2.37)$$

hence $h(X,Y) = \{1 + \tanh(X)\}/2$. Since $h \to 0$ and $h \to 1$ as $X \to -\infty$ and $X \to \infty$ respectively, the qualitative behaviour of the solutions will follow the analysis given in Subsection 3.2.3 for the case $0 \le h \le A^* < \infty$. Figures 10, 11 and 12 illustrate the spatial structure of the modon translation speed $c=1+\mu c^{(1)}$, modon radius $a=1+\mu a^{(1)}$ and modon wavenumber $\kappa=\kappa_0+\mu\kappa_0\kappa^{(1)}$ respectively, with $\mu=0.2$ for the sequence of slow times T=0.0, 0.2, 0.6, 1.4 and 4.0.

These figures represent space-like slices (i.e., T held constant) in space-time of the solutions for the modon translation speed, modon radius and modon wavenumnber. As stated in Subsection 3.2.3 the particular values of a, c and κ that the modon experiences at a given time are determined by the interSection of the characteristic on which the modon is propagating and the characteristics defining the individual solution components in (3.2.20), (3.2.21) and (3.2.22). The modon characteristic is defined by (3.2.26) or (3.2.27) or asymptotically (i.e., $T \ll 1$) by (3.2.28) with h(X) given in (3.2.37).

The qualitative analysis of the interaction between the escarpment topography in this Subsection follows that of the description given last Subsection. Thus we only briefly comment on the similar aspects and highlight the differences. Figure 10 shows space-like slices in space-time of the slowly varying modon translation speed. As in Subsection (3.2.3) the westward-travelling transient acts to reduce the modon translation speed (see Figure 10a) for $X<0$ and the eastward-travelling transient acts to increase the translation speed for $X>0$. Similarly, the modon radius (wavenumber) is increased (decreased) by the westward-travelling transient and decreased (increased) by the eastward=travelling transient.

However the fact that $h(X)\to 1$ as $X\to+\infty$ is of crucial importance here. The escarpment forces a permanent deformation in the modon once initial interaction begins. The westward-travelling and eastward-travelling transients have the role of transmitting information of the eastward and westward topographic configurations. If a modon has initial position $\epsilon\xi_0<0$, after sufficient time the modon characteristic will intersect the characteristics containing the $X>0$ topographic information. However since the upstream topography does not eventually approach zero all subsequent westward-travelling characteristics will carry a nonzero signal. Therefore the spatial structure of the modon parameters is continuously deformed.

This spatial deformation is shown in Figures 10, 11 and 12. The westward-travelling transient results in a continued

reduction in the modon translation speed for X<0 and a continued increase in the modon translation speed for X>0 (see Figures 10b, 10c and 10d for the transient behaviour and Figure 10d for the local steady-state structure).

The modon radius is increased for the entire domain upstream of the leading edge of the westward-travelling transient. There is relative decrease in the radius across X=0 since the coefficient of the stationary component of the solution is negative (see Subsection 3.2.3). Figures 11b, 11c and 11d illustrate the transient behaviour and Figure 11e the local steady-state structure.

The modon wavenumber is decreased for the entire domain upstream of the leading edge of the westward-travelling transient. There is a relative increase in the modon wavenumber across X=0 since the amplitude of the stationary component is positive (see Subsection 3.2.3). Figures 12b, 12c and 12d illustrate the transient structure and Figure 12e the local steady-state solution.

As an example of the qualitative behaviour of the slow evolution of the modon as it goes up and over a escarpment of the form (3.2.39) suppose initially that the modon center is at $\epsilon\xi_0=-10$. The modon initially propagates eastward unaffected by the upstream topography. Eventually after sufficient time the modon characteristic intersects the characteristics carrying the nonzero upstream topographic information. The modon translation speed decreases, its radius increases and its wavenumber decreases. Since the upstream topography remains nonzero as X

increases and the westward-travelling transient carries this information, the modon characteristic continues to intersect nontrivial westward-travelling transient characteristics. Thus the translation speed remains reduced, the radius remains increased and the wavenumber remains decreased. After sufficient further time the modon propagates up over the escarpment and the translation speed increases, the radius decreases and the wavenumber increases since the modon characteristic is intersecting the characteristics associated with the stationary part of the perturbation solutions.

This qualitative analysis assumed that the escarpment increased from $X<0$ to $X>0$. If the reverse had been assumed, the above behaviour would be reversed. If the initial position of the modon is positive (e.g., $\epsilon\xi_0>0$), the modon will initially be unaffected by the topography. If $\epsilon\xi_0$ is large (e.g., 10), the characteristics associated with the westward-travelling transient and the stationary component carry constant information (i.e., $h(X)\simeq 1$ for $X>10$). However as the modon characteristic begins to intersect characteristics associated with the topographic structure for $X<0$, the modon translation speed will increase, the modon radius will increase and the modon wavenumber will decrease.

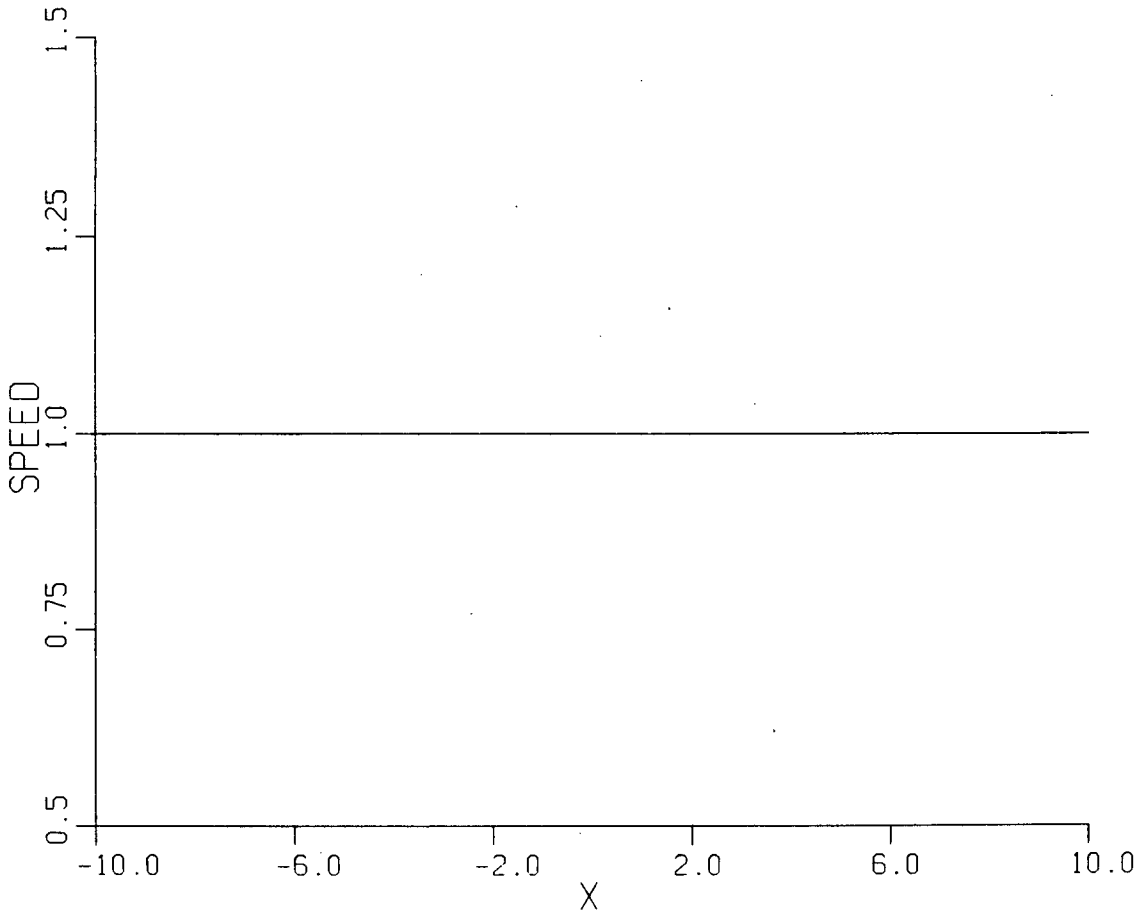

Figure 10a. Sequence of space-like slices showing the space-time evolution of the modon translation speed for modon propagation over a slowly varying hyperbolic-tangent escarpment centered at X=0. This plot shows the initial condition (i.e. at T=0.0) on the translation speed (i.e. c(X,Y,0)=1).

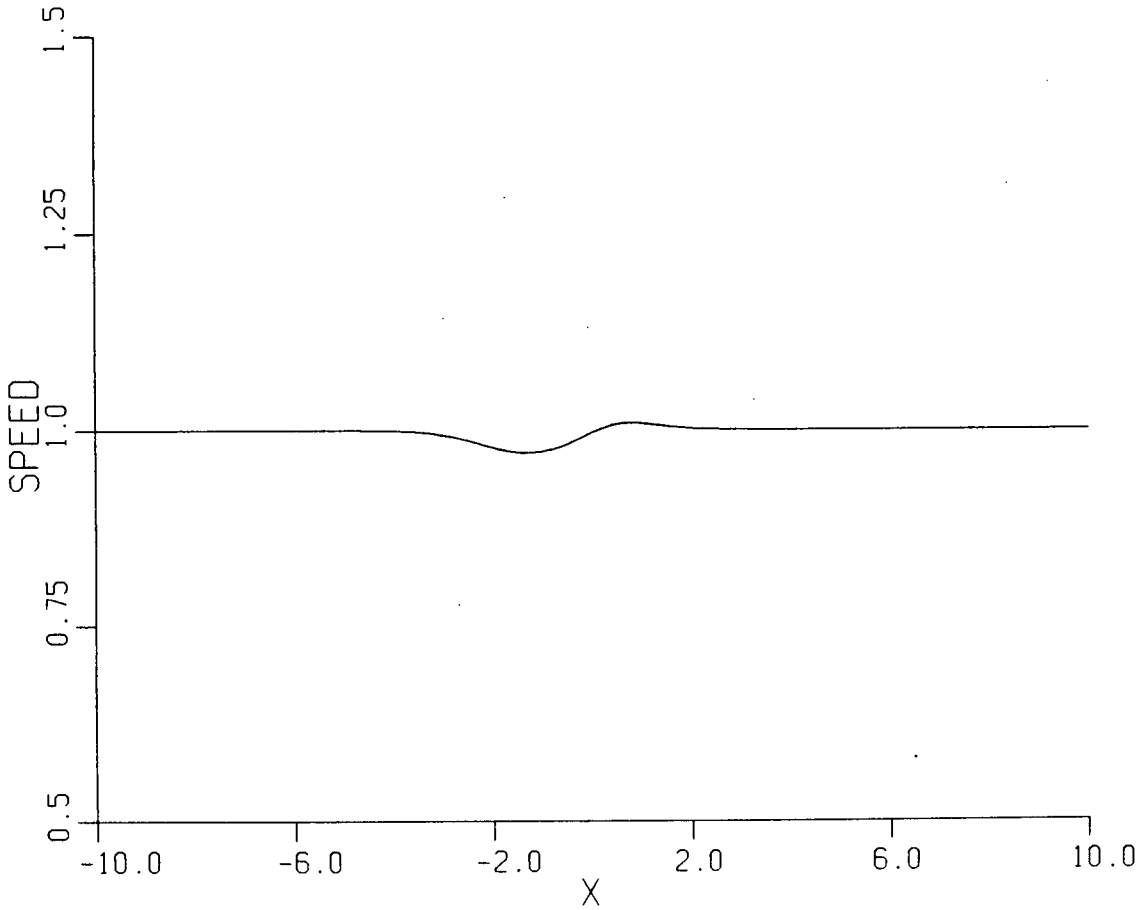

Figure 10b. Space-like structure of the modon translation speed induced by a hyperbolic-tangent escarpment at T=0.2.

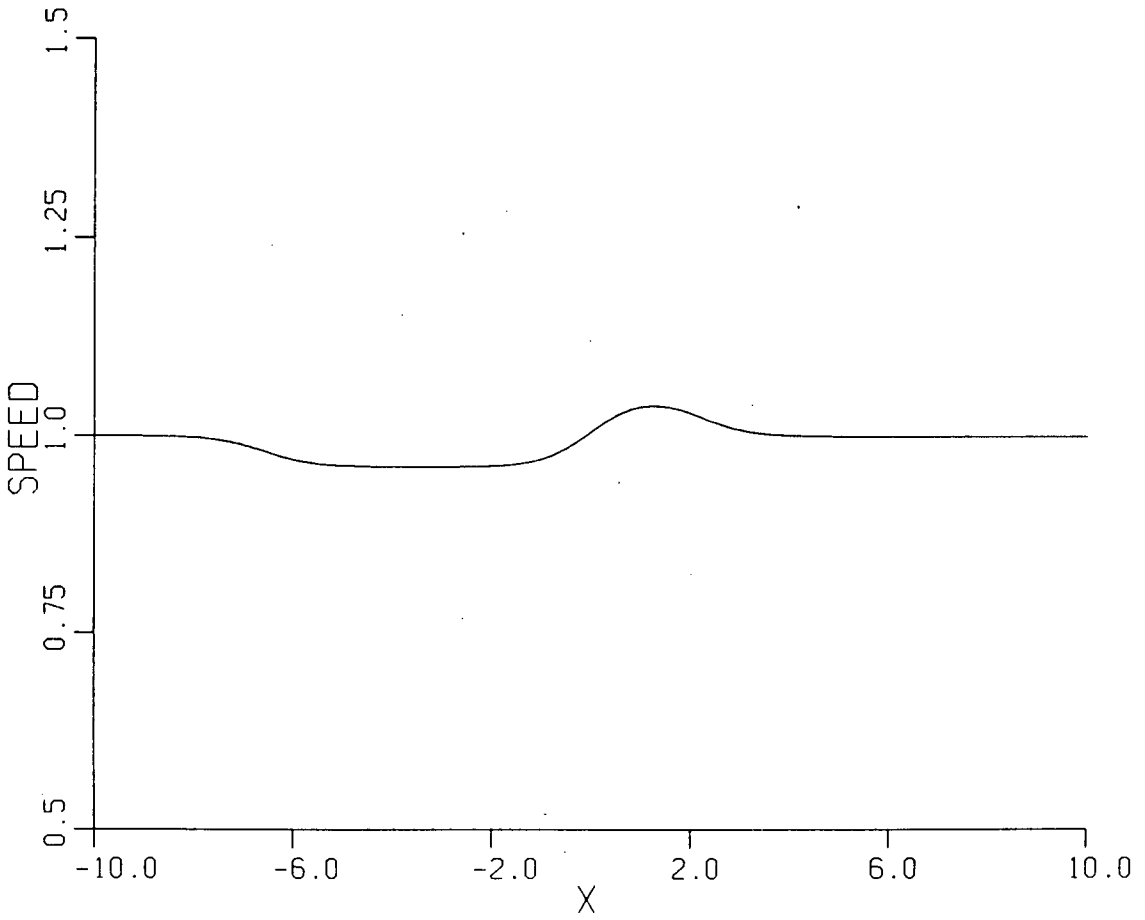

Figure 10c. Space-like structure of the modon translation speed induced by a hyperbolic-tangent escarpment at T=0.6.

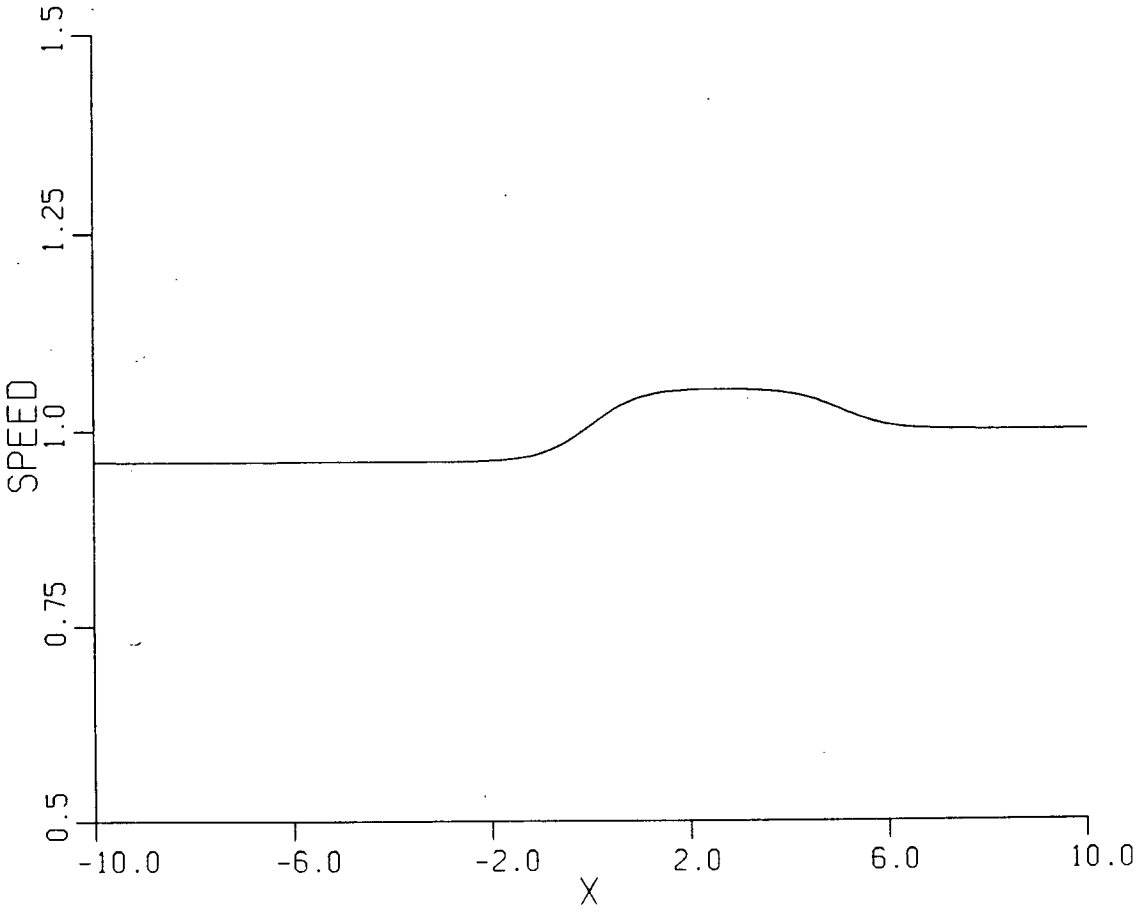

Figure 10d. Space-like structure of the modon translation speed induced by a hyperbolic-tangent escarpment at T=1.4.

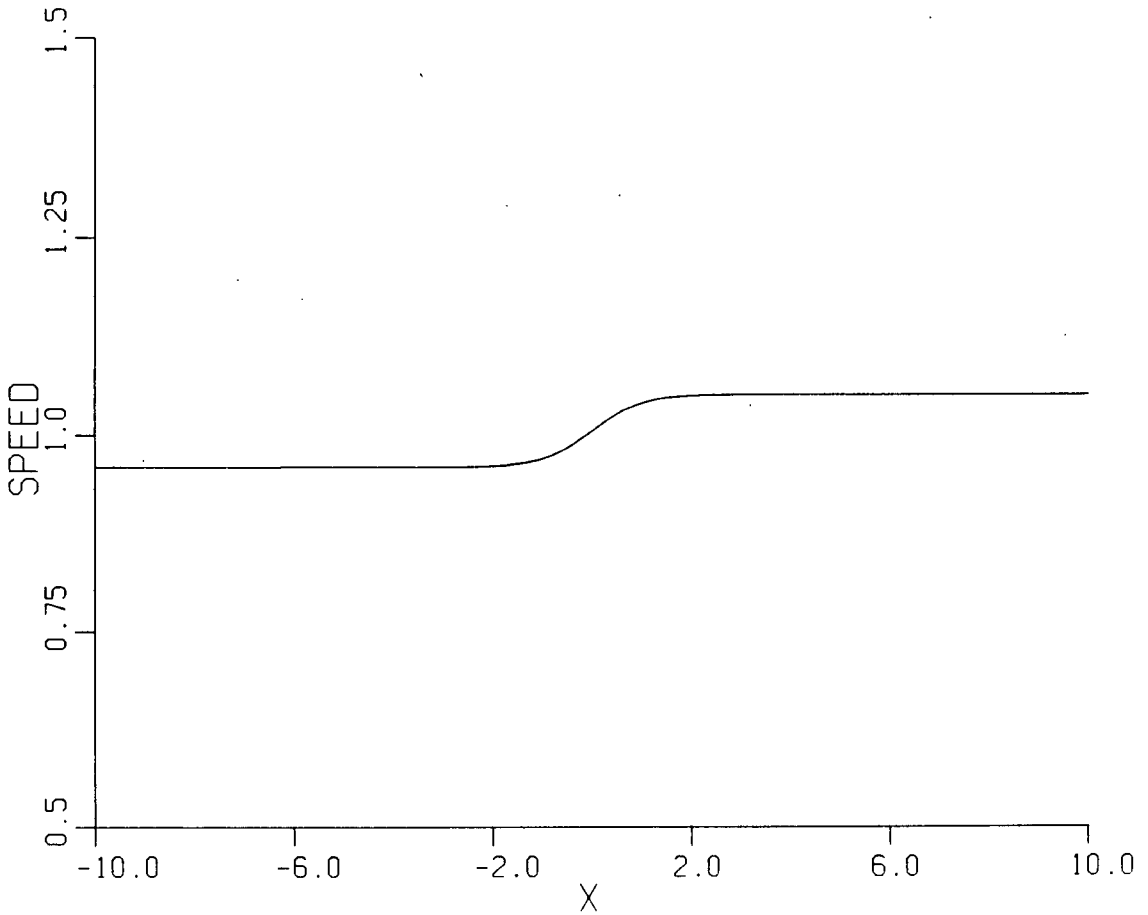

Figure 10e. Space-like structure of the modon translation speed induced by a hyperbolic-tangent escarpment at T=4.0.

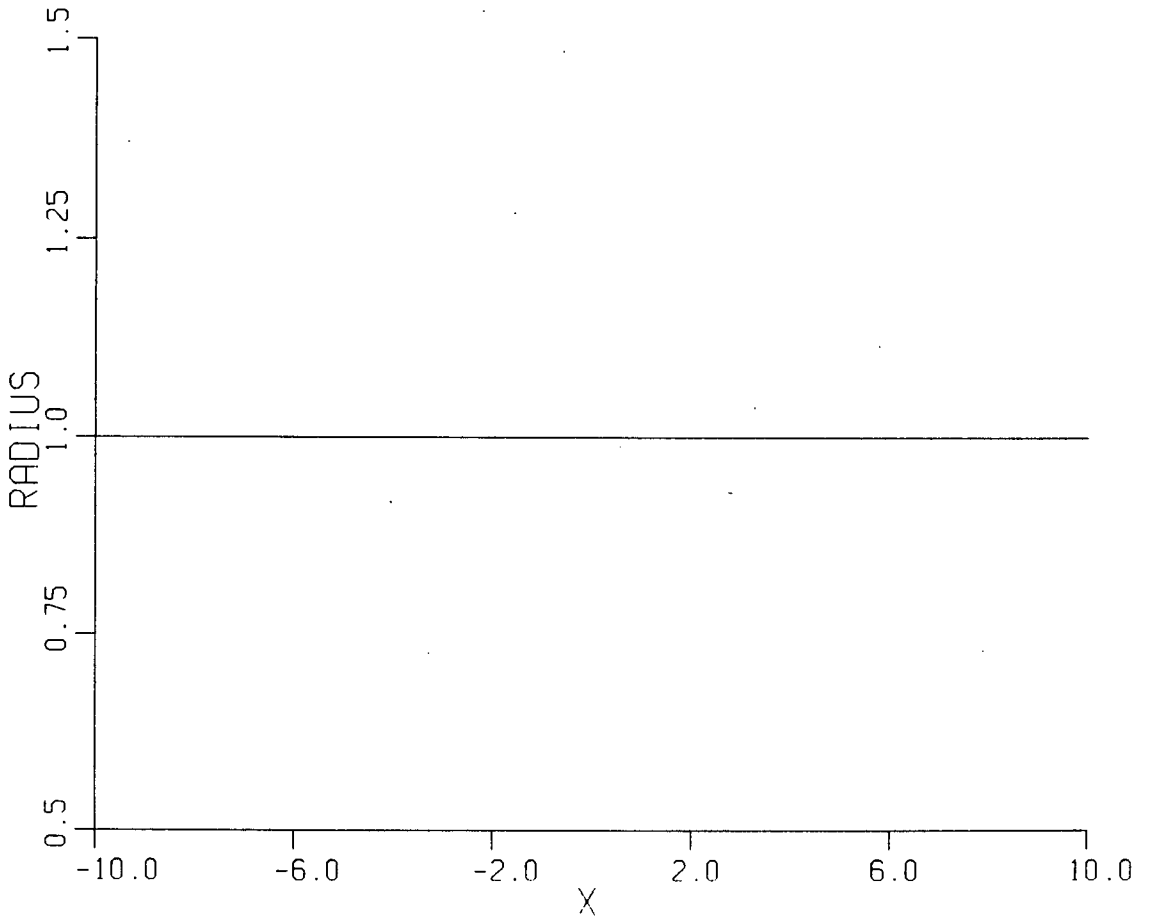

Figure 11a. Sequence of space-like slices showing the space-time evolution of the modon radius for modon propagation over a slowly varying hyperbolic-tangent escarpment centered at X=0. This plot shows the initial condition (i.e. at T=0.0) on the radius (i.e. a(X,Y,0)=1).

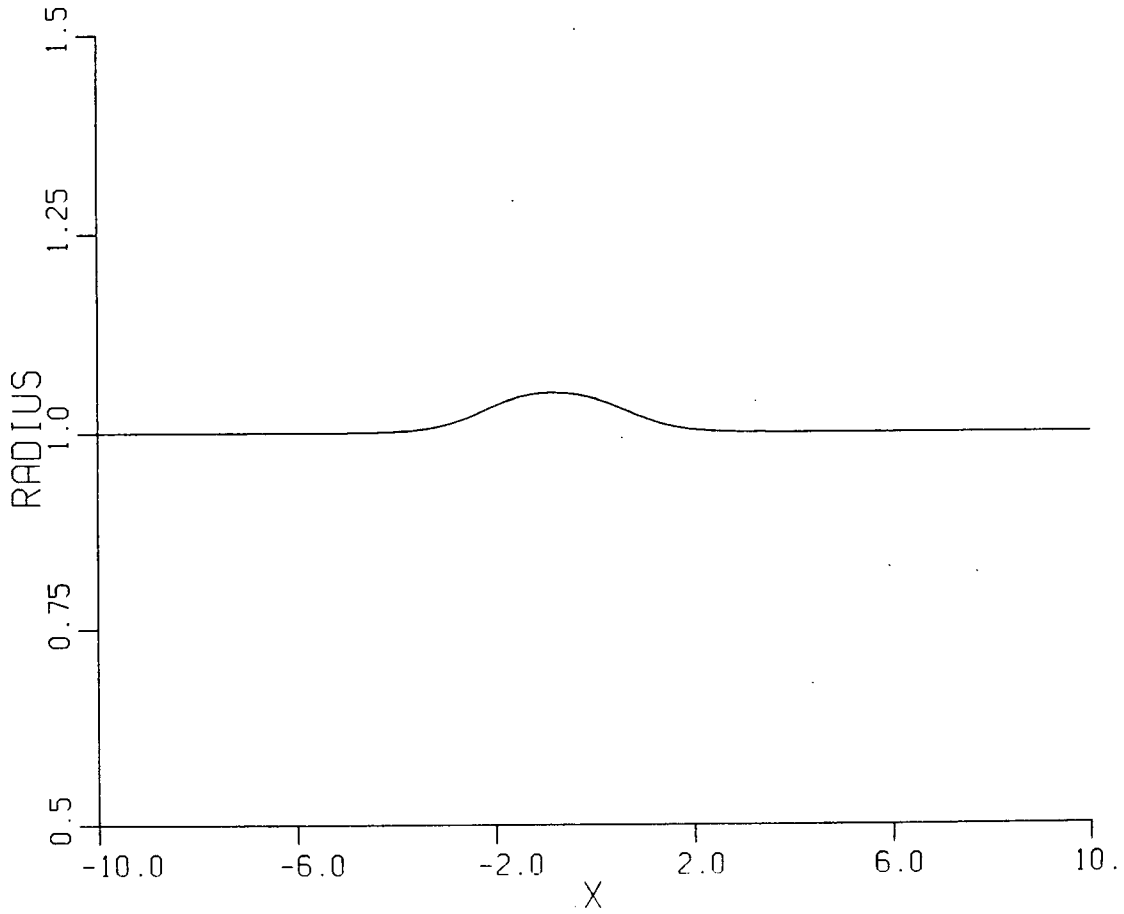

Figure 11b. Space-like structure of the modon radius induced by a hyperbolic-tangent escarpment at T=0.2.

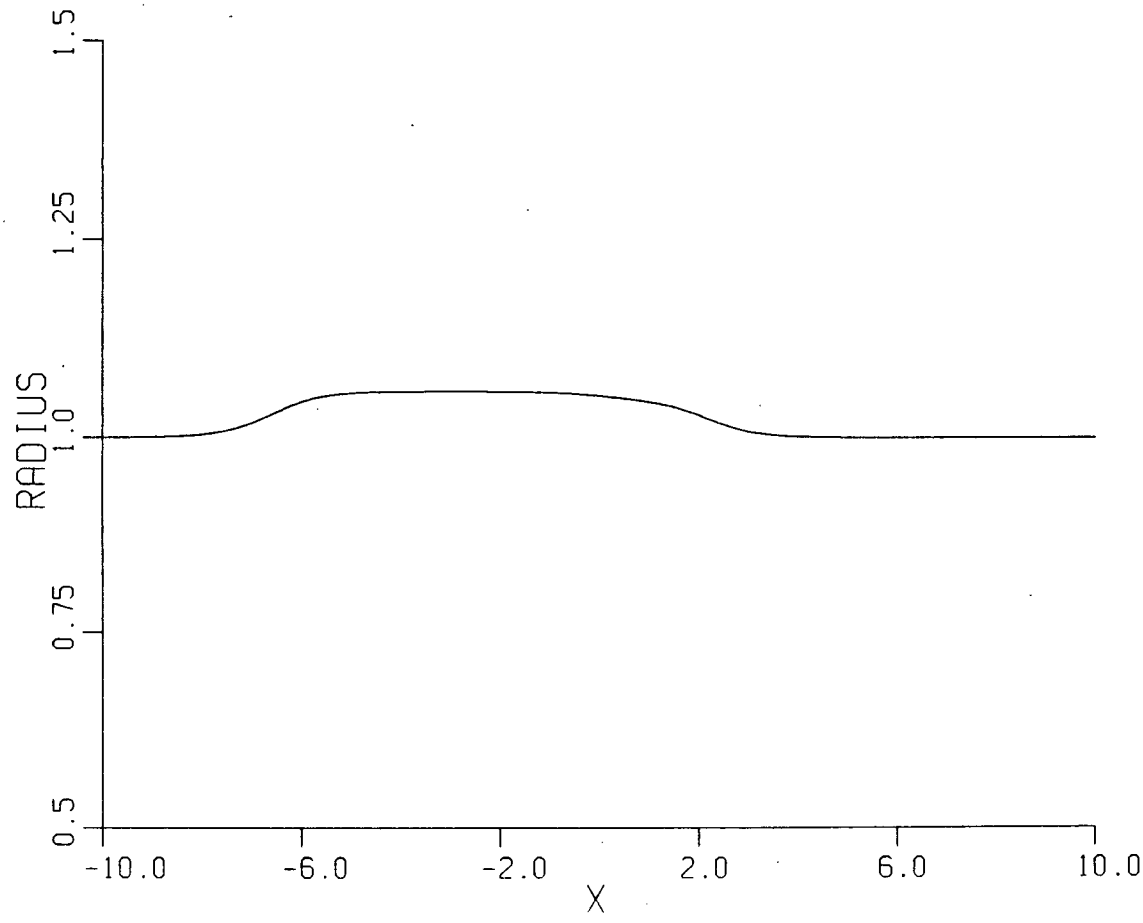

Figure 11c. Space-like structure of the modon radius induced by a hyperbolic-tangent escarpment at T=0.6.

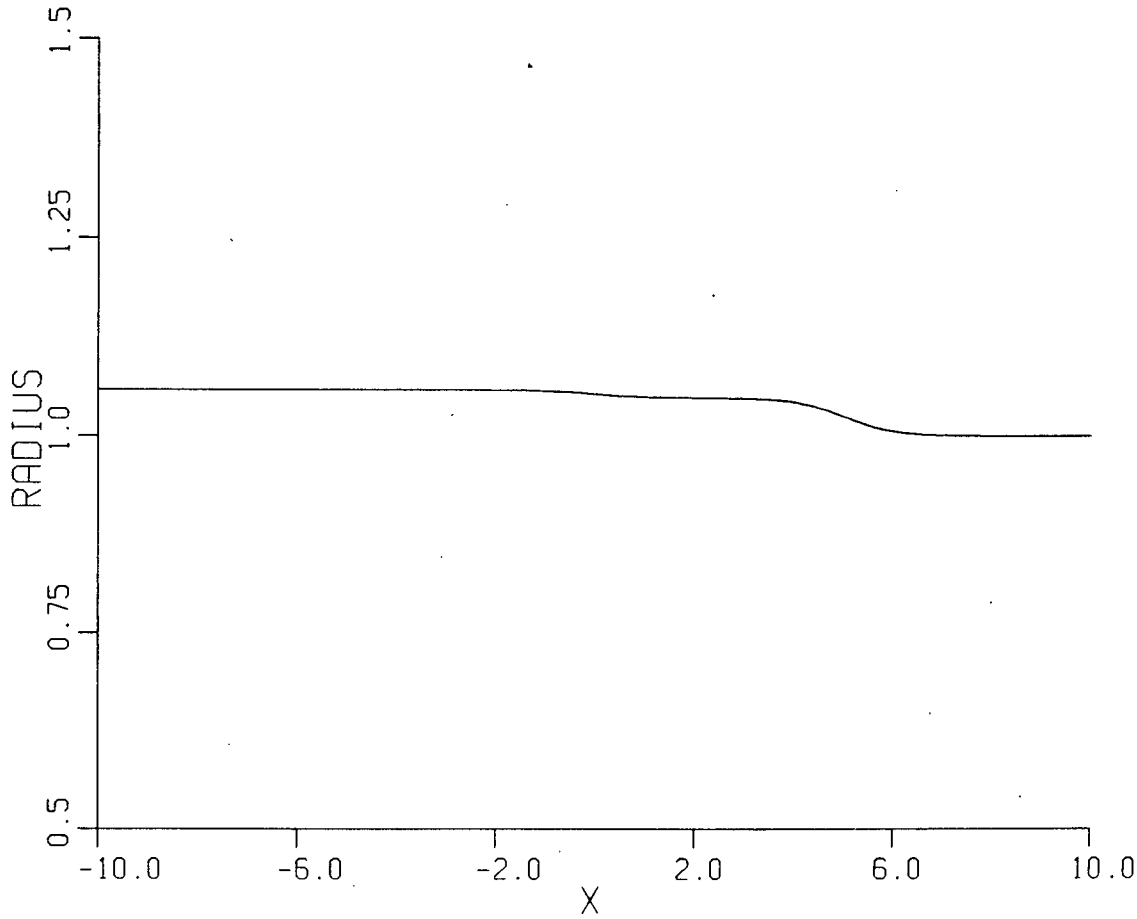

Figure 11d. Space-like structure of the modon radius induced by a hyperbolic-tangent escarpment at T=1.4.

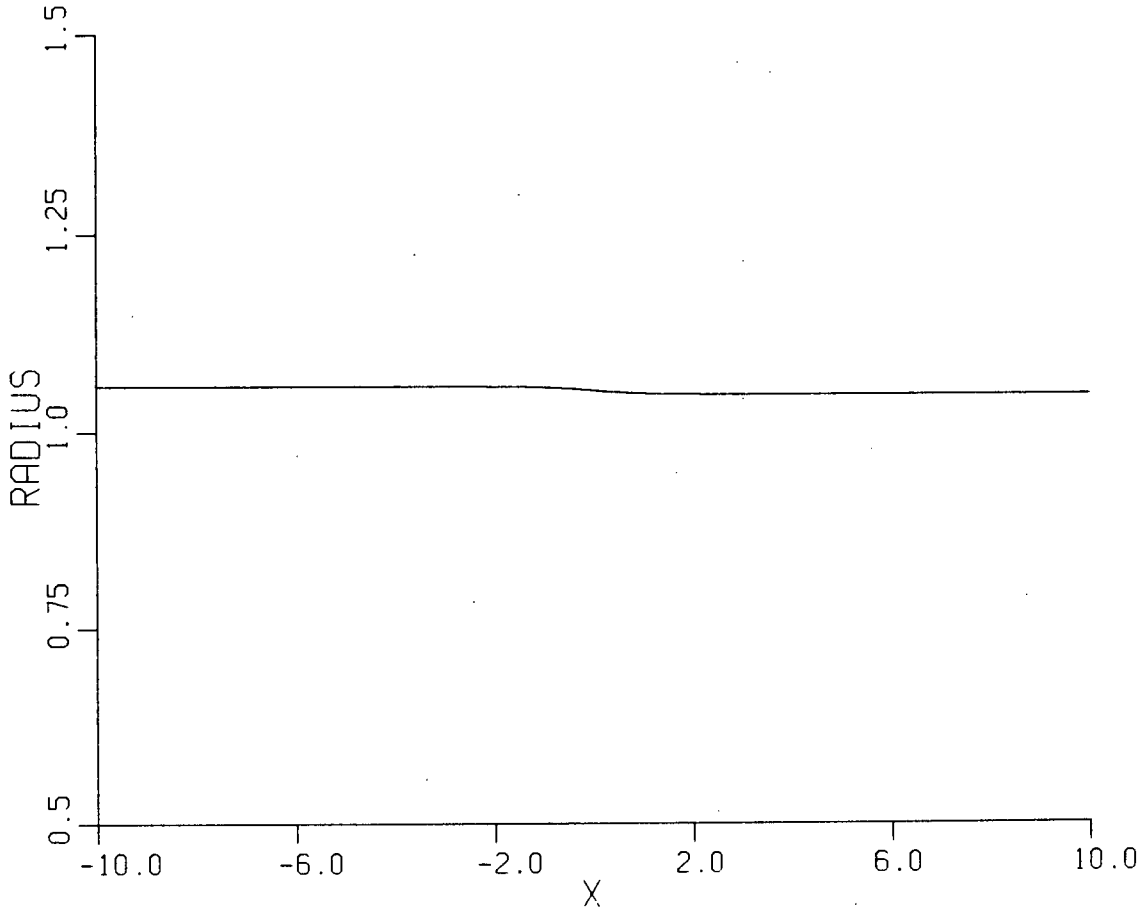

Figure 11e. Space-like structure of the modon radius induced by a hyperbolic-tangent escarpment at T=4.0.

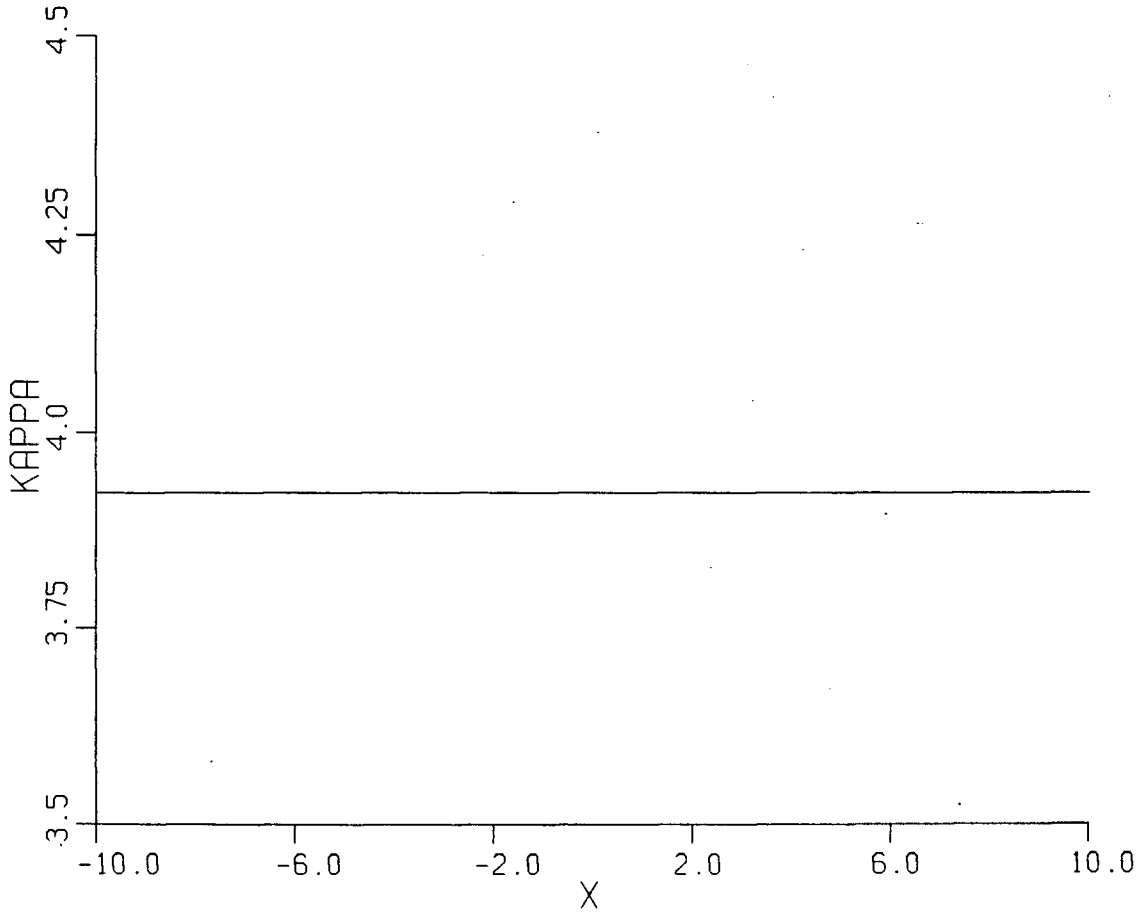

Figure 12. Sequence of space-like slices showing the space-time evolution of the modon wavenumber for modon propagation over a slowly varying hyperbolic-tangent escarpment centered at X=0. This plot shows the initial condition (i.e. at T=0.0) on the wavenumber (i.e. $\kappa(X,Y,0)=\kappa_0$).

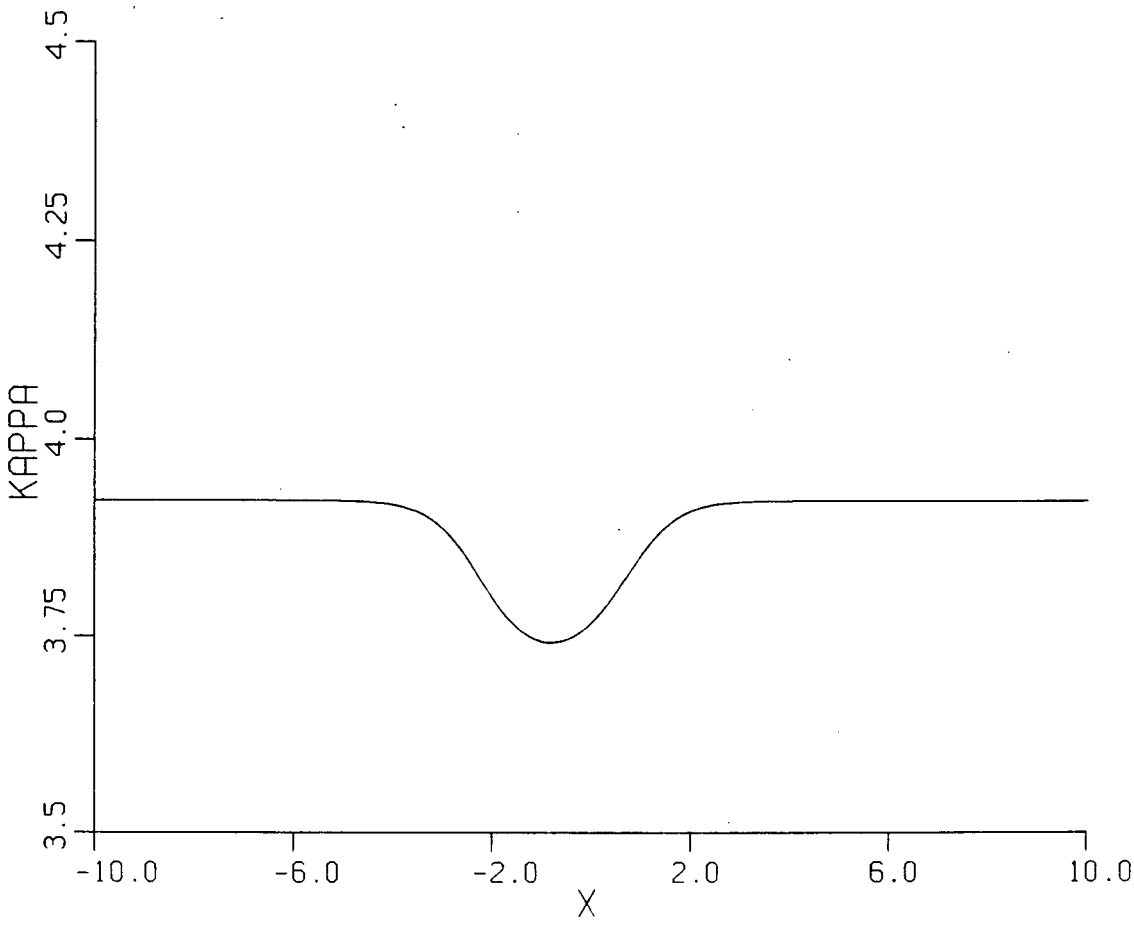

Figure 12b. Space-like structure of the modon wavenumber induced by a hyperbolic-tangent escarpment at T=0.2.

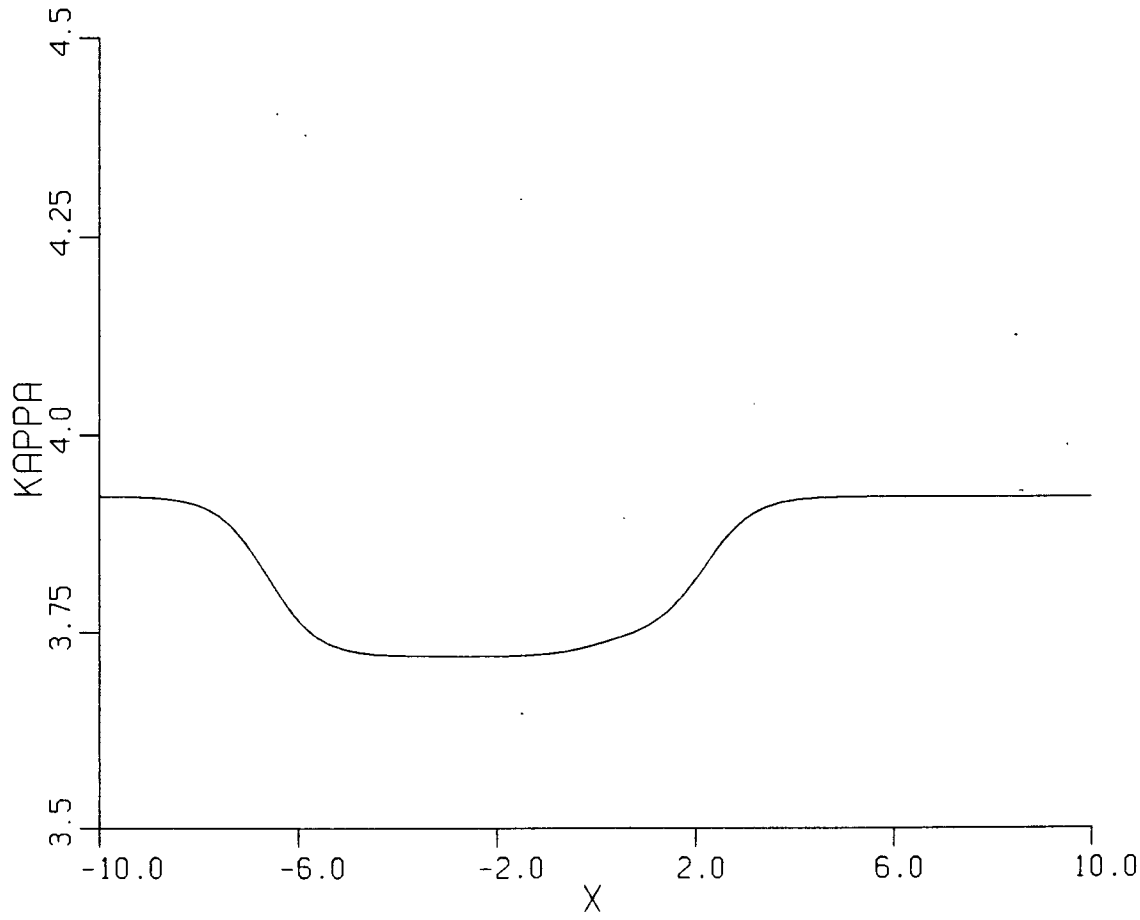

Figure 12c. Space-like structure of the modon wavenumber induced by a hyperbolic-tangent escarpment at T=0.6.

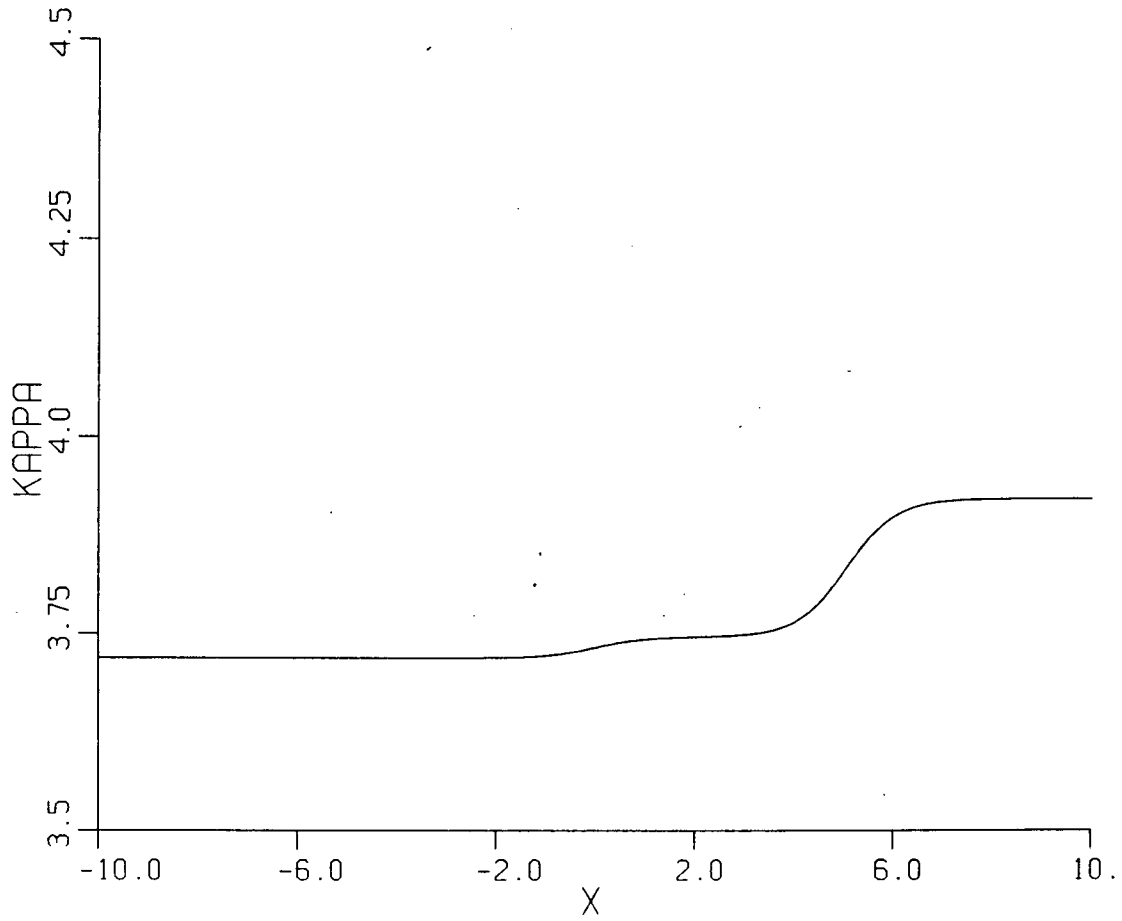

Figure 12d. Space-like structure of the modon wavenumber induced by a hyperbolic-tangent escarpment at T=1.4.

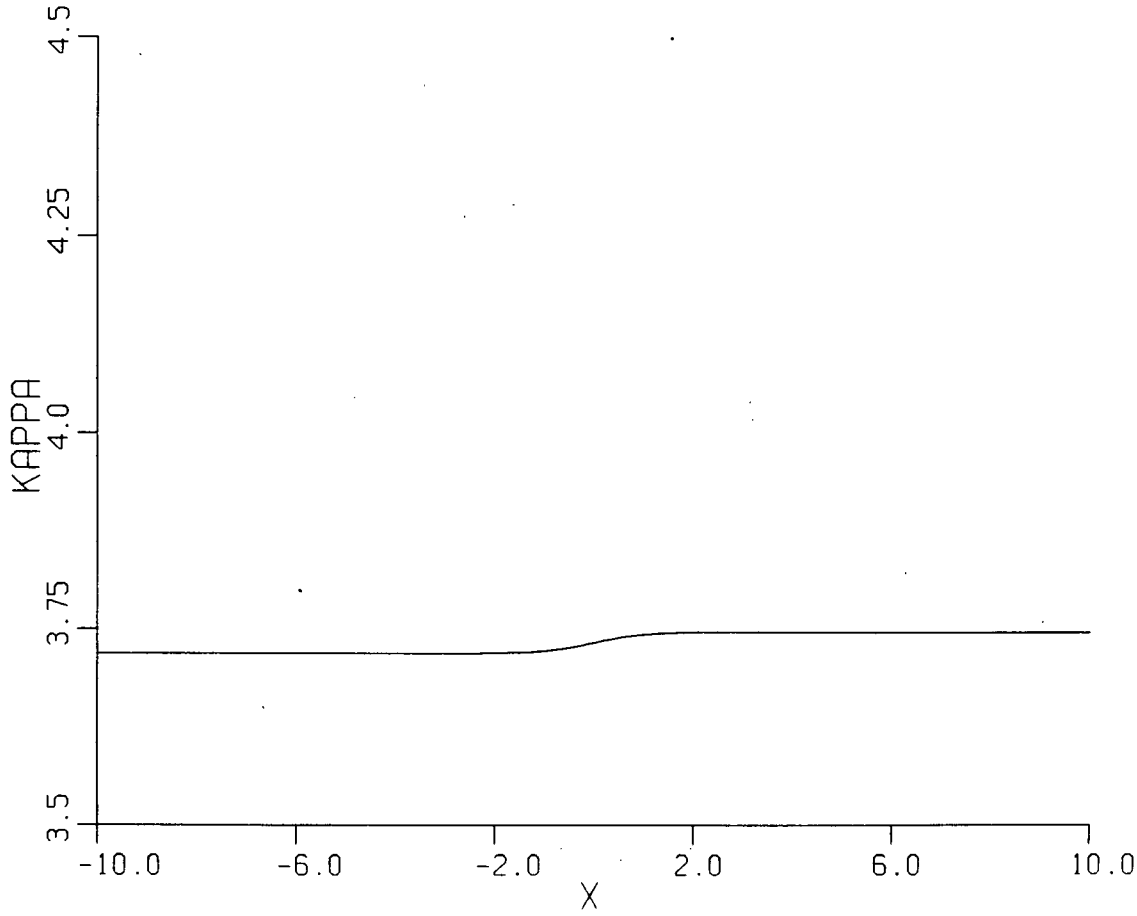

Figure 12e. Space-like structure of the modon wavenumber induced by a hyperbolic-tangent escarpment at T=4.0.

IV. CONCLUSIONS

This thesis has examined two aspects of the theory of barotropic modons. The first aspect was examined in Chapter II in which a sufficient neutral stability condition (in the form of an integral constraint) for barotropic modons was obtained. Eastward-travelling modons are neutrally stable to perturbations solely composed with wavenumber magnitudes ($|\eta|$) satisfying $|\eta|<\kappa$ where κ is the modon wavenumber. Westward-travelling modons are neutrally stable to perturbations composed solely of spectral components satisfying $|\eta|>\kappa$ (or else the modon is stable).

The eastward-travelling modon neutral stability condition implies that when $\kappa/|\eta|>1$ the slope of the neutral stability curve proposed by McWilliams et al.(1981) should begin to increase as $|\eta|$ decreases. A similar trend in the neutral stability curve has been numerically determined for topographically-forced planetary eddies (Malanotte-Rizzoli, 1982).

As an atmospheric application, the stability condition was calculated based on the 300, 500 and 700 mb eddy kinetic energy spectrum described by Tomatsu(1979), Saltzman and Fleisher(1962) and Eliasen and Machenhauer(1965). Eastward-travelling modons satisfy the stability condition and thus we conclude that for typical mid-latitude 700 mb to 300 mb atmosphere energetics eastward-travelling modons are neutrally stable. A similar calculation for westward-travelling modons fails to satisfy the

stability condition and thus the stability or instability for westward-travelling modons cannot be determined.

Simple scaling arguments suggested that only eastward-travelling barotropic modons would have realistic translation and particle speeds in the ocean. The stability integral was tested with the Fu(1983) mesoscale wavenumber eddy energy spectrum. The stability of oceanic modons could not be inferred. However due to the short period over which the data for the Fu(1983) spectrum was collected (24 days) arguments were presented to suggest that the Fu(1983) spectrum may not be representative of either the total eddy energy or its wavenumber distribution. Therefore the oceanic calculation using the Fu(1983) spectrum should only be considered a very preliminary estimate of modon stability in the oceans.

The second aspect of this thesis is contained in Chapter III. A leading order perturbation theory was developed to describe the propagation of a barotropic modon in a slowly varying medium. The perturbation method developed here represents an extension to a two-dimensional solitary wave of various calculations made of slowly varying one dimensional solitary waves (e.g., Luke(1966), Grimshaw(1970, 1971, 1977, 1978, 1979a,b, 1981), Zakharov and Rubenchik(1974) and Kodama and Ablowitz(1980,1981), among others).

Two problem were posed and solved. In Section 3.1 a perturbation solution for the propagation of an eastward travelling modon with a bottom boundary layer was obtained. The geostrophic pressure has been expanded in the damping

coefficient $\epsilon = E^{1/2}/(2r_0) \simeq 10^{-1}$ with E the vertical Ekman number and r_0 the Rossby number.

The modon radius (a), translation speed (c) and wavenumber (κ) are allowed to be functions of the slow time $T = \epsilon t$. The $0(\epsilon)$ equations require a necessary compatibility condition on the 0(1) solutions (taken to be an eastward-travelling modon) resulting in nonlinear initial-value problems for the modon parameters.

The solutions $a = \exp(-T)$, $c = \exp(-2T)$ and $\kappa = \kappa_0 \exp(T)$ leave the modon dispersion relationship invariant during the decay. The amplitude of the modon streamfunction and vorticity decays like $\exp(-3T)$ and $\exp(-T)$, respectively. The maximum distance over which the modon travels before complete dissipation is about 5 modon (initial) radii. Based on a comparison with a numerical solution (McWilliams et al., 1981) for the frictional dissipation of an eastward-travelling modon the asymptotic solution obtained here describes the decay over a 100 day time scale for oceanic parameters and a 10 day time scale for atmospheric parameters.

In Section 3.2 a leading order perturbation theory is developed to describe modon propagation over slowly varying topography. As in previous work on the effects of variable topography on barotropic planetary waves (e.g., Veronis(1966), Rhines(1969a,b), Clarke(1971) and LeBlond and Mysak(1978), among others) the theory is developed in the context of the rigid-lid shallow water equations on the β-plane.

Nonlinear hyperbolic equations are derived for the slow

evolution of the leading order modon radius, translation speed and wavenumber. These equations are valid for arbitrary slowly varying finite-amplitude topography. In general they must be solved numerically. It is shown that to leading order the evolution of the modon is independent of the meridional topographic structure. This result is interpreted using simple vorticity arguments.

Analytical perturbation solutions for the modon radius, translation speed and wavenumber are obtained for small-amplitude topography (which is the case in many atmospheric and oceanic applications). The solutions take the form of eastward and westward-travelling hyperbolic transients and a stationary component proportional to the topography. The general properties of the solution are described in Subsection 3.2.2. Subsections 3.2.3 and 3.2.4 describe the slowly varying modon for the specific examples of a topographic ridge and escarpment, respectively.

BIBLIOGRAPHY

1. Ablowitz, M. J., 1971: Application of slowly varying nonlinear dispersive wave theories. Stud. in Appl. Math., 54, 329-344.

2. Ablowitz, M. J. and Kodama, Y., 1979: Transverse instability one dimensional transparent optical pulses in resonant media. Phys. Lett., A70, 83-86.

3. Ablowitz, M. J., and H. Segur, 1981: Solitons and the inverse scattering transform. SIAM, 425 pp.

4. Arnol'd, V. I., 1965: Conditions for the nonlinear stability of stationary plane curvilinear flows of an ideal fluid. Dokl. Akad. Nauk SSSR, 6, 773-777.

5. Arnol'd, V. I., 1969: On an a priori estimate in the theory of hydrodynamical stability. Am. Math. Soc. Transl., 79, 267-269.

6. Benzi, R., S. Pierini, A. Vulpiani and E. Salusti, 1982: On nonlinear hydrodynamic stability of planetary vortices. Geophys. Astrophys. Fluid Dynamics, 20, 293-306.

7. Bernstein, R. L. and W. B. White, 1974: Time and space scales of baroclinic eddies in the central north Pacific. J. Phys. Oceanogr., 4, 613-624.

8. Blumen, W., 1968: On the stability of quasigeostrophic flow. J. Atmos. Sci., 25, 929-933.

9. Charney, J. G. and G. R. Flierl, 1981: Oceanic analogues in large scale atmospheric motions. In "Evolution of Physical Oceanography", edited by B. Warren and C. Wunsch, MIT Press, pp. 502-546.

10. Clarke, R. A., 1971: Solitary and cnoidal planetary waves. Geophys. Fluid Dyn., 2, 342-354.

11. Csanady, G. T., 1979: The birth and death of a warm core ring. J. Geophys. Res., 84, 777-780.

12. Drazin,, P. G. and W. H. Reid, 1981: Hydrodynamic Instability. Cambridge University Press, 527 pp.

13. Ebin, D. G. and J. Marsden, 1970: Groups of diffeomorphisms and the motion of an incompressible fluid. Ann. Math., 92, 102-163.

14. Eliasen, E. and B. Machenhauer, 1965: A study of the fluctuations of the atmospheric planetary flow patterns represented by spherical harmonics. Tellus, 7, 220-238.

15. Flierl, G. R., 1976: Contributions to the theory and modelling of eddies. In "Theory and modelling of ocean eddies: Contribution of the U.S. delegation to the Yalta Polymode Theoretical Institute", edited by P. B. Rhines, 23pp.

16. Flierl, G. R., 1977: The application of linear quasigeostrophic dynamics to Gulf Stream rings. J. Phys. Oceanogr., 7, 365-379.

17. Flierl, G. R., 1979: A simple model for the structure of warm and cold rings. J. Geophys. Res., 84, 781-785.

18. Flierl, G. R., V. D. Larichev, J. D. McWilliams and G. M. Reznik, 1980: The dynamics of baroclinic and barotropic solitary eddies. Dyn. Atmos. Oceans, 5, 1-41.

19. Flierl, G. R., M. S. Stern and J. A. Whitehead, Jr., 1983: The physical significance of modons: Laboratory experiments and general integral constraints. Dyn. Atmos. Oceans, 7, 233-263.

20. Fu, L. L., 1983: On the wavenumber spectrum of oceanic mesoscale variability observed by the SEASAT altimeter. J. Geophys. Res., 88, 4331-4341.

21. Grimshaw, R. H. J., 1970: The solitary wave in water of variable depth., Part 1. J. Fluid Mech., 42, 639-656.

22. Grimshaw, R. H. J., 1971: The solitary wave in water of variable depth., Part 2. J. Fluid Mech., 46, 611-622.

23. Grimshaw, R. H. J., 1977: Nonlinear aspects of long shelf waves. Geophys. Astrophys. Fluid Dyn., 8, 3-16.

24. Grimshaw, R. H. J., 1978: Long nonlinear internal waves in channels of arbitrary cross-Section. J. Fluid Mech., 86, 415-431.

25. Grimshaw, R. H. J., 1979a: Slowly varying solitary waves. I. Korteweg-de Vries equation. Proc. R. Soc. Lond., A368, 359-375.

26. Grimshaw, R. H. J., 1979b: Slowly varying solitary waves. II. Nonlinear Schroedinger equation. Proc. R. Soc. Lond., A368, 377-388.

27. Grimshaw, R. H. J., 1981: Slowly varying solitary waves in deep fluids. Proc. R. Soc. Lond., A376, 319-332.

28. Holm, D. D., J. E. Marsden, T. Ratiu and A. Weinstein, 1983: Nonlinear stability conditions and a priori estimates for barotropic hydrodynamics. Phys. Lett., A98, 1, 15-21.

29. Ikeda, M., L. A. Mysak and W. J. Emery, 1984: Observation and modelling of satellite-sensed meanders and eddies off Vancouver Island. J. Phys. Oceanogr., 14, 3-21.

30. Johnson, R. S., 1973: On an asymptotic solution of the Korteweg-de Vries equation with slowly varying coefficients. J. Fluid Mech., 60, 813-824.

31. Karpman, V. I. and E. M. Maslov, 1977a: A perturbation theory for the Korteweg-de Vries equation. Phys. Lett., A60, 307-308.

32. Karpman, V. I. and E. M. Maslov, 1977b: Perturbation theory for solitons. Soviet Phys. JETP, 46, 281-291.

33. Kaup, D. J. and A. C. Newell, 1978: Solitons as particles, oscillators, and in slowly changing media: A singular perturbation theory. Proc. R. Soc. Lond., A361, 413-446.

34. Kloeden, P. E., 1985a: Uniqueness of the Larichev-Reznik solitary wave solutions. Ocean Modelling, 61, 11-13.

35. Kloeden, P. E., 1985b: Uniqueness of solitary Rossby waves, Submitted to Quart. J. Mech. Appl. Math..

36. Ko, K., and H. H. Kuehl, 1978: Korteweg-de Vries soliton in a slowly varying medium. Phys. Rev. Lett., 40, 233-236.

37. Kodama, Y. and M. J. Ablowitz, 1980: Transverse instability of breathers in resonant media. J. Math. Phys., 21, 928-931.

38. Kodama, Y. and M. J. Ablowitz, 1981: Perturbations of solitons and solitary waves. Stud. in Appl. Math., 64, 225-245.

39. Lai, Y. L. and P. L Richardson, 1977: Distribution and movement of Gulf Stream rings. J. Phys. Oceanogr., 7, 671-683.

40. Larichev, V. and G. Reznik, 1976: Two-dimensional Rossby soliton: an exact solution. Polymode News, 19, 5-7.

41. LeBlond, P. H. and L. A. Mysak, 1978: Waves in the ocean. Elsevier, 602 pp.

42. Luke, J. C., 1966: A perturbation method for nonlinear dispersive wave problems. Proc. Roy. Soc., A292, 403-412.

43. Malanotte-Rizzoli, P. and M. C. Hendershott, 1980: Solitary Rossby waves over variable relief and their stability. Part 1. The analytical theory. Dyn. Atmos. Oceans, 4, 247-260.

44. Malanotte-Rizzoli, P., 1982: Planetary solitary waves in geophysical flows. Adv. Geophys., 24, 147-224.

45. Malanotte-Rizzoli, P., 1984: Boundary forced planetary radiation. J. Phys. Oceanogr., 14, 1032-1046.

46. Marsden, J. E. and R. Abraham, 1970: Hamiltonian mechanics on Lie groups and hydrodynamics. Proc. Symp. Pure Math., Am. Math. Soc., 16, 237-243.

47. Maxworthy, T. and L. G. Redekopp, 1976: Theory of the Great Red Spot and other observed features of the Jovian atmosphere. Icarus, 29, 261-271.

48. Matsuura, T., and T. Yamagata, 1982: On the evolution of nonlinear planetary eddies larger than the radius of deformation. J. Phys. Oceanogr., 12, 440-456.

49. McWilliams, J. C., 1980: An application of equivalent modons to atmospheric blocking. Dyn. Atmos. Oceans, 5, 43-66.

50. McWilliams, J. C., G. R. Flierl, V. D. Larichev and G. M. Reznik, 1981: Numerical studies of barotropic modons. Dyn. Atmos. Oceans, 5, 219-238.

51. McWilliams, J. C. and N. J. Zabusky, 1982: Interactions of isolated vortices I: Modons colliding with modons. Geophys. Astrophys. Fluid Dyn., 19, 207-227.

52. McWilliams, J. C., 1983: Interactions of isolated vortices II: Modon generation by monopole collision. Geophys. Astrophys. Fluid Dyn., 24, 1-22.

53. Mied, R. P. and G. J. Lindemann, 1982: The birth and evolution of eastward propagating modons. J. Phys. Oceanogr., 12, 213-230.

54. Mode Group, 1978: The mid-ocean dynamics experiment. Deep-Sea Res., 24, 859-910.

55. Mysak, L. A., 1983: Generation of annual Rossby waves in the north Pacific. J. Phys. Oceanogr., 13, 1908-1923.

56. Pedlosky, J., 1979: Geophysical Fluid Dynamics. Springer-Verlag, 624 pp.

57. Purini, R., and E. Salusti, 1984: Nonlinear hydrodynamic stability of oceanic flow. Geophys. Astrophys. Fluid Dyn., 30, 261-270.

58. Rhines, P. B., 1969a: Slow oscillations in an ocean of varying depth. Part 1. Abrupt topography. J. Fluid Mech., 37, 161-189.

59. Rhines, P. B., 1969b: Slow oscillations in an ocean of varying depth. Part 2. Islands and seamounts. J. Fluid Mech., 37, 191-205.

60. Richardson, P. L., 1983: Eddy kinetic energy in the north Atlantic from surface drifters. J. Geophys. Res., 88, 4355-4367.

61. Saltzman, B. and A. Fleisher, 1962: Spectral statistics of the wind at 500 mb. J. Atmos. Sci., 19, 195-204.

62. Stern, M. E., 1975: Minimal properties of planetary eddies. J. Mar. Res., 33, 1-13.

63. Swaters, G. E. and L. A. Mysak, 1985: Topographically induced baroclinic eddies near a coastline, with application to the northeast Pacific. J. Phys. Oceanogr., 15, in press.

64. Swaters, G. E., 1985: Ekman layer dissipation in an eastward-travelling modon. J. Phys. Oceanogr., 15, in press.

65. Tomatsu, K., 1979: Spectral energetics of the troposphere and lower stratosphere. Adv. Geophys., 21, 289-405.

66. Tribbia, J. J., 1984: Modons in spherical geometry. Geophys. Astrophys. Fluid Dyn., 30, 131-168.

67. Verkley W. T. M., 1984: The construction of barotropic modons on a sphere. J. Atmos. Sci., 41, 2492-2504.

68. Veronis, G., 1966: Rossby waves with bottom topography. J. Mar. Res., 24, 338-349.

69. Warn, T., and B. Brasnett, 1983: The amplification and capture of atmospheric solitons by topography: A theory of the onset of regional blocking. J. Atmos. Sci., 40, 28-38.

70. White, W. B. and J. F. T. Saur, 1981: A source of annual baroclinic waves in the eastern subtropical north Pacific. J. Phys. Oceanogr., 11, 1452-1462.

71. Whitham, G. B., 1965: A general approach to linear and nonlinear dispersive waves using a Lagrangian. J. Fluid Mech., 22, 273-283.

72. Willmott, A. J. and L. A. Mysak, 1980: Atmospherically forced eddies in the northeast Pacific. J. Phys. Oceanogr., 10, 1789-1791.

73. Wunsch, C., 1981: Low-frequency variability of the sea, In "Evolution of Physical Oceanography", edited by B. Warren and C. Wunsch, MIT Press, pp. 342-374.

74. Wyrtki, K., L. Magaard and J. Hagar, 1976: Eddy energy in the oceans. J. Geophys. Res., 81, 2641-2646.

75. Yamagata, T., 1982: On nonlinear planetary waves: A class of solutions missed by the traditional quasigeostrophic approximation. J. Oceanogr. Soc. Japan, 38, 263-244.

76. Zakharov, V. E., and A. M. Rubenchik, 1974: Instability of waveguides and solitons in nonlinear media. Sov. Phys. JETP, 38, 494-501.

APPENDIX A - CALCULATION OF SOLVABILITY INTEGRALS IN TOPOGRAPHIC PROBLEM

This appendix describes the calculations of the compatibility conditions (3.2.7) and (3.2.9). The exterior computations (i.e., (3.2.7)) are presented first and the interior computations (i.e., (3.2.9)) follow.

Exterior Calculations

The compatibility condition (3.2.7) involves 18 integrals. The terms are described in the order of their appearance in (3.2.6) and are denoted I_1 through to I_{18}.

Recall that for r>a

$$\psi^{(0)} = -caK_1(\delta c^{-1/2}r)\sin(\theta)/K_1(\delta a c^{-1/2})$$

$$\Delta\psi^{(0)} = -\delta^2 aK_1(\delta c^{-1/2}r)\sin(\theta)/K_1(\delta a c^{-1/2})$$

i.e.,
$$\Delta\psi^{(0)} = (\delta^2/c)\psi^{(0)}.$$

It will be convenient to let

$$R(r) = -caK_1(\delta c^{-1/2}r)/K_1(\delta a c^{-1/2}),$$

so that $\psi^{(0)} = R(r)\sin(\theta)$, and define the operators $D = d/dr$ and $D_0F[(\cdot)] = dF[(\cdot)]/d(\cdot)$ (i.e., differentation with respect to r and arguments, respectively). Recall $r^2 = (\xi-\xi_0)^2 + y^2$ and $\tan(\theta)=y/(\xi-\xi_0)$, hence

$$(\partial_T, \partial_X, \partial_Y)r = -\cos(\theta)(\partial_T, \partial_X, \partial_Y)\xi_0$$

$$(\partial_T, \partial_X, \partial_Y)\theta = r^{-1}\sin(\theta)(\partial_T, \partial_X, \partial_Y)\xi_0.$$

And finally it is helpful to recall that by definition

$$D^2R + DR/r - (r^{-2} + \delta^2/c)R = 0.$$

The integral calculations for r>a are as follows;

I_1:

$$I_1 = (\delta^2/c)H^{-1}g_Y \int_{-\pi}^{\pi}\int_a^{\infty} \psi^{(0)}\psi^{(0)}_{\xi}\, r\,dr\,d\theta$$

Note that $\psi^{(0)}_{\xi} = (DR - R/r)\sin(\theta)\cos(\theta)$. Therefore the trigonometric part of the integral contains $\cos(\theta)\sin^2(\theta)$ which integrates to zero due to the periodicity in θ. Thus $I_1 = 0$.

I_2:

$$I_2 = -\int_{-\pi}^{\pi}\int_{a}^{\infty} \psi^{(0)}_{T}\Delta\psi^{(0)}_{T}\, rdrd\theta$$

Note that

$$\Delta\psi^{(0)}_{T} = \{ a^{-1}a_{T} - [D_0K_1(\delta ac^{-1/2})/K_1(\delta ac^{-1/2})]\delta ac^{-1/2}[a^{-1}a_{T} - (2c)^{-1}c_{T}]\}\Delta\psi^{(0)}_{T} + c^{1/2}(rc^{-1/2})\,\Delta\psi^{(0)}_{r} - (\delta^2/c)\cos(\theta)\sin(\theta)\xi_{0_T}\, DR + (\delta^2/c)r^{-1}\sin(\theta)\cos(\theta)\xi_{0_T}\, R.$$

The trigonometric component of the integral associated with the last two terms (i.e., the terms containing ξ_{0_T}) is $\sin^2(\theta)\cos(\theta)$ and thus integrates to zero. The remaining calculation gives

$$I_2 = -\pi\delta^2 ca^4 Q[A_1 a^{-1}a_{T} - (A_1 - 1)(2c)^{-1}c_{T}]$$

where

$$A_1 = \gamma K_2(\gamma)/K_1(\gamma) - (2Q)^{-1} - 1 \qquad \text{(A1a)}$$

$$Q = -[\gamma K_1^2(\gamma) - 2K_0(\gamma)K_1(\gamma) - \gamma K_0^2(\gamma))/(2\gamma K_1^2(\gamma)], \qquad \text{(A1b)}$$

recalling $\gamma^2 = \delta^2 a^2/c$.

I_3:

$$I_3 = 2c\int_{-\pi}^{\pi}\int_{a}^{\infty} \psi^{(0)}_{\xi\xi}\psi^{(0)}_{X}\, rdrd\theta$$

We require

$$\psi^{(0)}_{\xi\xi X} = \sin(\theta)\cos^2(\theta)(D^2 - 2DR/r - 2R/r^2)_X + \sin^3(\theta)(DR/r - R/r^2)_X +$$

$$r^{-1}\xi_{0_X}(\cos^3(\theta)\sin(\theta) - 2\sin^3(\theta)\cos(\theta)(D^2R - 2DR/r - 2R/r^2) -$$

$$\xi_{0_X}\cos^3(\theta)\sin(\theta)D(D^2 - 2DR/r - 2R/r^2) +$$

$$3r^{-1}\xi_{0_X}\sin^3(\theta)\cos(\theta)(DR/r - R/r^2)_X -$$

$$\xi_{0_X}\cos(\theta)\sin^3(\theta)D(DR/r - R/r^2).$$

The trigonometric component of the integrals containing ξ_{0_X} have $\cos^3(\theta)\sin^2(\theta)$ or $\sin^4(\theta)\cos(\theta)$ both of which integrate to zero. The remaining integration gives

$$I_3 = (1/2)\pi\delta^2c^2a^4Q[A_1a^{-1}a_X - (A_1 - 1)(2c)^{-1}c_X].$$

I_4:

$$I_4 = -\delta^2\int_{-\pi}^{\pi}\int_a^{\infty}\psi^{(0)}\psi^{(0)}_X\,rdrd\theta$$

The calculation of I_4 is essentially the same as I_2 (modulo the δ^2/c factor associated with $\Delta\psi^{(0)}$ compared to $\psi^{(0)}$ and the X-derivative rather than the T-derivative). The result is

$$I_4 = -\delta^2\pi c^2a^4Q[A_1a^{-1}a_X - (A_1 - 1)(2c)^{-1}c_X + c^{-1}c_X].$$

I_5:

$$I_5 = (\delta^2/c)_X\int_{-\pi}^{\pi}\int_a^{\infty}\psi^{(0)}\psi^{(0)}\psi^{(0)}_y\,rdrd\theta$$

We note that

$$\psi^{(0)}\psi^{(0)}\psi^{(0)}_y = (1/3)[\sin\theta D + r^{-1}\cos(\theta)\partial/\partial\theta)R^3\sin^3(\theta)$$

which gives

$$I_5 = -(\delta^2\pi c^2a^4/2)(2c)^{-1}c_X.$$

I_6:

$$I_6 = -2 \int_{-\pi}^{\pi} \int_{a}^{\infty} \psi^{(0)} J(\psi^{(0)}, \psi^{(0)}_{\xi X}) \, r dr d\theta$$

We require

$$(r^{-1}\psi^{(0)}_{\xi\theta})_X = (\cos^2(\theta) - \sin^2(\theta))(DR/r - R/r^2)_X -$$

$$2r^{-1}\sin^2(\theta)\cos(\theta)\xi_{0X}(DR/r - R/r^2) -$$

$$\cos(\theta)(\cos^2(\theta) - \sin^2(\theta))\xi_{0X} D(DR/r - R/r^2)$$

and

$$(\psi^{(0)}_{\xi r})_X = \cos(\theta)\sin(\theta)(D^2R - DR/r + R/r^2)_X -$$

$$r^{-1}\sin(\theta)(\cos^2(\theta) - \sin^2(\theta))\xi_{0X}(D^2R - DR/r + R/r^2) -$$

$$\cos^2(\theta)\sin(\theta)\xi_{0X} D(D^2R - DR/r + R/r^2).$$

Note that

$$J(\psi^{(0)}, \psi^{(0)}_{\xi X}) = \psi^{(0)}_{r}(r^{-1}\psi^{(0)}_{\xi\theta})_X - r^{-1}\psi^{(0)}_{\theta}(\psi^{(0)}_{\xi r})_X .$$

The trigonometric component of the terms containing ξ_{0X} is $\sin^4(\theta)\cos(\theta)$ or $\sin^2(\theta)\cos^3(\theta)$, both of which integrate to zero. The remaining integration gives

$$I_6 = -\pi a^2 c^3 \gamma K_2(\gamma)(2K_1(\gamma))^{-1}[(2c)^{-1}c_X + B(a^{-1}a_X - (2c)^{-1}c_X)]$$

where

$$B = \gamma[K_2(\gamma)/K_1(\gamma) - K_1(\gamma)/K_2(\gamma) - 3/\gamma)]. \qquad (A2)$$

I_7:

$$I_7 = c(H^{-1}H)_X \int_{-\pi}^{\pi}\int_a^{\infty} \psi^{(0)}_{\xi\xi}\psi^{(0)}_{\xi}\, r\,dr\,d\theta$$

We require

$$\psi^{(0)}_{\xi\xi} = \sin(\theta)\cos^2(\theta)(D^2R - 2DR/r + 2R/r^2) + \sin^3(\theta)(DR/r - R/r^2)$$

which results in

$$I_7 = (1/4)\delta^2\pi a^4 c^2 Q(H^{-1}H)_X .$$

I_8:

$$I_8 = -\delta^2(H^{-1}H)_X \int_{-\pi}^{\pi}\int_a^{\infty} \psi^{(0)}\psi^{(0)}\, r\,dr\,d\theta$$

Straightforward calculation results in

$$I_8 = -\delta^2 a^4 c^2 \pi Q(H^{-1}H)_X .$$

I_9:

$$I_9 = -(H^{-1}H)_X \int_{-\pi}^{\pi}\int_a^{\infty} \psi^{(0)} J(\psi^{(0)}, \psi^{(0)}_{\xi})\, r\,dr\,d\theta$$

We require

$$\psi^{(0)}_{\xi\theta} = (\cos^2(\theta) - \sin^2(\theta))(DR - R/r)$$

$$\psi^{(0)}_{\xi r} = \cos(\theta)\sin(\theta)(D^2R - DR/r + R/r^2),$$

which gives

$$I_9 = -\pi a^2 c^3 \gamma K_2(\gamma)(4K_1(\gamma))^{-1}(H^{-1}H)_X .$$

I_{10}:

$$I_{10} = -(H^{-1}H_X) \int_{-\pi}^{\pi} \int_{a}^{\infty} \psi^{(0)}[(r_0)^{-1} + \delta^2 y]\psi^{(0)}_y \, rdrd\theta$$

We require

$$\psi^{(0)}_y = \sin^2(\theta)DR + \cos^2(\theta)R/r.$$

The trigonometric components of the integral with the Rossby number as a coefficient are $\sin^3(\theta)$ or $\cos^2(\theta)\sin(\theta)$ both of which integrate to zero. The remaining integration gives

$$I_{10} = (3/8)\delta^2\pi a^4 c^2 H^{-1}H_X + (1/2)\delta^2\pi a^4 c^2 Q H^{-1}H_X .$$

I_{11}:

$$I_{11} = -(2\delta^2/c)(H^{-1}H_X) \int_{-\pi}^{\pi} \int_{a}^{\infty} \psi^{(0)}\psi^{(0)}\psi^{(0)}_y \, rdrd\theta$$

The evaluation of I_{11} is similar to I_5 the result is

$$I_{11} = -(1/2)\delta^2\pi a^4 c^2 H^{-1}H_X .$$

I_{12}:

$$I_{12} = 2c \int_{-\pi}^{\pi} \int_{a}^{\infty} \psi^{(0)}\psi^{(0)}_{\xi y Y} \, rdrd\theta$$

We require

$$\psi^{(0)}_{\xi y Y} = \cos(\theta)\sin^2(\theta)(D^2R - 2DR/r + 2R/r^2)_Y +$$

$$\cos^3(\theta)(DR/r - R/r^2)_Y +$$

$$r^{-1}(\cos^2(\theta)\sin^2(\theta) - \sin^4(\theta))\xi_{0Y}(D^2R - DR/r + 2R/r^2) -$$

$$\cos^2(\theta)\sin^2(\theta)\xi_{0Y} D(D^2R - 2DR/r + 2R/r^2) -$$

$$3r^{-1}\cos^2(\theta)\sin^2(\theta)\xi_{0Y}(DR/r - R/r^2) - \cos^4(\theta)\xi_{0Y} D(DR/r - R/r^2).$$

The trigonometric part of these terms is integrated against $\sin(\theta)$ (belonging to $\psi^{(0)}$). It is easy to see that each term integrates to zero due to the periodicity in θ, consequently $I_{12}=0$.

I_{13}:

$$I_{13} = -(\delta^2/c) \int_{Y} \int_{-\pi}^{\pi} \int_{a}^{\infty} \psi^{(0)}\psi^{(0)}\psi^{(0)}_{\xi} \, r dr d\theta$$

We require

$$\psi^{(0)}_{\xi} = \cos(\theta)\sin(\theta)(DR - R/r).$$

When this term is integrated against the $\sin^2(\theta)$ trigonometric component of $(\psi^{(0)})^2$ the resulting integral vanishes, consequently $I_{13}=0$.

I_{14}:

$$I_{14} = -2 \int_{-\pi}^{\pi} \int_{a}^{\infty} \psi^{(0)} J(\psi^{(0)}, \psi^{(0)}_{yY}) \, r dr d\theta$$

We require

$$(r^{-1}\psi^{(0)}_{y\theta})_{Y} = 2\sin(\theta)\cos(\theta)(DR/r - R/r^2)_{Y} +$$

$$2r^{-1}(\cos^2(\theta)\sin(\theta) - \sin^3(\theta))\xi_{0\,Y}(DR/r - R/r^2) -$$

$$2\sin^2(\theta)\cos(\theta)\xi_{0\,Y} D(DR/r - R/r^2).$$

$$(\psi^{(0)}_{yr})_{Y} = \sin^2(\theta)(D^2R)_{Y} + \cos^2(\theta)(D^2R - R/r^2)_{Y} -$$

$$\sin^2(\theta)\cos(\theta)\xi_{0\,Y}(D^3R - 2D^2R/r) -$$

$$2r^{-1}\sin^2(\theta)\cos(\theta)\xi_{0\,Y}(D^2R - R/r^2) - \cos^3(\theta)\xi_{0\,Y} D(D^2R - R/r^2).$$

The first term is multiplied by $(DR)R\sin^2(\theta)$ which integrates to zero due to the trigonometric integration. The second term is multiplied by $R^2\sin(\theta)\cos(\theta)$ which integrates to zero due to the trigonometric integration. Therefore $I_{14}=0$.

I_{15}:

$$I_{15} = c(H^{-1}H_Y)\int_{-\pi}^{\pi}\int_{a}^{\infty}\psi^{(0)}\psi^{(0)}_{\xi y}\,rdrd\theta$$

We require

$$\psi^{(0)}_{\xi y} = \cos(\theta)\sin^2(\theta)(D^2R - 2DR/r + 2R/r^2) + \cos^3(\theta)(DR/r - R/r^2)$$

which when integrated against $R\sin(\theta)$ is zero due to the trigonometric integration. Therefore $I_{15}=0$.

I_{16}:

$$I_{16} = -(H^{-1}H_Y)\int_{-\pi}^{\pi}\int_{a}^{\infty}\psi^{(0)}J(\psi^{(0)}, \psi^{(0)}_{y})\,rdrd\theta$$

We require

$$\psi^{(0)}_{yr} = \sin^2(\theta)D^2R + \cos^2(\theta)[DR/r - R/r^2),$$

$$\psi^{(0)}_{y\theta} = 2r^{-1}\sin(\theta)\cos(\theta)(DR/r - R/r^2).$$

The first term is integrated against $R^2\sin(\theta)\cos(\theta)$ and the second term is integrated against $(DR)R\sin^2(\theta)$ which integrate to zero due to the trigonometric integration. Therefore $I_{16}=0$.

I_{17}:

$$I_{17} = (H^{-1}H_Y)\int_{-\pi}^{\pi}\int_{a}^{\infty}\psi^{(0)}[(r_0)^{-1} + \delta^2 y]\psi^{(0)}_{\xi}\,rdrd\theta$$

The integrand is

$$((r_0)^{-1} + \delta^2 r\sin(\theta))R\sin^2(\theta)\cos(\theta)(DR - R/r)$$

which integrates to zero due to the trigonometric integration. Therefore $I_{17}=0$.

I_{18}:

$$I_{18} = 2(\delta^2/c)(H^{-1}H_Y)\int_{-\pi}^{\pi}\int_{a}^{\infty}\psi^{(0)}\psi^{(0)}\psi^{(0)}_{\xi}\, rdrd\theta.$$

This integral is trigonometrically indentical to I_{13}. Therefore $I_{18}=0$.

The compatibility condition (3.2.7) is therefore

$$0 = \int_{-\pi}^{\pi}\int_{a}^{\infty}\psi^{(0)}(\text{RHS}[3.2.6])\, rdrd\theta = \sum_{n=1}^{18} I_n,$$

which after a little algebra results in (3.2.10) where A_1 is given by (A1) and

$$A_2 = 2 + Q/2 - K_2(\gamma)Q[2\gamma K_1(\gamma)]^{-1}(B-1) \qquad (A3)$$

$$A_3 = K_2(\gamma)Q[2\gamma K_1(\gamma)]^{-1}B \qquad (A4)$$

$$E_1 = 1/4 + Q/8 + K_2(\gamma)Q[2\gamma K_1(\gamma)]^{-1} \qquad (A5)$$

with B is given by (A2).

Interior Calculations

The interior compatibility condition (3.2.9) contains 19 integrals denoted I_1 through I_{19}. Recall that for $r<a$

$$\psi^{(0)} = \delta^2\kappa^{-2}aJ_1(\kappa r)\sin(\theta)/J_1(\kappa a) - (\delta^2 + \kappa^2 c)\kappa^{-2}r\sin(\theta)$$

$$\Delta\psi^{(0)} = -\delta^2 aJ_1(\kappa r)\sin(\theta)/J_1(\kappa a)$$

i.e., $$\Delta\psi^{(0)} = -\kappa^2\psi^{(0)} - (\delta^2 + c\kappa^2)r\sin(\theta).$$

As in the previous calculation it will be convenient to let

$$R(r) = \delta^2\kappa^{-2}aJ_1(\kappa r)/J_1(\kappa a) - (\delta^2 + \kappa^2 c)\kappa^{-2}r$$

so that $\psi^{(0)} = R(r)\sin(\theta)$, and define the operators $D = d/dr$ and $D_0F[(\cdot)] = dF[(\cdot)]/d(\cdot)$ (i.e., differentation with respect to r and arguments, respectively). Recall $r^2 = (\xi-\xi_0)^2 + y^2$ and $\tan(\theta)=y/(\xi-\xi_0)$, hence

$$(\partial_T, \partial_X, \partial_Y)r = -\cos(\theta)(\partial_T, \partial_X, \partial_Y)\xi_0$$

$$(\partial_T, \partial_X, \partial_Y)\theta = r^{-1}\sin(\theta)(\partial_T, \partial_X, \partial_Y)\xi_0.$$

And finally it is helpful to recall that by definition

$$D^2R + DR/r - (r^{-2} - \kappa^2)R = 0.$$

The integrals are given as follows.

I_1:

$$I_1 = -\kappa^2 H^{-1} g_Y \int_{-\pi}^{\pi} \int_0^a \psi^{(0)}_\xi \psi^{(0)} \, r dr d\theta$$

This integral is trigonometrically identical to I_1 in the exterior calculations. Therefore $I_1=0$.

I_2:

$$I_2 = -\int_{-\pi}^{\pi} \int_0^a \psi^{(0)} \Delta\psi^{(0)}_T \, r dr d\theta$$

Note that $\Delta\psi^{(0)}_T = \{ a^{-1}a_T - [D_0 J_1(\kappa a)/J_1(\kappa a)]\kappa a[a^{-1}a_T + \kappa^{-1}\kappa_T]\}\Delta\psi^{(0)} + \kappa^{-1}(\kappa r)_T \Delta\psi^{(0)}_r - \cos(\theta)\xi_{0T}\Delta\psi^{(0)}_r + r^{-1}\sin(\theta)\xi_{0T}\Delta\psi^{(0)}_\theta.$

The trigonometric component of the terms with ξ_{0T} is $\sin^2(\theta)\cos(\theta)$ which integrates to zero due to the periodicity in θ. The remaining calculation gives

$$I_2 = Ga^{-1}a_T + L[a^{-1}a_T + \kappa^{-1}\kappa_T]$$

where

$$G = C_2[D_2 - (1 + k^2/\gamma^2)J_2(k)[kJ_1(k)]^{-1} \qquad \text{(A6)}$$

$$L = C_2[-kD_2/J_1^2(k) + (kJ_0(k)/J_1(k) + 2)(1 + k^2\gamma^{-2}).$$

$$J_2(k)[kJ_1(k)]^{-1} - 1/2 - (k/\gamma)^2] \tag{A7}$$

$$C_2 = \delta^4 a^4 \pi \kappa^{-2} \tag{A8}$$

$$D_2 = (1/2)[J_2^2(k) - 2J_2(k)J_1(k)k^{-1} + J_1^2(k)]/J_1^2(k) \tag{A9}$$

recalling $k=\kappa a$.

I_3:

$$I_3 = 2c \int_{-\pi}^{\pi} \int_0^a \psi^{(0)}_{\xi\xi X} \psi^{(0)} \, r dr d\theta$$

We require

$$\psi^{(0)}_{\xi\xi X} = \sin(\theta)\cos^2(\theta)(D^2 - 2DR/r - 2R/r^2)_X +$$

$$\sin^3(\theta)(DR/r - R/r^2)_X +$$

$$r^{-1}\xi_{0X}(\cos^3(\theta)\sin(\theta) - 2\sin^3(\theta)\cos(\theta)(D^2R - 2DR/r - 2R/r^2) -$$

$$\xi_{0X}\cos^3(\theta)\sin(\theta)D(D^2 - 2DR/r - 2R/r^2) +$$

$$3r^{-1}\xi_{0X}\sin^3(\theta)\cos(\theta)(DR/r - R/r^2)_X -$$

$$\xi_{0X}\cos(\theta)\sin^3(\theta)D(DR/r - R/r^2).$$

The trigonometric component of the integrals containing ξ_{0X} have $\cos^3(\theta)\sin^2(\theta)$ or $\sin^4(\theta)\cos(\theta)$ both of which integrate to zero. The remaining integration gives

$$I_3 = -(c/2)Ga^{-1}a_X - (c/2)L(a^{-1}a_X + \kappa^{-1}\kappa_X).$$

I_4:

$$I_4 = \kappa^2 c \int_{-\pi}^{\pi} \int_0^a \psi^{(0)}_X \psi^{(0)} \, r dr d\theta$$

Note that

$$\psi^{(0)}_{X} = \{ a^{-1}a_{T} - [D_0 J_1(\kappa a)/J_1(\kappa a)]\kappa a[a^{-1}a_{X} + \kappa^{-1}\kappa_{X}]\}\psi^{(0)} + \kappa^{-1}(\kappa r)\ \psi^{(0)}_{X\,r} - \cos(\theta)\xi_{0X}\ \psi^{(0)}_{X\,r} + r^{-1}\sin(\theta)\xi_{0X}\ \psi^{(0)}_{X\,\theta}.$$

The trigonometric component of the terms with ξ_{0X} is $\sin^2(\theta)\cos(\theta)$ which integrates to zero due to the periodicity in θ. The remaining calculation gives

$$I_4 = cGa^{-1}a_{X} + cL[a^{-1}a_{X} + \kappa^{-1}\kappa_{X}] - 2cG\kappa^{-1}\kappa_{X} + cC_2[-J_2(k)/(kJ_1(k)) + (1 + (k/\gamma)^2)/4]\cdot(\kappa^2 a^{-1}\delta^{-1}\{(\delta^2 + c\kappa^2)a\kappa^{-2}\}_{X}.$$

I_5:

$$I_5 = -(\kappa^2)_X \int_{-\pi}^{\pi}\int_{0}^{a} \psi^{(0)}\psi^{(0)}\psi^{(0)}_{y}\ rdrd\theta$$

We note that

$$\psi^{(0)}\psi^{(0)}\psi^{(0)}_{y} = (1/3)[\sin\theta D + r^{-1}\cos(\theta)\partial/\partial\theta)R^3\sin^3(\theta)$$

which gives

$$I_5 = cC_2(k/\gamma)^4\kappa^{-1}\kappa_{X}/2.$$

I_6:

$$I_6 = -2\int_{-\pi}^{\pi}\int_{0}^{a} \psi^{(0)}J(\psi^{(0)}, \psi^{(0)}_{\xi X})\ rdrd\theta$$

We require

$$(r^{-1}\psi^{(0)})_{\xi\theta\,X} = (\cos^2(\theta) - \sin^2(\theta)(DR/r - R/r^2)_X -$$

$$2r^{-1}\sin^2(\theta)\cos(\theta)\xi_{0\,X}(DR/r - R/r^2) -$$

$$\cos(\theta)(\cos^2(\theta) - \sin^2(\theta)\xi_{0\,X} D(DR/r - R/r^2)$$

and

$$(\psi^{(0)})_{\xi r\,X} = \cos(\theta)\sin(\theta)(D^2R - DR/r + R/r^2)_X -$$

$$r^{-1}\sin(\theta)(\cos^2(\theta) - \sin^2(\theta))\xi_{0\,X}(D^2R - DR/r + R/r^2) -$$

$$\cos^2(\theta)\sin(\theta)\xi_{0\,X} D(D^2R - DR/r + R/r^2).$$

Note that

$$J(\psi^{(0)}, \psi^{(0)})_{\xi X} = \psi^{(0)}_r(r^{-1}\psi^{(0)})_{\xi\theta\,X} - r^{-1}\psi^{(0)}_\theta(\psi^{(0)})_{\xi r\,X}.$$

The trigonometric component of the terms containing $\xi_{0\,X}$ is $\sin^4(\theta)\cos(\theta)$ or $\sin^2(\theta)\cos^3(\theta)$, both of which integrate to zero. The remaining integration gives

$$I_6 = cJ_2(k)C_2k(2J_1(k)\gamma^2)^{-1}[-\kappa^{-1}\kappa_X + B_2(a^{-1}a_X + \kappa^{-1}\kappa_X)]$$

where

$$B_2 = k[J_1(k)/J_2(k) + J_2(k)/J_1(k) - 3/k].$$

I_7:

$$I_7 = c(H^{-1}H)_X \int_{-\pi}^{\pi}\int_0^a \psi^{(0)}\psi^{(0)}_{\xi\xi}\, rdrd\theta$$

We require

$$\psi^{(0)}_{\xi\xi} = \sin(\theta)\cos^2(\theta)(D^2R - 2DR/r + 2R/r^2) +$$

$$\sin^3(\theta)(DR/r - R/r^2)$$

which results in

$$I_7 = -cC_2(G/4)H^{-1}H_X .$$

I_8:

$$I_8 = \kappa^2 c(H^{-1}H_X) \int_{-\pi}^{\pi}\int_0^a \psi^{(0)}\psi^{(0)}\, rdrd\theta$$

Straightforward calculation results in

$$I_8 = cC_2[D_2 - 2(1 + (k/\gamma)^2)J_2(k)/(kJ_1(k)) + (1 + (k/\gamma)^2)^2/4]H^{-1}H_X .$$

I_9:

$$I_9 = -(H^{-1}H_X) \int_{-\pi}^{\pi}\int_0^a \psi^{(0)}J(\psi^{(0)}, \psi^{(0)}_{\xi})\, rdrd\theta$$

We require

$$\psi^{(0)}_{\xi\theta} = (\cos^2(\theta) - \sin^2(\theta))(DR - R/r)$$

$$\psi^{(0)}_{\xi r} = \cos(\theta)\sin(\theta)(D^2R - DR/r + R/r^2),$$

which gives

$$I_9 = cC_2k(4\gamma^2)^{-1}(J_2(k)/J_1(k))H^{-1}H_X .$$

I_{10}:

$$I_{10} = (H^{-1}H_X) \int_{-\pi}^{\pi}\int_0^a \psi^{(0)}[(r_0)^{-1} - \kappa^2 cy]\psi^{(0)}_{y}\, rdrd\theta$$

We require

$$\psi_y^{(0)} = \sin^2(\theta)DR + \cos^2(\theta)R/r.$$

The trigonometric components of the integral with the Rossby number as a coefficient are $\sin^3(\theta)$ or $\cos^2(\theta)\sin(\theta)$ both of which integrate to zero. The remaining integration gives

$$I_{10} = cC_2[(3/8)(k/\gamma)^4 - D_2/2 +$$

$$(1 + (k/\gamma)^2)J_2(k)/(kJ_1(k)) - (1/8)(1 + (k/\gamma)^2)^2]H^{-1}H_X .$$

I_{11}:

$$I_{11} = 2\kappa^2(H^{-1}H_X)\int_{-\pi}^{\pi}\int_{0}^{a}\psi_y^{(0)}\psi^{(0)}\psi^{(0)}\,rdrd\theta$$

The evaluation of I_{11} is similar to I_5, the result is

$$I_{11} = -(1/2)cC_2(k/\gamma)^4H^{-1}H_X .$$

I_{12}:

$$I_{12} = 2c\int_{-\pi}^{\pi}\int_{0}^{a}\psi^{(0)}\psi_{\xi yY}^{(0)}\,rdrd\theta$$

This integral is trigonometrically indentical to I_{12} in the exterior calculations. Therefore $I_{12}=0$.

I_{13}:

$$I_{13} = (\kappa^2)_Y\int_{-\pi}^{\pi}\int_{0}^{a}\psi^{(0)}\psi^{(0)}\psi_{\xi}^{(0)}\,rdrd\theta$$

This integral is trigonometrically identical to the I_{13} integral in the exterior calculation. Therefore $I_{13}=0$.

I_{14}:

$$I_{14} = \int_{-\pi}^{\pi}\int_{0}^{a} \psi^{(0)}[r\sin(\theta)(\delta^2 + \kappa^2 c)]_{Y}\, \psi^{(0)}_{\xi}\, r\,dr\,d\theta$$

We require

$$[r\sin(\theta)(\delta^2 + \kappa^2 c)]_{Y} = -\cos(\theta)\sin(\theta)\xi_0 (\delta^2 + \kappa^2 c)_{Y} +$$

$$\cos(\theta)\sin(\theta)\xi_0 (\delta^2 + \kappa^2 c)_{Y} +$$

$$\sin(\theta)[r(\delta^2 + \kappa^2 c)]_{Y},$$

and $\psi^{(0)}_{\xi} = (DR - R/r)\sin(\theta)\cos(\theta)$. The trigonometric component of the integral is therefore $\sin^3(\theta)\cos^2(\theta)$ or $\sin^3(\theta)\cos(\theta)$, both of which integrate to zero due to the periodicity in θ.

The integrals I_{15} through I_{19} are trigononmetrically indentical to the exterior integrals I_{14} through I_{18}, respectively. Therefore all the remaining integrals are zero.

I_{15}:

$$I_{15} = -2\int_{-\pi}^{\pi}\int_{0}^{a} \psi^{(0)} J(\psi^{(0)}, \psi^{(0)}_{yY})\, r\,dr\,d\theta$$

I_{16}:

$$I_{16} = c(H^{-1}H_{Y}) \int_{-\pi}^{\pi}\int_{0}^{a} \psi^{(0)}\psi^{(0)}_{\xi y}\, r\,dr\,d\theta$$

I_{17}:

$$I_{17} = -(H^{-1}H_{Y}) \int_{-\pi}^{\pi}\int_{0}^{a} \psi^{(0)} J(\psi^{(0)}, \psi^{(0)}_{y})\, r\,dr\,d\theta$$

I_{18}:

$$I_{18} = (H^{-1}H_{Y}) \int_{-\pi}^{\pi}\int_{0}^{a} \psi^{(0)}[(r_0)^{-1} - \kappa^2 cy]\psi^{(0)}_{\xi}\, r\,dr\,d\theta$$

I_{19}:

$$I_{19} = -2\kappa^2(H^{-1}H_Y)\int_{-\pi}^{\pi}\int_{0}^{a}\psi^{(0)}\psi^{(0)}\psi^{(0)}_{\xi}\,rdrd\theta.$$

The compatibility condition (3.2.9) is therefore

$$0 = \int_{-\pi}^{\pi}\int_{0}^{a}\psi^{(0)}(\text{RHS[3.2.8]})\,rdrd\theta = \sum_{n=1}^{19} I_n . \qquad \text{(A10)}.$$

In order to obtain (3.2.11) the terms $\kappa^{-1}\kappa_T$ and $\kappa^{-1}\kappa_X$ in (A10) are eliminated in favour of $a^{-1}a_T$, $(2c)^{-1}c_T$, $a^{-1}a_X$ and $(2c)^{-1}c_X$ by differentiating the dispersion relation (3.1.5) to obtain

$$\kappa^{-1}\kappa_T = N[a^{-1}a_T - (2c)^{-1}c_T] - (2c)^{-1}c_T$$

$$\kappa^{-1}\kappa_X = N[a^{-1}a_X - (2c)^{-1}c_X] - (2c)^{-1}c_X$$

where $N = -\{\gamma R + k^2R/\gamma\}/\{4 + \gamma/R + k^2R/\gamma\}$ and $R=K_2(\gamma)/K_1(\gamma)$.

After a little alegbra, (3.2.11) is obtained from (A10) where B_1, B_2, B_3 and E_2 are given by the following hierarchy of definitions;

$$M = L/G + 1,$$

$$E = [-J_2(k)/(kJ_1(k)) + (1 + (k/\gamma)^2)/4]/G,$$

$$B_1 = NM + M - N, \qquad \text{(A11)}$$

$$B_2 = 2(1 + N) + E(N + 2 + 2(k/\gamma)^2) + (k/\gamma)^4(2G)^{-1}(N - 1) + kJ_2(k)[2\gamma^2J_1(k)G]^{-1}(1 - B_1N - B_1 + N), \qquad \text{(A12)}$$

$$B_3 = -2N + E(1 - N + (k/\gamma)^2) + k^4N(2\gamma^4G)^{-1} + k(2\gamma^2J_1(k)G)^{-1}J_2(k)[B_1N + B_1 - N], \qquad \text{(A13)}$$

$$E_2 = 1/4 + E/2 - k^4(8\gamma^4G)^{-1} + kJ_2(k)[4\gamma^2J_1(k)G]^{-1}. \qquad \text{(A14)}$$